PROTEASOMAL PROTEOLOYSIS DURING PORCINE FERTILIZATION

A Dissertation

Presented to

The Faculty of the Graduate School

At the University of Missouri

In partial fulfillment

Of the requirements for the degree

Doctorate of Philosophy

By

Shawn William Zimmerman

Dr. Peter Sutovsky, Dissertation Supervisor

May 2012

The undersigned, appointed by the dean of the Graduate School,
have examined the dissertation entitled

PROTEASOMAL PROTEOLOYSIS DURING PORCINE FERTILIZATION

Presented by SHAWN ZIMMERMAN

A candidate for the degree of

Doctor of Philosophy

And hereby certify that, in their opinion, it is worthy of acceptance.

Professor Peter Sutovsky

Professor Randall Prather

Professor Rocio Rivera

Professor Heide Schatten

ACKNOWLEDGEMENTS

I would like to thank the members of my committee Dr. Peter Sutovsky, Dr. Randall Prather, Dr. Rocio Rivera and Dr. Heide Schatten for all of their guidance throughout my PhD program. As a whole, I could not have asked for a better committee; you have been both challenging and understanding, and for that I am truly thankful. I would especially like to thank my advisor Dr. Sutovsky, for his patience and guidance throughout my PhD studies.

To the members of the Sutovsky lab, I thank you for being there not just as lab mates but also as friends; you made my time here truly memorable. Along with being there as my friends, I would like to thank you all for your time and participation in my various projects. I would like to thank Miriam Sutovsky for taking the time to teach me numerous procedures that became essential to the completion of my dissertation projects. I would also like to thank you for assisting with westerns so that I may move forward with other projects. To Dr. Yi, I thank you for the countless conversations we had about my projects and for your contributions to several of them by performing IVF trials.

Thank you to Melissa Samuel and Dr. Walters for providing me with tissue samples when I was in need of them, you truly gave me the “hands on” experience when it comes to tissue collection. To Lonnie Dowell a special thanks to you for

collecting semen for me on a weekly basis. While it is not the most glamorous job you always managed to smile when you brought it to me. I would like to say thank you to Lee Spate for coordinating ovaries every week, without this my projects surely would have suffered.

To the many graduate friendships I have developed over the years I thank you all. Each one of you has brightened my day in one way or another and I couldn't imagine my time here without you. To my family a special thank you for supporting me throughout my PhD program. To my mother and father Susan and Ervin Zimmerman I could not have asked for more supportive parents. You got me through the rough parts and celebrated with me during the high and I can't thank you enough. To my sister and brother-in-law Heather and AJ Mills thank you for supporting me throughout my PhD studies and for never letting me lose sight of the big picture. Finally thank you to my grandparents for your understanding when I couldn't come home to see you due to work and for your continued support throughout my degree.

Table of Contents

LIST OF FIGURES

LIST OF SUPPLEMENTAL FIGURES

NOMENCLATURE

AA	Amino Acid
ACUC	Animal Care and Use Committee
AE	Acrosome Exocytosis
AM	Acrosomal Membrane
ANOVA	Analysis of Variance
AR	Acrosome Reaction
ATP	Adenosine triphosphate
Bp	Base pair
BSA	Bovine Serum Albumin
cDNA	complementary DNA
CLβL	clasto-Lactacystin β-Lactone
CO_2	Carbon Dioxide
COC	Cumulus Oocyte Complex
DAPI	4',6-diamidino-2-phenylindole
DMSO	Dimethyl sulfoxide
DNA	Deoxyribonucleic acid
DUB	Deubiquitinating Enzyme
EDTA	Ethylenediaminetetraacetic acid
EGF	Epidemial Growth Factor
EST	Expressed Sequence Tags
EtOH	Ethanol
FITC	Fluorescein isothiocyanate

FSH	Follicle Stimulating Hormone
HRP	Horseradish peroxidase
IAM	Inner Acrosome Membrane
IgG	Immunoglobulin G
IVF	In Vitro Fertilization
IVM	In Vitro Maturation
K	Lysine
kDa	kilo Dalton
LC	Liquid Chromatography
LH	Luteinizing Hormone
MII	Metaphase II
MS	Mass Spec
MW	Molecular Weight
NaCl	Sodium Chloride
NGS	Normal Goat Serum
OAM	Outer Acrosomal Membrane
PBS	Phosphate Buffer Solution
PCR	Polymerase Chain Reaction
PIC	Proteasomal Inhibitor Cocktail
PMSF	Phenylmethanesulfonylfluoride
PNA	Peanut agglutinin
PVA	Polyvinyl alcohol
PVDF	Polyvinylidene fluoride
RNA	Ribonucleic Acid

SEM	Standard Error Mean
sZP	Solublized Zona Pellucida
TBS	Tris Buffer Solution
TOF	Time of Flight
Tris	Tris(hydroxymethyl)aminomethane
TRITC	Tetramethylrhodamine-5-(and 6)-isothiocyanate
UBAL	Ubiquitin Aldehyde
UPS	Ubiquitin Proteasome System
Zn	Zinc
ZP	Zona Pellucida
ZPC	Zona Pellucida Glycoprotein C

PROTEASOMAL PROTEOLOYSIS DURING PORCINE FERTILIZATION

Shawn William Zimmerman

Dr. Peter Sutovsky, Dissertation Supervisor

ABSTRACT

Protein degradation is essential for maintaining a healthy cellular state. One such protein degradation pathway is the Ubiquitin Proteasome System (UPS) that consists of a small chaperone protein ubiquitin, a proteolytic holoenzyme known as the 26S proteasome and three key ubiquitin-activating and ubiquitin-conjugating enzymes (E1, E2, E3). The UPS participates in multiple reproductive processes in various species including spermatogenesis, oocyte maturation and fertilization. Based on this knowledge, the first objective ot this thesis was to determine if the UPS was active during the penetration of fertilizing boar spermatozoa through the porcine egg coat, zona pellucida (ZP). The second objective was to determine if the UPS was actively targeting acrosomal proteins for degradation during the zona induced acrosome reaction. Activity of the UPS was determined based on the protection of both zona and acrosomal proteins from degradation by the 26S proteasome, via addition of specific proteasomal inhibitors. It was concluded that the UPS is active during ZP penetration of porcine oocytes and acrosome reaction of fertilizing boar spermatozoa. Furthermore, it was shown that by adding specific proteasomal inhibitors, these proteins could be

protected from degradation by the UPS. While attempting to determine which proteins were being protected from degradation, a member of the UBR box family of E3 enzymes, known as the, the ubiquitin ligase UBR7 was identified in the boar testis and spermatozoa. Collectively, these results provide a unique window by which to gain a better understanding of the activity of the UPS during mammalian fertilization.

CHAPTER ONE

RECENT PROGRESS IN THE STUDY OF THE SPERM PROTEASOME DURING SPERM CAPACITATION AND FERTILIZATION

by

Shawn Zimmerman and Peter Sutovsky

Key words: Ubiquitin, proteasome, sperm, acrosome, fertilization, zona pellucida,

Short Title: Sperm proteasome during fertilization

Reference: Zimmerman S & Sutovsky P 2009 The sperm proteasome during sperm capacitation and fertilization. Journal of Reproductive Immunology 83 19–25.

Abstract

The 26S proteasome is a multi-subunit protease specifically targeting ubiquitinated proteins. Consensus emerged from studies by multiple laboratories on the role of sperm-borne proteasomes in human, mouse, pig, bovine, ascidian and echinoderm fertilization. Major findings from the studies in various mammalian and non-mammalian fertilization systems are: **1**) proteasomes are present in the mammalian sperm acrosome and on the acrosomal surface; **2**) ubiquitinated proteins are present on the mammalian, ascidian and echinoderm egg coat; **3**) proteasomal proteolytic and ubiquitin-deconjugating (deubiquitinating) activities can be detected in viable, motile mammalian spermatozoa; **4**) proteasomes remain associated with the sperm head following ZP-induced acrosomal exocytosis; **5**) inhibition of ubiquitination and proteasomal proteolysis blocks fertilization in mammals, ascidians and echinoderms; **6**) inhibition of proteasomal proteolysis alters the course of mammalian sperm capacitation and acrosomal exocytosis induced by sperm binding to the egg coat, zona pellucida (ZP); **7**) depletion of the sperm-surface associated ATP blocks porcine and echinoderm fertilization, most likely by affecting the integrity of sperm proteasomes, of which several subunits are ATPases; **8**) inhibition of proteasomal proteolysis blocks sperm-ZP penetration, but does not alter the rate of sperm-ZP binding in mammals; and **9**) experimental modification of sperm-associated deubiquitinating activities shifts the balance of monospermic fertilization to polyspermic fertilization *in vitro.* Altogether, these studies provide evidence for the involvement of the 26S proteasome in multiple

steps of animal and human fertilization, offering a novel model of sperm-egg coat interactions, and identifying a range of potential new sperm quality markers and contraceptive targets.

Introduction

The ubiquitin-proteasome pathway is a crucial, regulated route for substrate specific protein degradation in eukaryotic cells (Coux et al. 1996). The 26S proteasome is a multi-subunit complex consisting of a barrel shaped 20S core capped on one or both sides with a 19S regulatory complex (**Figure 1.1**). Within the hollow core of the 20S proteasome reside two β-rings consisting of seven subunits, β1-7 (PSMB1-7). Contained within these rings are proteolytic enzymes, subunits PSMB5-7, that have trypsin-like, chymotrypsin-like, and postglutamyl peptide hydrolyzing activities that are responsible for degrading the proteins that enter the core chamber (Wojcik et al. 2000). On each side of these β-rings are single α-rings also consisting of seven subunits per ring and designated in the same order as those seen in the β-rings, i.e. α1-7 (PSMA1-7). The α-rings modulate the entrance of the targeted proteins into the β-rings allowing for full degradation of a given protein (Glickman and Ciechanover 2002).

The 19S regulatory complex/cap contains the isopeptidase, oxidoreductase, ATPase, and protein-unfolding activities. It is responsible for the recognition, binding and removal of multi-ubiquitin chains on the ubiquitinated substrate proteins destined for degradation (Lupas et al. 1993). The 19S cap consists of two types of subunits that are intermingled throughout the cap, the first being the ATP dependent subunits (Rpt1-6 or PSMC1-6), and the second type, non-ATP dependent ones (Rpn1-12 or PSMD1-14) (Hendil 1988). The 19S cap is divided into two multisubunit sections, the base and the lid. The base contains ATPases Rpt1-6 (PSMC1-6) and non-ATPases Rpn1 (PSMD2), Rpn2

(PSMD1), and Rpn10 (PSMD4). Recognition of ubiquitinated proteins occurs in the base through the non-ATPase subunit Rpn10/PSMD4. Recently, subunit Rpn 13/ARM1 was proposed to participate in the ubiquitin chain recognition process (Husnjak et al. 2008). Upon recognition, the ATPases (Rpt 1-6/PSMC1-6) are thought to rotate and allow for the protein to enter into the 20S core (Husnjak et al. 2008). The remaining non-ATPase subunits (Rpn3-9, Rpn11-12) make up the lid of the 19S complex. Some of these non-ATPase subunits may be responsible for recruiting deubiquitinating enzymes (DUBs) that release the ubiquitin molecules from the ubiquitinated substrate protein. Following this deubiquitination step, the substrate protein alone can enter into the core for degradation and the uncoupled ubiquitin molecules can be reused by the cell to target other proteins for recycling (Yao and Cohen 2002). Intriguingly, the inhibition of the deubiquitinating activity associated with the 19S complex actually promotes and accelerates proteasomal proteolysis (Guterman and Glickman 2004). In the presence of DUB inhibitors, the multiubiquitin chains are not released from the substrate docked to the 19S complex; instead, these multi-ubiquitin chains are degraded along with the substrate to which they are linked. The inhibitors of deubiquitination appear to not only stop deubiquitination but also stimulate proteasomal proteolysis (Guterman and Glickman 2004). As will be discussed below, such a proteasome-stimulating effect of DUB inhibitors may account for an increase in polyspermy observed in the presence of a DUB inhibitor, ubiquitin-aldehyde, during porcine fertilization *in vitro* (Yi et al. 2007b).

Besides the 19S regulatory complex/cap there are alternative caps that can be found attached to the 20S core. These caps are capable of replacing the 19S regulatory complex in certain situations involving proteasomes and are known as the PA200 and the 11S regulatory particle (PA28) or REG. The PA200 (PMSE4) is a 200 kDa protein that was originally believed to be present only in the nucleus of cells where it was thought to assist in repairing double stranded DNA breaks (Ortega et al. 2005; Ustrell et al. 2002). It is now known that PA200 is also required for normal post-meiotic spermatogenesis (i.e. spermiogenesis) in mice (Khor et al. 2006). Unlike the PA200 the 11S particle/REG is typically found in proteasomes outside the nucleus and is tasked with the recognition of MHC class I molecules (Kloetzel 2004). The 11S particle is a ring of seven subunit molecules, comprised of three subunit types, REGα (PSME1), REGβ (PSME2) and REGγ (PSME3). The subunits arrange themselves such that the 11S will be composed of either a homodimer of seven REGγ (PSME3) subunits or a heterodimer of REGα (PSME1) and REGβ (PSME2) subunits. Determination of the correct configuration is based on the function; the heterodimer is known to recognize the presence of MHC class I molecules while the substrate affinity of the homodimer is not fully understood (Kloetzel 2004; Mao et al. 2008). Both PA200 and 11S particle can associate with the 20S core. These alternative proteasomes are believed to be able to mediate the degradation of non-ubiquitinated proteins though this role has yet to be firmly established (Rechsteiner and Hill 2005).

In order for the canonical 26S proteasome to properly recognize its target proteins, these proteins must be expressing a multiubiquitin chain. Ubiquitination is a series of enzymatic reactions that are choreographed specifically with the goal of forming this multiubiquitin chain. The ubiquitination process is comprised of three key enzymes and begins with the activation of the ubiquitin activating enzyme E1 (UBA1). UBA1 becomes active through phosphorylation; this active state then allows for initial association with a single ubiquitin molecule that is destined for ligation to a specific substrate protein (Baker et al. 2010). The association of ubiquitin to the E1 enzyme is short lived for the E1 is quickly removed and replaced with the second enzyme in the ubiquitination pathway, the ubiquitin conjugating enzyme E2. As of today there are about a dozen E2 enzymes in mammals and only two known testis-specific E2 enzymes. The testis-specific enzymes UBE2R and UBC4 are present in an ascidian *Ciona intestinalis* (Yokota et al. 2010a) and rat (Wing et al. 1996), respectively. Concurrently, as the E2 enzyme replaces the E1 enzyme, the final enzyme in the ubiquitination pathway is seeking out a protein that has out lived its use, this enzyme is known as the ubiquitin E3-type ligating enzyme. In mammals there are several hundred E3-type ligases known and a large portion of those enzymes present in the male germ line including spermatozoa (Yin, 2011). These E3-type ligases have been classified into two primary groups: the Hect-domain and the Ring-finger (Glickman and Ciechanover 2002). It is these classes of enzymes that are responsible for recognizing protein degron sequences and misfolded or compromised proteins in order for the transfer of the ubiquitin molecule to the

protein to occur. The initial single-molecule ubiquitination (monoubquiitnation) is completed by formation of a covalent bond between the C-terminal Gly-residue (G76) of ubiquitin and an internal Lysine-residue (K) of the targeted protein. Once monoubiquitination has occurred, the ubiquitin chain begins to elongate through the action of the E1, E2 and E3 enzymes in conjunction with a fourth enzyme E4. The E4 enzyme is believed to allow for elongation of the ubiquitin chain past the initial cycle of ubiquitination. E4 appears to never form bonds with the substrate itself but rather interacts with the incoming monoubiquitin molecule (Koegl et al. 1999). To be recognized by the 19S proteasomal regulatory complex, a substrate protein has to be tagged with a mutli-ubiquitin chain of four or more ubiquitin molecules.

A substantial body of work addressing the presence of proteasomes in mammalian spermatozoa has been generated since 2000, but the initial work was done in an ascidian, *Halocynthia roretzi.* Such studies showed that trypsin-like and chymotrypsin-like activities, consistent with those of a 20S proteasomal core, were occurring during *H. roretzi* fertilization (Hoshi et al. 1981). When these protease activities were inhibited by leupeptin analogs with a high affinity for proteasomal proteases, sperm penetration through the egg vitelline coat failed. However, when the same inhibitor treatment was performed with oocytes deprived of the vitelline coats, fertilization occurred (Sawada et al. 1984). These findings provided some of the first evidence that proteases consistent with the 26S proteasome were required for sperm penetration in an animal species.

While this early work showed that proteasomes are required for sperm-egg coat penetration in ascidians, evidence is now mounting that the gamete-borne proteasomes participate in numerous, and possibly all, gamete activities throughout the entire process of mammalian fertilization. Proteasomes may be essential for the removal of membrane-associated proteins during the remodeling of the sperm plasma membrane occurring during the capacitation process (Kong et al. 2009). Following sperm capacitation, the proteasomes may assist with acrosomal exocytosis (AE), possibly by degrading proteins associated with the outer acrosomal membrane (OAM) causing the OAM to become vesiculated and resulting in the release of the acrosomal matrix (AM) and the formation of an acrosomal shroud/ghost (S. Zimmerman and P. Sutovsky, unpublished data). Furthermore, proteasomes found in the AM may assist with sperm penetration through the mammalian egg coat, zona pellucida (ZP), by degrading proteins residing on the ZP surface (Sutovsky et al. 2004). Ultimately, such a proteolytic event could explain how the fertilization slit is created, through which the fertilizing spermatozoon is able to penetrate the egg coat (Buffone et al. 2008). Proteasomes that reside on the inner acrosomal membrane (IAM) and are retained after AE may provide a continuous proteolytic activity as the sperm head advances through the thick egg coat found in mammals, and may also be involved in the fertilization process as the sperm enters into the cytoplasm of the oocyte. Once there, these proteasomes could participate in the degradation of proteins found in the cytoplasm or within the sperm nucleus as it is being remodeled into a male pronucleus.

Subcellular localization of the sperm proteasomes

Location and distribution of the proteasomes is vital to cells' ability to efficiently degrade ubiquitinated proteins. Proteasomes have been found to reside in the cytoplasm and nucleus of all eukaryotic cells, and proteasomal subunits make up 1% of the total cell protein (Hendil 1988). Within the nucleus, the proteasomes appear to reside near the promyelocytic leukemia (PML) bodies present in many human cell types; from this position, the proteasomes are able to degrade nuclear proteins on site before the proteins are transported out into the cytoplasm where they would be degraded by resident proteasomes (Glickman and Ciechanover 2002). In the cytoplasm, the proteasomes are associated with the external layer of the endoplasmic reticulum (ER), the cytoskeleton and the centrosome (Wojcik and Di Napoli 2004). In human spermatozoa, proteasomes have been located on the plasma membrane overlying the sperm acrosome, allowing for degradation of proteins prior to or during sperm capacitation (Morales et al. 2004). Underneath the sperm plasma membrane, active proteasomes may reside on the outer acrosomal membrane, in the acrosomal matrix and in the inner acrosomal membrane (Morales et al. 2003; Sutovsky et al. 2004; Yi et al. 2010b). Besides being located in the acrosomal cap, proteasomes are detectable in the sperm tail connecting piece where they may participate in the release of the sperm-borne centriole following fertilization (Rawe et al. 2008). Finally, proteasomes are also located in the sperm tail mid-piece; it was proposed that they degrade structural

proteins of the sperm flagellum during epididymal sperm maturation (Mochida et al. 2000). During spermiogenesis/spermatid differentiation, proteasomal subunits can be detected associated with the nascent inner and outer acrosomal membranes of the acrosomal cap during acrosomal biogenesis as well as the caudal manchette, a transitory accessory structure of elongating spermatids (Rivkin et al. 1997; Rivkin et al. 2009).

Requirement of proteasomal activity during sperm capacitation and acrosomal exocytosis

During sperm capacitation, changes are occurring in the sperm plasma membrane, the outer acrosomal membrane and the acrosomal matrix in preparation for acrosomal exocytosis (AE). The interior pH of mouse acrosome is initially acidic, which is believed to serve as a means to keep the protease proacrosin inactive (Honda et al. 2002a). As the spermatozoa undergo capacitation the pH increases toward a basic pH; this change in pH causes proacrosin to become proteolytically processed into active acrosin, which then initiates proteolytic processes in the acrosomal matrix (Buffone et al. 2008; Nakanishi et al. 2001). Not only does a change in pH cause activation of resident proteases in sperm but phosphorylation also causes it (Bailey 2010). Recently, it was shown that acrosin binding protein sp32, located in the acrosomal matrix, was being tyrosine phosphorylated during the capacitation of boar spermatozoa (Arcelay et al. 2008). Proteasomal subunit α-6 (PSMA1) and the valosin contain protein (VCP),

which is a cofactor of substrate presentation to the 19S proteasomal regulatory complex, were also phosphorylated. Protein spots recognized by antibodies against 20S core subunits α-3 (PSMA4) and β-6 (PSMB1) were shown to increase in size when compared on 2-D PAGE gels before and after boar sperm capacitation; this suggests that changes in sperm proteasomal structure may occur during sperm capacitation (Choi et al. 2008). This increase in 20S core subunit detection could reflect the activation of the 20S core while it is also possible that changes in phosphorylation of the 20S core subunits cause this increase, similar to that seen in sp32 (Arcelay et al. 2008). Kong *et al.,* noted a change in overall protein tyrosine phosphorylation pattern in normal human capacitated spermatozoa incubated in the presence of proteasomal inhibitor epoxomicin (Kong et al. 2009). They determined that proteasomes were active during the capacitation process and their inhibition resulted in incomplete capacitation. Also, proteasomal activity may contribute to the release of capacitated spermatozoa from the oviductal sperm reservoir *in vivo;* this release has been documented in an *in vitro* sperm-oviductal epithelial cell co-culture system as being the result of a rapid loss of a sperm plasma-membrane bound seminal plasma protein, the spermadhesin AQN1 (Ekhlasi-Hundrieser et al. 2005). One can speculate that this acrosome-associated protein is removed by resident proteasomes located on the OAM, allowing the capacitated spermatozoa to detach from the oviductal epithelium and travel to the fertilization site. While more work is still required to confirm such a hypothesis, our preliminary data indicate that the acrosomal AQN1 in boar spermatozoa is

ubiquitinated. Along with active proteasomal subunits, the ubiquitinating enzymes may become active during capacitation. One enzyme known to be activated during capacitation is the UBE1 enzyme which has been shown to become phosphorylated during rat sperm capacitation (Baker et al. 2010). Furthermore, inhibition of activating enzyme UBE1 results in incomplete capacitation and a reduced ability to undergo AE or fertilization (Yi et al. 2011). Altogether, ubiquitinating enzymes and proteasomes appear to be participating in the removal of membrane bound proteins during the capacitation process, but not all proteasome activities are accounted for by the capacitation process. Proteasomal activities may assist with other aspects of the fertilization process, such as the acrosomal exocytosis.

According to Gerton's definition, acrosomal exocytosis (AE) can be defined as externalization of acrosomal contents at varying rates depending on acrosomal matrix and membrane compartmentalization (Kim and Gerton 2003). The AE is thought to start at capacitation and its completion to be a result of ZP-induced fusion and vesiculation of the OAM and plasma membrane (Buffone et al. 2008; Jin et al. 2011; Kim and Gerton 2003). As spermatozoa bind to ZP and undergo AE, proteasomes could degrade some of the ZP proteins. Proteasomes located in the acrosome appear to be located predominately in two compartments. Prior to AE, proteasomes are detectable on the OAM (Morales et al. 2004) and may allow for AE to occur, as suggested by studies of acrosomal exocytosis induced in the capacitated human spermatozoa by recombinant human ZP3 and ZP4 proteins (Chakravarty et al. 2008; Morales et al. 2004). A second

population of proteasomes is revealed after AE on the IAM where they may support the secondary binding mechanism for sperm and provide a sustained proteolytic activity while the sperm head advances through the zona pellucida (Sutovsky et al. 2004; Yi et al. 2007a; Yi et al. 2010b). Thus, it is now established that proteasomal activities are essential for spermatozoa to undergo capacitation and AE. However, the mechanism for sperm penetration through the ZP has been the subject of a spirited debate for several decades.

Do sperm proteasomes degrade sperm receptor on mammalian ZP during fertilization?

The debate between the proponents of enzymatic and mechanical sperm-zona penetration hypotheses has labored for years (Bedford 1998; Olds-Clarke 2003). While some theorize that spermatozoa penetrate through the ZP solely by a mechanical force exerted from the movement of the sperm flagellum, others believe it is the presence of proteolytic activity in the sperm acrosome that is essential for sperm-ZP penetration. Studies on acrosin favored an enzymatic pathway of sperm-zona penetration, but the finding that the acrosin-null mice are fertile (Baba et al. 1994a) shifted the pendulum back towards the acceptance of the mechanical hypothesis. Recently, several review papers once again discussed the merit of the enzymatic hypothesis, mentioning the work on sperm proteasome (Bedford 2008; Hedrick 2008; Kim et al. 2008; Yanagimachi

2009). If spermatozoa were to penetrate through the zona pellucida by force alone, then the presence of proteasomal inhibitors would have no effect on the sperm-ZP penetration. Furthermore, the physical attributes of the sperm head make it difficult for purely mechanical penetration in most species. With the human sperm head having a round shape, it requires greater force than the tail is able to exert to achieve egg coat penetration. It has been shown that a force exceeding 50 kN/m^2 was not sufficient for mechanical zona penetration. This force far exceeds the estimated force produced by the flagellar motility of the zona-bound spermatozoa (Green 1987). So while the mechanical thrust of flagellar motility undoubtedly provides some assistance as the spermatozoon advances through the ZP, it is not likely to be the sole mechanism of penetration. In the case of ascidians, the main component of the vitelline coat, HrVC70 (Urayama et al. 2008), which is the homologue of mammalian ZP3, acts as the sperm receptor and upon sperm binding is degraded by the sperm proteasomes as the fertilizing spermatozoon begins penetration (Sawada et al. 2002). In the presence of proteasomal inhibitor MG132, pig spermatozoa are unable to penetrate the intact zona, but when the zona is removed, the spermatozoa are able to fertilize even in the presence of MG132 (Sutovsky et al. 2004). Similar results were obtained in bovine, when capacitated spermatozoa were incubated with the proteasomal inhibitor epoxomicin for either 30 or 60 min and were unable to penetrate intact ZP or undergo AE during IVF (Sanchez et al. 2011). Human spermatozoa exposed to epoxomicin for 45 min showed a similar inability to undergo AE even when in the presence of progesterone (Tapia et al.

2011). It follows that if proteasomal inhibitors are able to stop penetration through the mammalian ZP, then the zona should be ubiquitinated either before or during fertilization. The aforementioned ascidian sperm receptor HrVC70 is ubiquitinated by the sperm–contributed ubiquitin at fertilization immediately prior to being degraded by the sperm proteasomes (Urayama et al. 2008). Work done in sea urchin showed that urchin egg coat is ubiquitinated; however, ubiquitination clearly occurred during oogenesis (Urayama et al. 2008). Zona pellucida of pigs also appears to be ubiquitinated primarily on the outer surface in both preantral and antral ovarian follicles (Sutovsky et al. 2004). However recently it was suggested that there may be active ubiquitination still occurring during porcine fertilization because a mutant form of ubiquitin (UBB^{+1}), which is known to block proteasomal degradation, was used to block fertilization during porcine IVF (Yi et al. 2010b). Similar observations were made in human binding studies when anti-20S subunit antibodies for PSMA4 and PSMB6 were shown to reduce sperm binding to zona-intact human oocytes (Redgrove et al. 2011). Because the porcine ZP proteins are heavily glycosylated, one would predict that their proteasomal degradation would go hand in hand with their deglycosylation. Accordingly, glycosidases and glycan desulfating enzymes such as arylsulfatase A, are associated with the sperm acrosome (Tantibhedhyangkul et al. 2002; Tulsiani and Abou-Haila 2001). The ubiquitination of zona proteins and the presence of proteasomes on the outer acrosomal membrane could appear to be the lock and key to successful fertilization, but that may not be all that is required for fertilization to occur properly.

Requirement of extracellular, sperm surface-associated ATP during proteasome-assisted fertilization events

The 19S cap houses two types of subunits, ATPases and non-ATPases, located in two distinct structures, the base and the lid respectively. The six ATPase subunit (Rpt 1-6/PSMC1-6) reside in the base of the 19S complex and provide a connection between the cap and the α-rings of the 20S core (Hendil 1988). When activated by the presence of ATP, these subunits allow substrate proteins that have been tagged with a multiubiquitin chain and deubiquitinated by the 19S complex to enter the core of the proteasome and be degraded.

ATP is required for the sustenance and functioning of these subunits. The presence of ATP may also be required for proper tyrosine phosphorylation of 20S core subunits during sperm capacitation (Arcelay et al. 2008). The production of intracellular ATP in the sperm mitochondria and sperm tail principal piece is undoubtedly essential for fertilization to occur, but it appears that the presence of ATP on the sperm surface also plays a part in fertilization success. Upon infusion of extracellular ATP, human spermatozoa change movement pattern and speed to the point of hyperactivation even before becoming fully capacitated (Edwards et al. 2007; Rodriguez-Miranda et al. 2008). However, in mouse spermatozoa, the addition of external ATP not only caused them to bind to the oocyte faster than normal during IVF, but also appeared to cause the oocytes to become fertilized faster (Rodriguez-Miranda et al. 2008). This ability to

fertilize at a faster rate provides evidence that extracellular or sperm-surface associated ATP is essential for sperm function, possibly including the activity of sperm acrosomal proteasomes that, as discussed above, are exposed to the sperm surface during fertilization. Further evidence has been shown during porcine *in vitro* fertilization. The addition of a high activity *Solanum tuberosum* apyrase, a large 49 kDa enzyme that is not cell permeable and efficiently depletes ATP from cell extracts, prevents fertilization and, as indicated by Western blotting, affects the integrity of sperm proteasomes (Yi et al. 2009a). These experiments were inspired by the work of Sawada's team showing that the addition of apyrase to sea water efficiently prevents fertilization in spawning sea urchin *Pseudocentrotus depressus* (Yokota and Sawada 2007). It is reasonable to propose that the presence of extracellular, sperm-surface associated ATP facilitates both sperm capacitation and sperm-egg coat interactions that rely on sperm proteasomal activity.

Are protein substrates in the sperm acrosome and on the ZP ubiquitinated during capacitation, AE or fertilization?

It has been well documented in the ascidian model that the sperm exudates topically ubiquitinate the sperm receptor on the vitelline coat prior to degrading it with sperm-borne proteasomes, resulting in fertilization (Sawada et al. 2002; Urayama et al. 2008). In contrast, the sperm receptor on the sea urchin vitelline coat is already

ubiquitinated prior to fertilization, which suggests that the echinoderm sperm receptor becomes ubiquitinated during oogenesis. The pig model for gamete ubiquitination is not yet completely understood, but early immunohistochemical studies detected ubiquitinated proteins on porcine ZP even at the earliest stages of folliculogenesis within the porcine ovary (Sutovsky et al. 2004). Ubiquitin-conjugating enzyme E2 has been detected in the boar sperm acrosome by immunocytochemistry (Fischer et al. 2005). Use of a yeast two-hybrid system showed that the ubiquitin-like protein UBAP2L was binding to the human glycoprotein ZP3 during hemizona assays and the inhibition/immunoblock of UBAP2L reduced sperm-zona binding (Naz and Dhandapani 2010). More recently, we have detected the ubiquitin-activating enzyme E1 by Western blotting and found changes in the Western blotting band patterns of unconjugated and substrate-linked ubiquitin present in the acrosome during the capacitation process (Yi et al. 2011). It is plausible that as the spermatozoa undergo capacitation, acrosomal proteins could be actively ubiquitinated and degraded by acrosomal proteasomes to facilitate acrosomal exocytosis upon sperm contact with the ZP. The remaining monoubiquitin molecules in the acrosomal matrix could be used to form multiubiquitin chains on the zona proteins in points of contact between the acrosomal shroud and ZP, allowing the proteasomal degradation of sperm receptors on ZP and subsequent sperm penetration. As in ascidians, boar spermatozoa could thus ubiquitinate the ZP proteins during fertilization, resulting in the digestion of the fertilization slit. The proper environment to assure the retention of ubiquitin-conjugating enzymes and

unconjugated monoubiquitin at the site of fertilization slit could be maintained within the acrosomal shroud. While acrosome reaction was traditionally defined as the dispersion of the acrosomal matrix, the acrosomal shroud is a solid structure that envelopes the sperm head on the zona surface and may maintain a gel-like environment in which biochemical reactions such as ubiquitination and proteasomal degradation could be sustained for hours after exocytosis. Some of the outstanding issues associated with this aspect of sperm-ZP interactions could be addressed by the inhibition of E1 and E2 enzymes during fertilization.

Role of deubiquitinating enzymes in sperm proteasome function and anti-polyspermy defense

Following the recognition of an ubiquitinated substrate protein by the 19S proteasomal regulatory complex, the multi-ubiquitin chain is released and the substrate protein enters the 20S core. Deubiquitinating enzymes (DUBs) are recruited into the 19S cap where they target the multi-ubiquitin chains on the docking ubiquitinated proteins. It is believed that the ubiquitin molecules are released from the multi-ubiquitin chains individually by the DUBs, and the substrate protein is then pulled into the 20S core and degraded (Coux et al. 1996). The newly liberated monoubiquitin molecules are then released from the cap to re-enter the ubiquitination-degradation cycle. The DUBs may regulate the rate of proteasomal proteolysis, but are not essential

for proteasomal degradation. The inhibition of deubiquitinating activities associated with the 19S regulatory complex actually increases the rate of proteasomal proteolysis (Guterman and Glickman 2004; Yi et al. 2009b). In the presence of DUB inhibitors such as the ubiquitin-aldehyde, the whole complex of a protein substrate covalently linked to a multi-ubiquitin chain is threaded through the 20S core and degraded. A specific type of DUB, the ubiquitin C-terminal hydrolase UCHL3, is present in the boar sperm acrosome, and the non-cell permeant UCH inhibitor, ubiquitin-aldehyde, increases the fertilization and polyspermy rates when mixed in fertilization medium during porcine IVF (Yi et al. 2007b). However, when ubiquitin-aldehyde was injected into developing oocytes, it prevented sperm incorporation into the ooplasm and reduced fertilization rates (Mtango et al. 2011). The failure of sperm incorporation in the injected ova was probably due to incomplete maturation of the oocyte cortex, accompanied by abnormal or missing oocyte meiotic spindle (Mtango et al. 2011). In turn, polyspermy is reduced and a high rate of monospermic fertilization can be achieved by the addition of recombinant UCHL3 in the IVF medium (Yi et al. 2007b). These results indicate that polyspermy can be manipulated by supplying either an extracellular UCH during IVF to reduce the occurrence of polyspermy or an extracellular ubiquitin-aldehyde to increase polyspermy (Yi et al. 2007b). The above described paper also identified a related enzyme, UCHL1 (synonymous with PGP9.5), in the porcine oocyte cortex. Sekiguchi *et al.,* suggested that oolemma bound UCHL1 participates in preventing polyspermy from occurring in the mouse ova. Accordingly, the gracile axonal dystrophy-affected *gad*

mutant mice, expressing a mutated form of UCHL1 in their oocytes, showed increased polyspermy during IVF and reduced litter sizes *in vivo* (Sekiguchi et al. 2006). Deubiquitinating enzymes continue to be expressed after fertilization and may be required for the removal of maternal proteins which are then replaced with zygotic proteins. Both UCHL1 and UCHL3 are highly expressed in the non-human primate zygote and still observed at high levels at the 2-cell stage (Mtango and Latham 2007). Apparently, the DUBs are not only needed for removal of ubiquitin molecules from substrates docked to the 19S regulatory complex, but also contribute to anti-polyspermy defense during fertilization by allowing for normal cortical granule configuration and expulsion during oocyte activation (Mtango et al. 2011; Susor et al. 2010). This unique combination of DUB activities plays right into the thought of using the modulation of ubiquitin-proteasome pathway to improve assisted fertilization and as a means of developing a non-hormonal contraceptive.

Proteasome as a possible contraceptive target

Evidence of complete inhibition of fertilization by proteasomal inhibitors and anti-proteasome antibodies make the 26S proteasome an attractive contraceptive target, especially if one considers that it is an excellent target for pharmacological inhibitor design. Testis specific isoforms of the conjugating enzyme UBE2 and proteasomal subunits α-4 (PSMA7) and α-6 (PSMA1) have been isolated in two subgenera of

Ascidians and *Drosophila* (Belote et al. 1998; Yokota et al. 2010a; Yokota et al. 2010b), but the ubiquitinating enzymes and proteasomal subunits in mammals do not appear to be testis/germ line specific gene products. The challenge is thus to target proteasomes exclusively on the sperm surface, primarily on the OAM and AM of the sperm acrosome at different stages of the fertilization process. While anti-proteasome, anti-sperm antibodies were found in the seminal plasma of male patients suffering from autoimmune infertility, the use of autoantibodies as a non-pharmacological inhibitor may not result in measurable success (Bohring et al. 2001; Bohring and Krause 2003; Brychcy et al. 2006). An additional requirement for specifically targeting the sperm surface-associated proteasomes with pharmacological inhibitors would be avoiding cell permeability required for such proteasomal inhibitor based contraceptives to reach their respective targets without impairing protein recycling in other cells and tissues. Such contraceptive design would make an easier transition into human medicine. The reversibility of the proteasomal inhibitors would be of merit; simple discontinuation of the contraceptive would make fertilization possible immediately when chosen by the subject without the need for a recovery period as with hormonal contraceptives.

Future challenges and opportunities

The future of research on gamete proteasomes looks bright and exciting. The requirement of proteasomal proteolysis not only during the fertilization process but also

during spermatogenesis, sperm maturation and sperm preparation for fertilization is now well established but leaves many questions still unanswered. The ubiquitin-proteasome pathway will continue to intrigue fertilization researchers for years to come, whether it's the part proteasomes could play in removal of protamines as the sperm nucleus decondenses into a male pronucleus after fertilization or the fate of sperm acrosomal proteasomes deposited in the ooplasm by intracytoplasmic sperm injection. Unexpected parallels could be found between fertilization and other non-reproductive systems. Studies of the brain, for example, show that the ubiquitin-proteasome pathway malfunction contributes to Alzheimer's and Parkinson's diseases (Oddo 2008; Ross and Pickart 2004; Tanaka et al. 2004). Mutant, frame shifted ubiquitin UBB^{+1} has been discussed as a possible cause of Alzheimer's disease (van Tijn et al. 2007). Studies are under way to determine if a similar mutation could have an effect on the reproductive system, or if UBB^{+1}, a naturally occurring non-cell permeant proteasomal inhibitor, could help with fertilization studies and contraceptive design. No matter how one looks at the ubiquitin-proteasome pathway, the list of its functions throughout the entire body is almost endless. Our particular challenge will be to further characterize the involvement of this pathway in the fertilization process and to map out how its utilization in fertilization differs between species and even between individuals.

Acknowledgements

We would like to thank Ms. Kathy Craighead for editorial assistance, and our colleagues Dr. Young-Joo Yi, Ms. Miriam Sutovsky and Dr. Gauri Manandhar for their continuous support of this effort. Our work on the gamete ubiquitin-proteasome pathway has been supported by National Research Initiative Competitive Grant # 2007-01319 from the USDA Cooperative State Research, Education and Extension Service to P.S., and by seed funding from the Food for the 21st Century Program to the University of Missouri-Columbia.

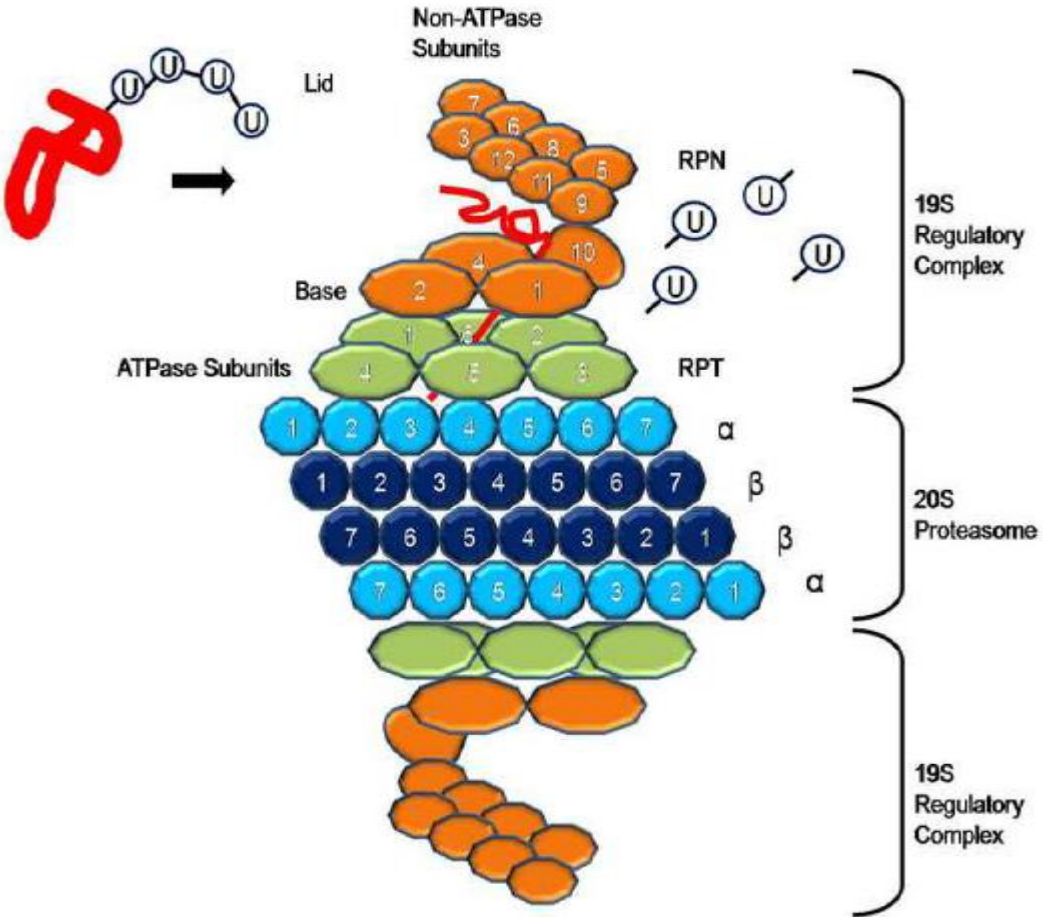

Figure 1.1: The 26S proteasome consists of the 19S regulatory complex and the 20S core, which contains two α- and two β- rings, each made of 7 subunits. Residing in the β-rings are the proteolytic sites (subunits β1/PSMB6, β2/PSMB7 and β5/PSMB5) where proteins are degraded once they enter into the core. Beside the β-rings are the α-rings that guide proteins through the core to the sites of degradation. On either side of the core resides the 19S regulatory complex; this complex recognizes proteins bound to multiubiquitin chains, removes the multiubiquitin chains and primes the substrate proteins for degradation. The 19S regulatory complex consists of a base containing ATPase subunits (RPT1-6) and a lid containing non-ATPases (RPN1-12). Recognition of ubiquitinated proteins occurs primarily through subunit RPN10; upon recognition the ubiquitin molecules are released through the recruitment of deubiquitinating enzymes to the 19S complex, and the deubiquitinated protein is unfolded and transported into the 20S core.

CHAPTER TWO

Sperm Proteasomes Degrade Sperm Receptor on the Egg Zona Pellucida during Mammalian Fertilization

Zimmerman S.W.[1], Manandhar G.[1], Yi Y-J [2], Gupta S. K.,[3] Sutovsky M.[1], Odhiambo J.F. [1], Powell M. D [4], Miller, D.J., [5] Sutovsky P.[1]

[1]Division of Animal Science, and Departments of Obstetrics, Gynecology, and Women's Health, University of Missouri –Columbia, Columbia, MO 62511; [2]Research Center for Transgenic Cloned Pigs4, Chungnam National University, Daejeon 305-764, SOUTH KOREA; [3]Reproductive Cell Biology Laboratory, National Institute of Immunology, Aruna Asaf Ali Marg, New Delhi-110 067, INDIA; [4]Morehouse School of Medicine[1], 720 Westview Dr. SW, Atlanta, GA 30310, USA; [5]Department of Animal Sciences, University of Illinois at Urbana-Champaign, Urbana, IL 61801, USA

Key words: Ubiquitin, proteasome, sperm, zona pellucida, acrosome

Short Title: Proteasomes degrade zona pellucida during mammalian fertilization

Summary sentence: Evidence of the degradation of zona pellucida glycoprotein C by proteasomes present in the sperm acrosomal matrix of porcine spermatozoa during *in vitro* culture

Reference: Zimmerman SW, Manandhar G, Yi Y-J, Gupta SK, Sutovsky M, Odhiambo JF, Powell MD, Miller DJ & Sutovsky P 2011 Sperm proteasomes degrade sperm receptor on the egg zona pellucida during mammalian fertilization. PLoS ONE 6 e17256.

Abstract

Despite decades of research, the mechanism by which the fertilizing spermatozoon penetrates the mammalian vitelline membrane, the zona pellucida (ZP) remains one of the unexplained fundamental events of human/mammalian development. Evidence has been accumulating in support of the 26S proteasome as a candidate for echinoderm, ascidian and mammalian egg coat lysin. Monitoring ZP protein degradation by sperm during fertilization is nearly impossible because those few spermatozoa that penetrate ZP leave behind a virtually untraceable residue of degraded proteins. We have overcome this hurdle by designing an experimentally consistent *in vitro* system in which live boar spermatozoa are co-incubated with ZP-proteins (ZPP) solubilized from porcine oocytes. Using this assay, mimicking sperm-egg interactions, we demonstrate that the sperm-borne proteasomes can degrade the sperm receptor protein ZPC. Upon coincubation with motile spermatozoa, the solubilized ZPP, which appear to be ubiquitinated, adhered to sperm acrosomal caps and induced acrosomal exocytosis/formation of the acrosomal shroud. The degradation of the sperm receptor protein ZPC was assessed by Western blotting band-densitometry and proteomics. A nearly identical pattern of sperm receptor degradation, evident already within the first 5 min of coincubation, was observed when the spermatozoa were replaced with the isolated, enzymatically active, sperm-derived proteasomes. ZPC degradation was blocked by proteasomal inhibitors and accelerated by ubiquitin-aldehyde (UBAL), a modified ubiquitin protein that stimulates proteasomal proteolysis. Such a degradation pattern of ZPC is consistent with in vitro fertilization studies, in which proteasomal

inhibitors completely blocked fertilization, and UBAL increased fertilization and polyspermy rates. Preincubation of intact zona-enclosed ova with isolated sperm proteasomes caused digestion, abrasions and loosening of the exposed zonae, and significantly reduced the fertilization/polyspermy rates after IVF, accompanied by en-mass detachment of zona bound sperm. Thus, the sperm borne 26S proteasome is a candidate zona lysin in mammals. This new paradigm has implications for contraception and assisted reproductive technologies in humans, as well as animals.

Introduction

Mammalian spermatozoa become fertilization-competent during capacitation in the female oviduct, a process that alters the sperm motility pattern and primes the sperm exocytotic organelle, the sperm head acrosome, for interactions with the egg zona pellucida (ZP)(Buffone et al. 2008; Yanagimachi 1994). Upon binding to the sperm receptor on the mammalian ZP (ZPC protein in the mouse or ZPB-ZPC heterodimer in the pig), the fertilizing spermatozoon undergoes acrosomal membrane vesiculation and exocytosis of the acrosomal cap, referred to as the acrosome reaction or acrosomal exocytosis (AE) (Bleil and Wassarman 1980; Yurewicz et al. 1998). This event results in the formation of the acrosomal shroud, a sperm head-enveloping cluster of acrosomal membrane vesicles and matrices that exposes the acrosome-borne proteolytic enzymes. The AE enables the spermatozoon to proceed with the formation of a fertilization slit and the penetration of the ZP (Yurewicz et al. 1998). Despite four decades of intense research, the mechanism of mammalian sperm-zona penetration remains elusive (Bedford 2008; Olds-Clarke 2003). Currently two different schools of thought interpret this major unresolved issue in developmental biology: Proponents of mechanical penetration hold that the motile force exerted from the sperm tail is sufficient to push the fertilizing spermatozoon through the ZP (Bedford 1998; Green and Purves 1984). However, physical forces generated by the sperm flagellum do not appear to fully account for sperm ability to push through the thick ZP (Green 1987). The second theory, introduced as early as 1958 by Austin and Bishop (Austin and Bishop 1958), proposes

that the fertilizing spermatozoa release an enzyme, a putative zona “lysin”, present in the sperm head acrosomal matrix (Austin 1975; Austin and Bishop 1958).

While the acrosomal protease acrosin was initially ruled out as a crucial enzyme in such a scheme (Baba et al. 1994a; Kawano et al.), the 26S proteasome has been gaining favor as a candidate mammalian, ascidian and invertebrate vitelline membrane lysin (reviewed in (Sakai et al. 2004; Yi et al. 2007a). It is hypothesized that the sperm acrosome-borne proteasomes degrade a sperm receptor protein on the ZP that becomes ubiquitinated either during oogenesis (as in echinoderms and mammals) (Sutovsky et al. 2004; Yokota and Sawada 2007) or directly by the sperm-released ubiquitination machinery during fertilization (as in ascidians)(Sawada et al. 2002). Recently, this hypothesis has been supported by yeast two-hybrid studies in which a proteasome-interacting, ubiquitin-binding protein UBAP2L has been identified as the most likely ZPC-interacting protein in human spermatozoa (Naz and Dhandapani).

Historically, it has been difficult to prove that mammalian ZP proteins and those with sperm-receptor function in particular, are degraded by the enzymes originating from the sperm acrosome during fertilization. Only one or very few spermatozoa actually penetrate ZP during fertilization and leave a virtually untraceable residue of degraded ZP proteins. We have overcome this hurdle by designing an experimentally consistent *in vitro* system (**Fig. 2.1a**) in which 10,000 live, freshly collected (never cryospreserved) and capacitated (i.e. fertilization competent) boar spermatozoa are co-incubated with ZP-proteins (ZPP) solubilized by non-degrading/non-reducing methods

from 100 meiotically mature, fertilization-competent porcine oocytes. Upon co-incubation, the soluble ZP-proteins bind to sperm acrosomal surface receptors as they would during fertilization and induce the process of acrosomal exocytosis, including the fusion of plasma and outer acrosomal membranes that results in the formation of the membrane vesicle-composed acrosomal shroud. This enables the interaction of acrosomal enzymes with ZPP. In the present study, this fertilization relevant *in vitro* assay is used to demonstrate the ability of sperm-borne proteasomes to degrade the mammalian sperm receptor on the oocyte zona pellucida.

Materials & Methods

Zona Pellucida Collection

Oocytes were aspirated using an 18 gauge needle and a 10 ml syringe from ovaries collected from a slaughterhouse (Farmland Foods, Milon, MO). Oocytes with cumulus cells were placed in 500 µl of TCM-199 media containing; FSH, LH, EGF, and follicular fluid. The oocytes remained in this media for 22 hrs, at which time they were moved into media containing no hormones for an additional 22 hrs. After maturation the cumulus cells were removed by agitation in TL-Hepes containing 0.1% polyvinylacohol (PVA) and 0.5% hyaluronidase. Oocytes were exposed to 10 µl TBS (213 mM NaCl, 50 mM Tris) pH 2.0. This solubilized the ZP and 10 µl of TBS pH 8.0 was then added to the oocytes to neutralize the solution. The solubilized zona pellucida proteins

(ZPP) were collected from the oocytes, placed in 500 µl tubes and stored in a -20°C freezer until required.

Sperm Capacitation and Fertilization In Vitro

All studies involving vertebrate animals were completed under the strict guidance of ACUC protocol number #A3394-01, approved by the Animal Care and Use Committee of the University of Missouri. Fresh boar spermatozoa were collected on the day of co-incubations. The collected spermatozoa were measured into a 15 ml Falcon tube and centrifuged at 350 x g in a Fisher Scientific Centrifuge for 5 min to remove the seminal plasma. The supernatant was removed and the pellet was resuspended in 14 ml TL-Hepes-PVA and centrifuged at 350 x g for 5 min. The sperm pellet was then resuspended in 6 ml TL-Hepes-PVA. In a new Falcon tube 30 million washed spermatozoa were added to 12 ml of capacitation media containing TL-Hepes, 11 mM glucose, 5mM pyruvic acid, and 20mg/ml BSA and capacitated for 6 hrs at 38.5˚C before being exposed to solubilized ZP. For IVF experiments, oocytes were maturated as described above, and fertilized with 500,000 sperm/ml according to a standard protocol (Yi et al. 2009c).

Sperm-ZPP Coincubation Experiments

Upon the completion of capacitation, the spermatozoa were centrifuged at 300 x g for 5 min, the supernatant was removed and the pellet resuspended in 13 ml TL-Hepes-PVA. The solution was centrifuged again at 300 x g for 5 min and the pellet was

resuspended in 6 ml TL-Hepes-PVA prior to being analyzed for final sperm concentration. New 15 ml Falcon tubes were marked for the individual groups, to these tubes 10,000 spermatozoa were added and then centrifuged at 300 x g for 5min. After removing the supernatant, appropriate amounts of TL-Hepes-PVA was added to the sperm pellets to bring the total reaction volume to 30 μl. Following the addition of TL-Hepes-PVA, the groups received either the Inhibitor cocktail containing 100 μm MG 132, 100 μm CLβL and 100 μm Epoxomicin, or vehicle solution containing 100 um EtOH, and 100 um DMSO, or ubiquitin-aldehyde at 5 μg/ml (all inhibitors were purchased from Enzo-Biomol; Plymouth Meeting, PA). Once the treatments were added to the sperm pellets, solubilized ZP protein purified from 100 oocytes was added and mixed with the sperm pellets. The incubations continued for 2 hrs at 38.5˚C and 5% CO_2 at which time the solutions were removed from the Falcon tubes, placed in 1.5 ml Eppendorf tubes and centrifuged at 300 x g for 5 min in the Sorvall Biofuge Fresco centrifuge. After centrifugation the supernatants and pellets were separated and kept for analysis of proteins by Western blotting.

Sperm Proteasome-Purification and Coincubation with ZPP

To isolate proteasomes, 30 ml of freshly collected boar semen were washed 3 times in PBS by centrifugation in a Fisher Scientific centrifuge at 350 x g for 5 min. The washed semen samples were sonicated with Branson Sonicator (Branson Ultrasonic Corp. Danbury, CT) at 30% intensity for 1 min in cold TBS (104mM NaCl, 96mM Tris, pH 7.4) supplemented with 1mM DTT, 1mM EDTA, and 10% glycerol. After sonication the

contents were separated into two 15 ml Falcon tubes and centrifuged at 300 x g for 10 min and the supernatants were collected. The supernatants were then centrifuged in Beckman centrifuge with 50.2 Ti-rotor at 100K x g for 2 hrs. The clear supernatants were collected and concentrated by additional centrifugation in 10K Centricon tubes (Millipore, Billerica, MA) at 4,000 x g until the total volume of the supernatant fractions were reduced down to 1.5 ml. The extracts were then aliquotted and stored at -80˚C. Upon being thawed, 5 μl of purified proteasomes was incubated with solubilized ZP protein from 100 oocytes either in the presence of the vehicles or the inhibitor cocktail as previously stated. The treatment groups were supplemented with 5 μM ATP.

Antibodies

The monoclonal antibody MA-467, reactive with the N-terminal domain of the peptide backbone of porcine ZPC glycoprotein and devoid of reactivity with pig ZPB by Western blotting, was generated and validated as described previously (Gupta and Gupta 1994; Gupta et al. 1993; Gupta et al. 1995). The ascites produced in inbred BALB/cj mice was used at a 1:2,000 dilution. It showed no reactivity with the related ZPB protein in ELISA and Western blotting. It also reacted with deglycosylated and reduced, and carboxyamidomethylated (RCM) forms of porcine ZPC, both in ELISA and Western blotting, thus suggesting that it reacts with the polypeptide backbone of ZPC. The epitope mapping studies using tryptic fragments of porcine ZPC followed by sequencing and mimotopes strategy revealed that MA-467 recognized the peptide corresponding to QPVWQDEGQRLR sequence (AA 23-34) of ZPC that is in the N-terminal part of the

mature, secreted porcine ZPC. Using single amino acid substitutions, the minimum binding motif was mapped to WQDE of ZPC. MA-467 also inhibited boar sperm binding to zona enclosed porcine oocytes.

Further characterization of the MA-467 revealed that prior incubation of porcine eggs with this antibody significantly delayed the time required for zona lysis by Trypsin. In Western blotting, this antibody reacted with 18 kDa band of recombinant ZPC digested with Lys-C and with the 37 and 30 kDa bands of recombinant ZPC digested with elastase. It is thus reasonable to assume that this antibody will recognize the N-terminal fragments of porcine ZPC protein produced by proteasomal proteolysis.

Mouse IgG against 20S proteasomal core subunits α1-7 (PW 8195; Enzo-Biomol) recognizes a common motif found in subunits α1 (PSMA6), α2 (PSMA2), α3 (PSMA4), α5 (PSMA5), α6 (PSMA1) and α7 (PSMA3). An anti-ubiquitin rabbit polyclonal antibody AB1690 (Chemicon, Rosemont, IL) was raised against KLH-conjugated full-length ubiquitin protein. Mouse anti-ubiquitin antibody KM691 was purchased from Kamiya Biomedical Company, Seattle, WA.

Western Blotting and Densitometry Analysis

The acrosomal shrouds containing ZP-bound proteins were separated from the sperm pellet by centrifugation at 500 x g for 5 min. The supernatant was boiled at 95°C for 5 min in 2X loading buffer containing; 100mM Tris, 300mM NaCl, 4% SDS, 10% β-mercaptoethanol, 40% glycerol, and Bromphenol Blue. Total loading volumes for the gel from the supernatants did not exceed 30 µl. Pellets from the coincubation

experiments were boiled as previously stated and then centrifuged at 3,000 x g for 10 min before loading 30 µl from each sample into a 4-20% gradient gel purchased from Lonza (Basel, Switzerland). Proteins were transferred on to PVDF membrane purchased from Millipore (Billerica, MA). Antibodies raised against ZP glycoprotein ZPC were used as primary antibodies at a 1:2,000 dilution. Primary antibody incubation occurred overnight at 4 °C, washing between antibodies was done using 1% nonfat dry milk in TBS with 0.1% Tween for 25 min. Secondary antibodies were anti-mouse IgG HRP antibody (Zymed) and were used at a 1:20,000 dilution for 40 min at room temperature in 1% nonfat dry milk in TBS /Tween. After secondary incubation, a final washing was done using TBS/Tween solution for 35 min. Antibodies raised against β tubulin (TUBB) were used as a loading control to assure equal loading between samples, and used to normalize for densitometry. The membrane was incubated in a volume of 3 ml of chemiluminescent HRP substrate for 5 min prior to being exposed to Kodak film. Differences in protein bands were determined by densitometry analysis using the Kodak 1D Image Analysis Software and Kodak films developed on the Hope micro-max developer. Statistics were performed on all three replicates by an ANOVA table.

1D Gel Proteomics of Sperm Acrosomal Fractions Coincubated with ZPP

Protein bands were excised from 1D SDS-PAGE gels stained with Coomassie Blue, followed by in-gel digestion with trypsin (Promega Gold MS grade). Peptides were partially purified by C-18 (ZIP tip) peptide clean-up prior to analysis by MALDI TOF-TOF MS & MS/MS. These results were then referenced for similarity of known porcine

proteins by using the Applied Biosystems' GPS Explorer software version 3.6 prior to being submitted for cross reference with the NCBInr mammalian protein database.

Nanospray LC-MS/MS of Zona Proteins

LC/MS/MS was also performed by first trapping the in-gel digested peptides on a C-18 CapTrap (Michrom) in 2% acetonitrile for 10 min. Peptides were then eluted onto a 0.6 x 100mm C-18 column (Agilent) using a linear 5-45% gradient of mass spectrometry grade acetonitrile (Sigma) in water (Burdick and Jackson, Honeywell) containing 0.1% formic acid (Fluka) over 80 min followed by 98% acetonitrile for 10 min and re-equilibration in 2% acetonitrile. Eluted peptides were analyzed using an LTQ ion-trap mass spectrometer running Excalibur 2.2 software. Excalibur was set to first collect a survey scan from 300 – 2000 Da followed by data-dependent scans on the top three ions. Dynamic exclusion was enabled and set for a repeat count of two, duration of 30s and a mass width of 1.0 Da. DTA generation parameters were set for a MW range of 500-4000, threshold of 200, precursor mass of 2.0Da, and a minimum ion count of 20. MS/MS spectra were then searched against an NCBInr protein database using both Proteome Discoverer 1.0 (ThermoFinnigan) and Peaks 5.2 (Bioinformatics Solutions Inc.) *de novo* search programs. Peptide mass tolerance was set at 3.0 Da and product ion tolerance was set to 0.8 Da. Variable modifications were set to include oxidation of methionine and Gly-Gly addition to lysines, fixed modifications were set to include carbamidomethylation of cysteine residues. Minimum acceptable quality peptides were set by false discovery rates of 0.05 generated from reverse database searches. At this

false discovery rate minimum acceptance criteria were: Xcorr = 1.5 sor 1+ charge, 2.2 for 2+ charge and 2.5 for 3+ charge.

Immunofluorescence and Epifluorescence Microscopy

Samples of 10 µl were taken from each sperm treatment group following the 40 min incubation with lectin PNA. Samples were placed on Super Frost microscope (Fisher) slides and covered with 22x22 Premium cover slips (Fisher). Once the cover slips were in place, clear nail polish was used to seal the edges of the cover slips. Immunofluorescence double-labeling of ZPC (see antibody details above) and ubiquitin (antibody KM691) was performed in the oocytes and zygotes as described previously (Sutovsky 2004). Slides were viewed on the Nikon Eclipse E800 microscope under the 40X magnification. Images were taken using the Nikon Cool Snap HQ camera and viewed through Metamorph Imaging Software Version 7.1.

Results

Sperm-Borne Proteasomes Degrade Solubilized Zona Proteins In Vitro

Western blot analysis of porcine sperm receptor component ZPC was conducted on the supernatant fraction which, after coincubation, contained partially degraded ZP proteins as well as acrosomal shrouds of acrosome-reacted spermatozoa. We submitted these co-incubated fractions to SDS-PAGE and Western blotting densitometry with a peptide-specific anti-ZPC antibody recognizing the N-terminal domain

(QPVWQDEGQRLR sequence; aa 23-34) of secreted porcine ZPC, and known to recognize proteolytic fragments of ZPC (Gupta and Gupta 1994; Gupta et al. 1993; Gupta et al. 1995)(see **Suppl. Fig.2.1** for zona staining with this antibody). We were thus able to trace the ZP degradation by spermatozoa (**Fig. 2.1b, c**) on a large scale (compared to fertilization). The proteolysis of ZPC was significantly inhibited in the presence of a cocktail of three specific proteasomal inhibitors, epoxomicin, clasto-lactacystin-beta lactone (CLβL) and MG132 (**Fig. 2.1b**). In turn, we accelerated the degradation of ZPC with ubiquitin-aldehyde (UBAL), a modified ubiquitin molecule that inhibits the proteasome-associated deubiquitinating enzymes, but increases proteasomal proteolytic activity (**Fig. 2.1c**). Comparison of the vehicle control group to the proteasomal inhibitor-treated group revealed a significant difference ($p<0.05$) in the density of ZPC-degradation product within the 12-19 kDa range (**Fig 2.1b**). Proteasomal inhibitors reduced the degradation product by 73% (**Fig 2.1b**). Further analysis of ZPC degradation revealed a unique, low molecular mass band of <9 kDa, present only in the UBAL-treated group (**Fig. 2.1c**).

Proteasomal Inhibitors Prevent the Breakdown of Acrosomal Shrouds Induced by Sperm Coincubation with Solubilized Zonae

Binding of soluble ZPC protein to capacitated spermatozoa in our co-incubation system was readily detectable by immunofluorescence with antibodies specific to porcine sperm receptor glycoprotein ZPC (**Fig. 2.2a**). This binding was not affected by proteasomal inhibitors, yet the proteasomal inhibitors altered the ZP-protein-induced

AE and resulted in the retention of the acrosomal shrouds on many spermatozoa (**Fig. 2.2a**). The observation that the inclusion of proteasomal inhibitors prevented the detachment and/or the disintegration of acrosomal shrouds from the ZPP-exposed sperm heads was further supported by the experiments showing lesser presence of acrosome-derived proteasomes in the supernatants in sperm-ZPP fractions coincubated in the presence of proteasomal inhibitors (**Fig 2.2b**). Sperm acrosomal status and formation of the acrosomal shrouds upon co-incubation were monitored by flow cytometry of live, ZPP-exposed and control spermatozoa in which the acrosomes were labeled with fluorescently-conjugated, outer acrosomal membrane-binding lectin PNA (Vazquez et al. 1996) (**Fig. 2.2c-e**). Patterns of acrosomal shroud labeling with PNA and their flow cytometry-measured fluorescence intensities are shown in **Fig. 2.3 a-d**.

Isolated Sperm Proteasomes Degrade Sperm Receptor ZPC in a Cell-Free System

To ascertain that the observed ZPC proteolysis was specifically due to the activity of sperm proteasomes, purified proteasomes were isolated from boar spermatozoa (see proteasome characterization data, **Suppl. Fig. 2.2**) and incubated with solubilized ZP-proteins. The reaction was supplied with energy in the form of ATP which is abundantly present and available to proteasomes in the intact boar spermatozoa (Yi et al. 2009c), but has to be supplied externally for the sustenance of isolated proteasomes. The pattern of ZPC degradation by the sperm-derived proteasomes was very similar to that observed after ZPP co-incubation with whole spermatozoa (**Fig. 2.4 a**). Also similar to whole sperm coincubation with ZP-proteins, proteasomal inhibitors reduced ZPC-

degradation by isolated sperm proteasomes by 86%, compared to vehicle group (**Fig. 2.4 b**). Furthermore, acceleration of proteasomal proteolysis with UBAL increased the density of the 12 kDa ZPC-degradation product by 23%, compared to proteasomes alone (**Fig. 2.4 b**). A time-lapse Western blotting experiment revealed a progressive degradation pattern with a most prominent degradation product observed at 30 min. of coincubation (**Fig. 2.4 c**). This degradation product was already visible after first 5 min. of coincubation (**Fig. 2.4 d**), suggesting that ZPC degradation by sperm proteasomes occurs very rapidly. No degradation products were observed in ZPP preparations incubated for up to 2 h without the addition of isolated proteasome (**Fig. 2.4 c, d**). Similar to two-hour incubation, the proteasomal inhibitor cocktail prevented the degradation of ZPC at 30 min and 1 hr after the onset of coincubation (**Fig. 2.4 e**).

Porcine Zona Proteins are Ubiquitinated

The hypothesis that sperm proteasomes are responsible for digesting a fertilization slit assumes that the target ZP-protein is already tagged with ubiquitin prior to fertilization, i.e. during oogenesis, as observed in the porcine ovarian follicles (Sutovsky et al. 2004) and also in the unfertilized sea urchin eggs (Yokota and Sawada 2007). This pattern of zona pellucida/vitelline membrane ubiquitination would be an alternative to ubiquitination of the sperm receptor by ascidian sperm exudates, observed during ascidian fertilization (Sawada et al. 2002). Therefore, we subjected the isolated porcine ZP protein to modified proteomic analysis capable of distinguishing the Gly-Gly-modification (Peng et al. 2003) characteristic of ubiquitinated proteins. Initially,

the solubilized ZP proteins isolated from porcine ovaries (Burkin et al. 2004) were subjected to affinity purification of ubiquitinated proteins using the recombinant UBA domain of ubiquitin-binding protein p62 (**Fig. 2.5 a**). A distinct protein band reactive to anti-ubiquitin antibodies was detected by Western blotting and the corresponding band from a PAGE gel was identified by MALDI-TOF mass spectroscopy as porcine sperm receptor component ZPC (**Fig. 2.5 b**), known to form the porcine sperm receptor complex by hetero-oligomerization with ZPB (Yurewicz et al. 1998). Compared to the ZPP band density in the initial protein load prior to affinity purification, the purified ubiquitinated protein band was relatively weak. This was likely due to low yield of the highly specific, low affinity purification procedure, or to the possibility that only some of the ZPP protein molecules are modified by ubiquitination. To identify the ubiquitinated internal lysine sites on porcine ZP proteins, we solubilized zonae from preselected, morphologically normal porcine metaphase-II oocytes matured *in vitro* (**Fig. 2.5c**) and subjected them to Nanospray LC-MS/MS spectroscopy. Database searches were adjusted to identify peptides containing lysine residues modified with a covalently attached di-aminoacid (Gly-Gly), which is a fingerprint of ubiquitinated internal Lys-residues (Peng et al. 2003). We found Gly-Gly modifications on all three components of porcine ZP, including ZPA, ZPB and ZPC (**Fig. 2.5d**). Such modifications were also identified in the positive control, the K-48 linked multi-ubiquitin chains, but not in the unconjugated monoubiquitin, in which ubiquitinated Lys-residues are not expected (**Fig.**

2.5d). Altogether, two different proteomic techniques found that ZPC was ubiquitinated in ZP proteins prepared using different methods.

ZPC Colocalizes with Ubiquitin on the Zona and in Corona Radiata Cells

Rather than being a homogeneous layer of extracellular matrix, porcine zona labeled with anti-ZPC antibody exhibits a bone-marrow like structure. A crisscrossed pattern of ECM cords on the surface appears to be due to uneven deposition of zona proteins in the gaps between corona radiata cells covering the zona inside an ovarian follicle (**Fig. 2.6 a, b**). It was in these cords that a most intensive overlap was observed between immunolabeled ubiquitin and ZPC protein (**Fig. 2.6 c, d; and Suppl. Fig. 2.3**). Overlapping accumulation of ZPC and ubiquitin was also observed in the cytoplasm of corona radiata cells surrounding the oocytes isolated from small/growing antral follicles (**Fig. 2.6 e**). Western blotting confirmed the presence of ZPC protein in both the zona free oocytes and in the isolated corona radiata cells (**Fig. 2.6 f**).

Proteasomal Inhibitors Protect the Proteins of Acrosomal Shroud from Degradation

In addition to actual degradation of the zona proteins, acrosomal proteasomes play a role in the process of acrosomal exocytosis (Chakravarty et al. 2008; Diaz et al. 2007; Morales et al. 2007). To determine if the proteasomal inhibitors were altering the proteolytic processing of acrosomal proteins in the capacitated spermatozoa stimulated by soluble ZP-proteins, we used 1D PAGE gels to separate the proteins from

supernatants containing acrosomal shrouds and soluble zona proteins. Based on differences in band patterns of fractions incubated with proteasomal inhibitors or with control vehicle solutions, several bands unique to these respective treatments (**Fig. 2.7**), were excised and subjected to LC-MS/MS identification. Among the identified proteins that were protected from proteasomal degradation by specific proteasomal inhibitors were Sperm Adhesion Molecule 1 (SPAM1), MFGE8 (aliases lactadherin, SED1, SP47), Zona Pellucida Binding Protein 2/ZPBP2 (alias IAM38) and a fragment of Acrosin-Binding Protein ACRBP (alias SP32). The Angiotensin I Converting Enzyme 1 Isoform 2/ACE2 was more abundant in vehicle group (**Fig 2.7).** Identified tryptic fragment sequences are shown in **Suppl. Fig. 2.4**). The same results were obtained in a repeated experiment. Most likely, these structural proteins of the acrosomal cap are degraded during AE to allow for the acrosomal membrane fusion and vesiculation of the outer acrosomal membrane.

Isolated Sperm Proteasomes Degrade Intact Zonae In Situ

The above data on proteasomal degradation of solubilized ZPC trigger expectation that isolated proteasomes would also degrade intact zonae surrounding mature, fertilization competent ova. Thus, we developed an assay in which in vitro maturing pig ova are incubated with purified, heat-activated sperm proteasomes during the last four hours of *in vitro* maturation (total 44 h of IVM). Heat activation for 20 min at 55˚C is an efficient method to activate purified proteasomes (Akopian et al. 1997; Reidlinger et al. 1997). After 4 h of coincubation, oocytes were washed, fertilized by

standard IVF and processed with antibody against ZPC (as also used for Western blotting/densitometry; see **Suppl. Fig. 2.1**), DNA stain DAPI and acrosomal shroud marker - lectin PNA-FITC. This coincubation of *in vitro* maturing ova with purified, heat-activated sperm proteasomes caused zona digestion, resulting in a striking abrasion and loosening of the zona (**Fig. 2.8 a-d**). This treatment coincided with a reduced rate of polyspermic fertilization (**Fig. 2.8 e**), which commonly occurs in porcine IVF systems. Strikingly, the rate of monospermic fertilization remained constant at ~50%, while the polyspermy rate was reduced from >30% to only 7% (**Fig. 2.8 f**). Control ova were incubated for 4 h with proteasomes that had only basal activity (they were not heat activated). Besides examining the fertilization rates of the proteasome-treated ova, groups of control and treated ova were also processed with anti-ZPC antibody immediately at the end of the 4 h coincubation. Patterns of zona digestion and abrasion similar to those seen after IVF were observed in unfertilized ova exposed to heat-activated proteasomes (**Fig 2.8 g**). Thus, it appears that the observed zona digestion was not occurring only after IVF. Altogether, this experiment demonstrates the ability of isolated sperm proteasomes to digest an intact pig zona, in addition to digesting soluble zona proteins.

Discussion

We show here for the first time that mammalian sperm proteasomes degrade ZP proteins in a coincubation system relevant to fertilization. Proteasomes purified from the acrosomal fractions as well as those carried by capacitated motile spermatozoa

were efficiently inhibited by a trio of specific proteasomal inhibitors including MG 132, CLβL, and Epoxomicin. Such an inhibition protected the solubilized sperm receptor glycoprotein ZPC from degradation during its coincubation with sperm cells or sperm proteasomes. Furthermore, ZPC degradation by sperm proteasome was accelerated by ubiquitin-aldehyde, a modified ubiquitin protein that has a stimulatory effect on proteasomal proteolysis by blocking the activity of ubiquitin C-terminal hydrolases (Guterman and Glickman 2004). The respective effects of proteasomal inhibitors and ubiquitin-aldehyde on ZPC degradation in a cell free system bear striking similarity to their action during *in vitro* fertilization. Proteasomal inhibitors block *in vitro* fertilization completely at the stage of sperm-ZP penetration (Sutovsky et al. 2004). Ubiquitin-aldehyde, in turn, stimulates fertilization overall, and causes a massive polyspermic fertilization in vitro (Yi et al. 2007b). These results provide strong support for the enzymatic hypothesis of sperm penetration through the mammalian ZP. While the entire act of fertilization may not be accounted for by the sperm associated proteolytic activity, one cannot dismiss the fact that enzymes found in the sperm acrosomal matrix are required for sperm penetration through the ZP (Green 1987). Not only are ZP proteins degraded by the sperm proteasomes in a coincubation system, but several acrosomal proteins are subject to proteasomal degradation as well. This finding explains why proteasomal inhibitors have the ability to stop acrosomal exocytosis at an early stage of its signaling cascade, i.e. upstream of calcium influx in the acrosome (Chakravarty et al. 2008; Morales et al. 2003).

The requirement of proteasomal proteolysis during sperm-ZP interactions is likely two-fold. First, the sperm acrosomal proteasomes degrade the sperm receptor protein on the ZP. This likely loosens up the structure of the ZP and is conducive to mechanical, motility-driven sperm-ZP penetration as well as to action of proteases other than 26S proteasome. Present data on proteasomal degradation/loosening of the intact porcine zonae support this interpretation. Second, sperm acrosomal proteasomes seem to degrade proteins associated with acrosomal membranes. This may lead to the formation and then to eventual breakdown of the sperm acrosomal shroud, which we have traced by flow cytometry. The formation of the acrosomal shroud may initially create a complex microenvironment consisting of zona-bound membrane vesicles, viscous acrosomal matrix and soluble as well as membrane anchored proteases and glycosidases. These enzymes may be held in place by the shroud and necessary for the digestion of the ZP surface around the leading edge of the zona-bound sperm head. Alternatively, proteasomal degradation of acrosomal zona-binding proteins, such as ACE2 and ZPBP2, observed during sperm-ZPP coincubation, could serve to terminate primary sperm-ZP binding as the ZP-bound sperm head starts to move forward and penetrate deeper into ZP. Both ACE2 and ZPBP2 have been implicated in the initial binding of the sperm acrosome to ZP (Hagaman et al. 1998; Yu et al. 2006).

The in vitro ZPC degradation assay was performed in the presence of extrinsic ATP. In somatic cells, ATP is almost exclusively intracellular. However, spermatozoa are sensitive to external ATP. Adding 2.5 mM extracellular ATP to the capacitated bull

spermatozoa stimulated acrosome reaction and increased the percentage of acrosome-reacted spermatozoa (Luria et al. 2002). Authors suggested that extracellular ATP activates a signaling cascade of acrosome reaction via ATP purinoreceptor of P_{2y} type. The addition of extracellular ATP also improved IVF results in humans (Rossato et al. 1999) and increased linear sperm motility in mice (Rodriguez-Miranda et al. 2008). The presence of extracellular, sperm-surface associated ATP was indirectly demonstrated in a free-spawning animal, sea urchin *Pseudocentrotus depressus,* via depletion of cell surface ATP by *Solanum tuberosum* apyrase, added directly to sea water with gametes. Apyrase is a large, 49 kDa enzyme that cannot penetrate the cellular plasma membrane. Consequently, it is expected to interact exclusively with the extracellular and cell-surface associated ATP when added in the fertilization medium. Therefore, similar to sea urchin fertilization, purified apyrase blocked fertilization in the porcine IVF system (Yi et al. 2009c). In these studies, sperm-surface associated ATP was measured directly by a fluorometric assay. A pool of extracellular/sperm surface ATP was found, associated with the acrosomal surface. It is plausible that ATP associated with sperm acrosomal surface can be utilized by the sperm proteasomes during fertilization. Although ATP is not required for substrate degradation in the 20S proteasomal core, it is required for maintaining the integrity of the 19S proteasomal regulatory complex, which contains six subunits with ATPase activity. In accordance, ATP depletion from boar sperm surface altered the integrity of sperm proteasomes, manifested by an altered proteasomal subunit migration on SDS-PAGE (Yi et al. 2009c).

Extracellular function of ubiquitin-proteasome pathway in mammalian gametes is unexpected in the context of general cell biology, yet the concept of extracellular ubiquitin systems has been gaining acceptance (see Reviews by (Sakai et al. 2004; Sixt and Dahlmann 2008)). Zona protein synthesis and secretion differs from species to species. While oocytes seem to be uniquely responsible for zona protein secretion in the mouse (Qi et al. 2002), localization of ZPA, ZPB, and ZPC mRNA changes with follicular stage in other mammals. Production of the canine ZP glycoprotein mRNAs starts from the oocyte cytoplasm in the primordial follicle, but gradually shifts toward adjacent cumulus cells in the growing follicle (Blackmore et al. 2004). Rabbit ZP glycoprotein ZP1 mRNA has been localized to both the oocyte and granulosa cells in primary follicles (Lee 2000). In the case of porcine oocyte-cumulus complex, both the oocyte and zona-adjacent cumulus/corona radiata cells express ZP-encoding genes (Kolle et al. 1996). Since zona deposition likely requires a high rate of ZP-protein secretion, it is possible that the zona proteins become ubiquitinated in the secretory pathway. The Endoplasmic Reticulum Associated Protein Degradation (ERAD) system is responsible for ubiquitination and proteasomal degradation of misfolded proteins in the ER, assuming that ubiquitination occurs during substrate translocation through ER membrane and proteasomal degradation occurs in the cell cytosol (reviewed by (Bagola et al.; Goeckeler and Brodsky)). Given the gaps in knowledge of ERAD mechanisms and possible limitations of ERAD efficiency in clearing defective proteins, it is possible that ubiquitinated proteins could be secreted. As such, ubiquitinated ZP-proteins could

escape degradation in the ER and be deposited in the oocyte zona. The observation that genes encoding ZP proteins appear to be expressed predominantly in the cumulus cells during the late stages of porcine oocyte/follicle growth (Kolle et al. 1996) agrees with the overlapping accumulation of ZPC and ubiquitin on the pig zona surface, and specifically in the cumulus cell cytoplasm and in the gaps between zona-adhering cumulus/corona radiata cells (see Fig. 6). Alternatively, zona proteins could be ubiquitinated after being secreted, as ubiquitin is present at a high concentration in the ovarian follicular fluid (Einspanier et al. 1993). Finally, ECM components other than zona glycoproteins are secreted by porcine oocyte and cumulus cells and bind to zona surface (Flechon et al. 2003); such ECM components could also be ubiquitinated and subject to degradation by the sperm proteasomes during fertilization.

There is now evidence that both the sperm acrosome (reviewed in (Zimmerman and Sutovsky 2009) and spermatid acrosomal cap (Rivkin et al. 2009; Tengowski et al. 2007) contain proteasomes. While the association of proteasomes with an organelle that ultimately undergoes exocytosis may appear unusual in the context of somatic cells, it is not uncommon for gametes to utilize cellular pathways such as the secretory pathway in an unorthodox manner. The sperm acrosome itself is a fitting example. Acrosomal membranes (outer and inner) and matrix are derivatives of trans-Golgi in a spermatid, but the secretory vesicles detaching from the spermatid are not docked to the inner face of the plasma membrane (Moreno and Alvarado 2006), as would be the case in somatic cells. Instead, they are directed toward the nucleus where they attach to

a specialized structure referred to as subacrosomal perinuclear theca, or acroplaxome. At this stage, the anchoring of proteasomes is already observed on the cytoplasmic face of the membranes of the future acrosomal cap (Rivkin et al. 2009).

While both *in vitro* fertilization (Sutovsky et al. 2004) and ZP-protein degradation (this study) is efficiently blocked by proteasomal inhibitors, consideration should be given to other proteases that may facilitate acrosomal exocytosis and sperm-zona penetration in mammals. Conventional protease inhibitors have been shown to prevent sperm penetration through the zona pellucida (Olds-Clarke 2003), though some of this inhibition may be due to an undetected inhibitory effect on sperm proteasomes. However, several acrosomal enzymes not related to proteasome, such as serine proteases ACR (acrosin) and PRSS21 (TESP5) may participate in the processing of the sperm acrosomal matrix and sperm penetration through the egg zona, resulting in fertilization (Baba et al. 1989; Honda et al. 2002b; Sutovsky et al. 2004). For instance, the male *Acr*-null mice are fertile but exhibit delayed AE during fertilization *in vitro* (Baba et al. 1994a) and the *Acr-Prss21* double-knockout mice are subfertile *in vivo,* and their sperm are unable to fertilize eggs *in vitro* (Kawano et al. 2010).

Collectively, our results validate the hypothesis that the sperm acrosome-borne 26S proteasomes recognize and degrade ubiquitinated zona pellucida proteins during mammalian fertilization. Such data point to evolutionary conservation of the proteasome-dependent mechanism adopted by animal spermatozoa for vitelline coat penetration: The sperm receptor on ascidian egg coat, called HrVC70, that is degraded

by sperm proteasomes during ascidian fertilization is in fact the ascidian homologue of mammalian sperm receptor ZPC (Sawada et al. 2002), shown to be targeted for proteasomal degradation in our coincubation system. Our findings have many implications for assisted fertilization in humans and animals. Simple, rapid methods for measuring of proteasomal activities in human and animal sperm samples using specific fluorometric substrates (e.g. (Yi et al. 2007b; Yi et al. 2009c)) could be adapted for male fertility testing in farm animals and for diagnostics of human male infertility. Since the proteasomes are uniquely exposed on the cell surface in human, pig, mouse and ascidian spermatozoa (Lambert et al. 2002; Morales et al. 2003; Pasten et al. 2005; Sakai et al. 2004; Sawada et al. 2002), they could be targeted to elicit a contraceptive effect by antibodies and proteasome-inhibiting molecules other than cell-permeant proteasomal inhibitors, which would likely exhibit side effects. Coincidentally, anti-proteasome antibodies are found among anti-sperm antibodies present in seminal plasma of men suffering from autoimmune infertility (Bohring and Krause 2003). Searching for possible immunocontraceptive targets in human spermatozoa by using yeast two-hybrid system, Naz and Dhandapani (Naz and Dhandapani) recently identified the ubiquitin-binding, proteasome-associating protein UBAP2L as the most likely binding partner of human ZPC protein. Furthermore, antibodies against UBAP2L inhibited human sperm-zona binding in a hemizona assay (Naz and Dhandapani).

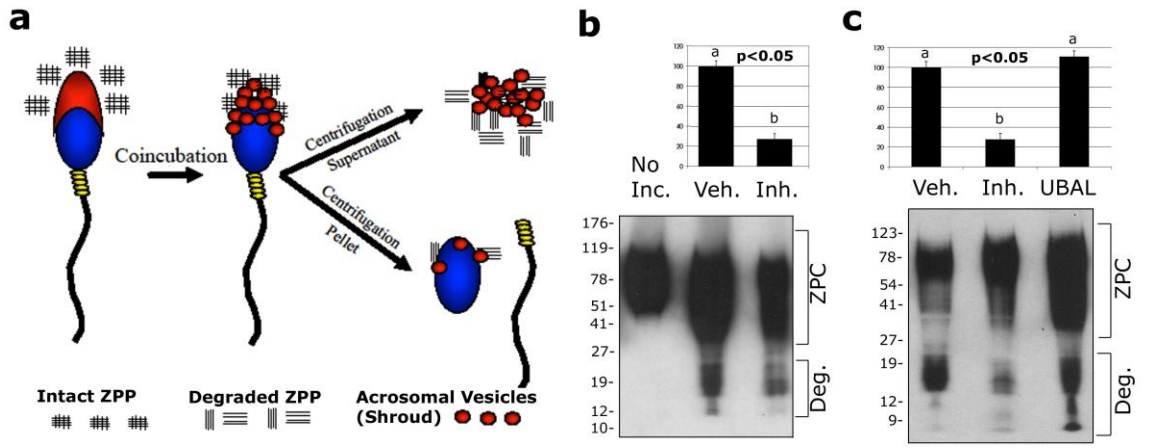

Fig. 2.1. Acrosome-borne 26S proteasomes degrade sperm receptor protein ZPC, solubilized from mature oocytes' zonae. (**a**) Diagram of the experimental setup in which the ZP-proteins (ZPP), solubilized by non-degrading/non-reducing methods from 100 meiotically mature, fertilization-competent porcine oocytes, were coincubated for 2 h with 10,000 capacitated boar spermatozoa. Each lane in the Western blots shown in panels b & c represent this number of gametes/proteins. The ZPP binding induced acrosomal exocytosis, enabling the separation of ZPC and sperm proteasome-containing acrosomal shrouds from the exocytosed spermatozoa. (**b**) Western blotting of ZPC in these co-incubated fractions detected a low mass degradation product ("Deg." bracket), which was present in the coincubated fraction after 2 h ("Veh." lane) or after 2 h of coincubation in the presence of a proteasomal inhibitor cocktail composed of epoxomicin, clasto-lactacystin-beta lactone (CLβL) and MG132 ("Inh." lane), but not detectable in the ZPP fraction prior to coincubation ("No Inc." lane). Densitometry revealed a statistically significant reduction (73% over the vehicle lane) in the density of the measured ZPC-degradation product (data from three replicates). (**c**) Accelerated degradation of ZPC was accomplished with the addition of ubiquitin-aldehyde (UBAL), a modified ubiquitin molecule that increases proteasomal proteolytic activity. Note a unique, low molecular mass band of <9 kDa that is prominent in the UBAL lane.

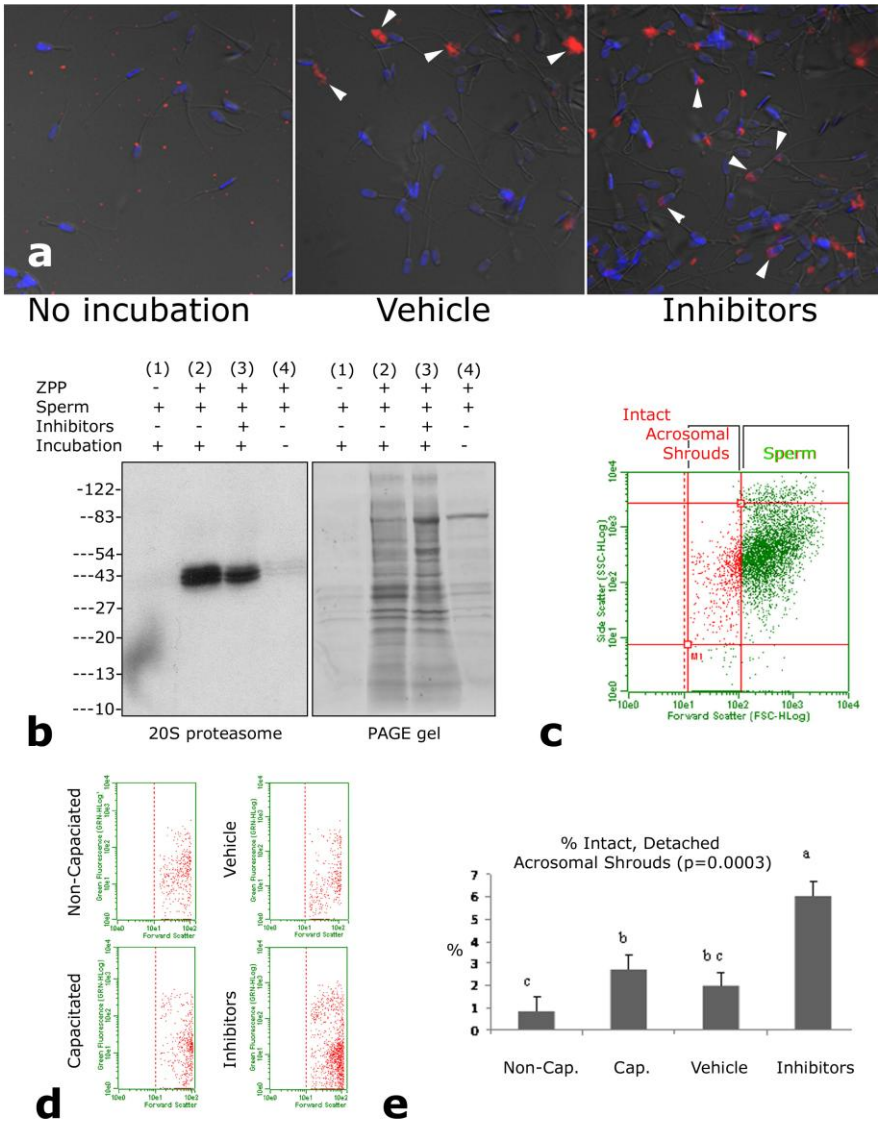

Fig. 2.2. Soluble ZPC protein binds to capacitated spermatozoa and triggers acrosomal exocytosis and separation of the acrosomal shrouds. (**a**). Immunofluorescence of sperm receptor protein ZPC (red) immediately after ZPP-sperm mixing (left), after 2 h of incubation (center; note the detached acrosomal shrouds-arrowheads) and after 2 h incubation with proteasomal inhibitors (right; arrows point to sperm with attached shrouds). (**b**). Addition of proteasomal inhibitors to sperm-ZPP coincubation limited the release of acrosomal proteasomes. Supernatant fractions (left panel) were collected from 10,000 sperm prior to mixing with ZPP (lane 1), after 2 h of coincubation (lane 2; appropriate vehicles were present), after 2 h co-incubation with proteasomal inhibitors added (lane 3) and immediately after sperm-ZPP mixing. Proteasomes were detected with a monoclonal antibody against alpha-type 20S proteasomal core subunits. The right panel shows the corresponding residual PAGE gel after protein transfer, confirming comparable protein loads between vehicle and inhibitor lanes (lanes 2&3). Lanes 1 and 4 contain only a small amount of protein because of limited acrosomal exocytosis. (**c-e**) Sperm acrosomal status and the formation and detachment of acrosomal shrouds upon co-incubation were monitored by flow cytometry of live spermatozoa in which the acrosomes were labeled with fluorescently-conjugated lectin PNA. (**c**) Gating of detached acrosomal shrouds (red dots) from spermatozoa (green dots) in scatter diagrams from flow cytometry of sperm-ZPP fractions. Each dot represents one flow cytometric event, a shroud or a sperm cell (2,000 events/fraction). (**d**) Number of intact acrosomal shrouds, gated in visible light scatter, is increased by addition of proteasomal inhibitors (lower right panel) to coincubation, compared to control sperm-ZPP fraction (upper right), and sperm fractions prior to (upper left) and after capacitation (upper right), not exposed to ZPP. A degree of spontaneous acrosomal exocytosis is expected during capacitation. (**e**) Percentage of detached acrosomal shrouds in the coincubation fraction (i.e. ratio of red dot-events to all events in the scatter diagrams gated on acrosomal shrouds), was increased significantly (ANOVA; $p<0.05$) by the addition of proteasomal inhibitor cocktail for the duration of sperm-ZPP coincubation.

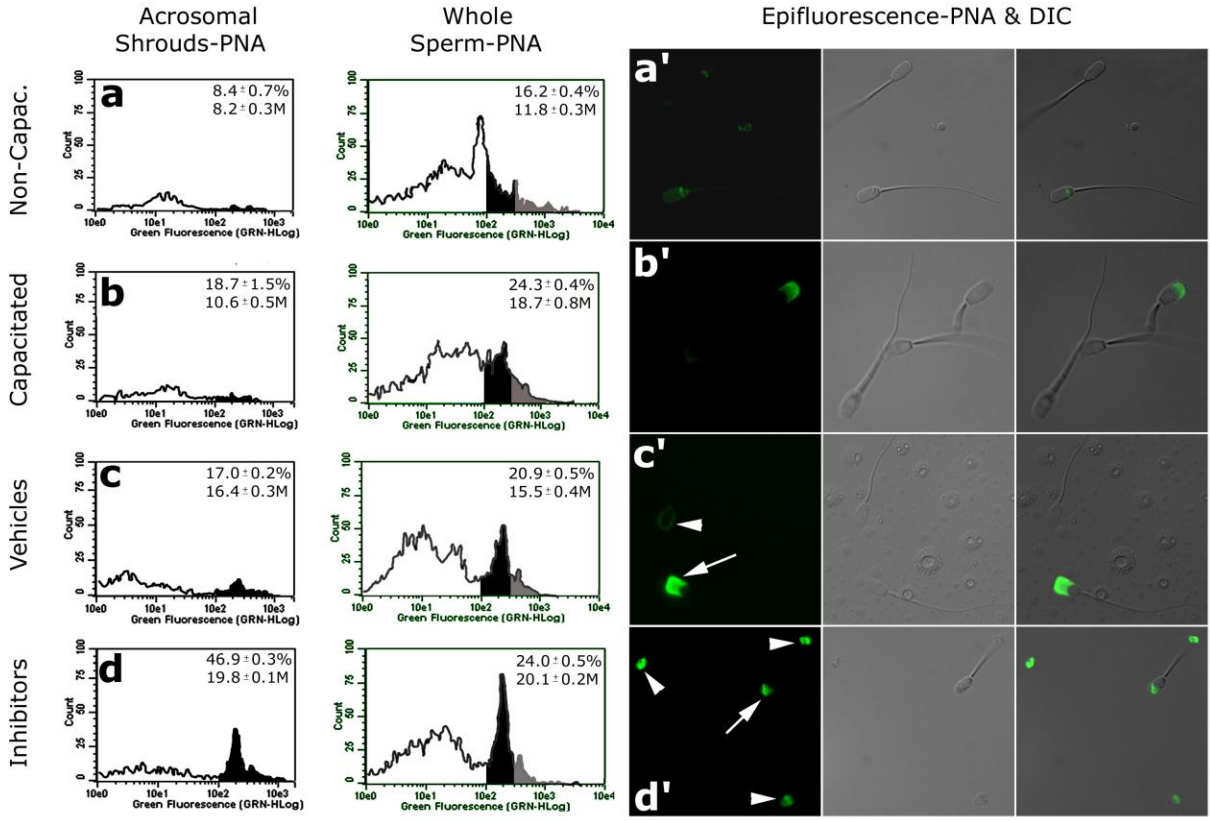

Fig. 2.3. The ZPP-induced formation, detachment and breakdown of acrosomal shrouds traced by flow cytometry and epifluorescence microscopy with lectin PNA-FITC**.** Lectin PNA binds to terminal β-galactose residues of disaccharides present on the outer acrosomal membrane (OAM), which is concealed in the non-capacitated spermatozoa, partially exposed in the capacitated ones and completely exposed during acrosomal exocytosis, which encompasses the vesiculation of OAM, and formation and eventual breakdown of the acrosomal shroud. During fertilization, the shroud remains attached to egg coat surface, forming a viscous cloud around the penetrating sperm head (Yanagimachi 1994). In a cell free system with live sperm and soluble ZPP, the shrouds eventually detach from the sperm heads of capacitated, ZPP-exposed spermatozoa and disintegrate, unless proteasomal inhibitors are included in coincubation mixture. The flow cytometric histograms of 5,000 cells/events per sample show an average from two replicates for the percentage of highly fluorescent cells (%-value; mean±SE) corresponding to the shadowed area of the histogram, and the median fluorescence of all flow cytometric events in the entire sample (M-value; mean±SE). Histograms of relative PNA-fluorescence are shown separately for gated acrosomal shrouds detached from sperm cells (left histogram column) and for the entire sample, including sperm cells and detached acrosomal shrouds (right histogram column). (**a**) The relative fluorescence of PNA is low prior to capacitation, in flow cytometer and by epifluorescence, because the OAM is concealed under sperm plasma membrane and not exposed for PNA-binding. (**b**) Fluorescence increases during capitation because OAM becomes exposed in the capacitated spermatozoa (Buffone et al. 2008); yet other spermatozoa undergo spontaneous acrosomal exocytosis. (**c**) Fluorescence level retreats back after sperm-ZPP coincubation under control conditions (only vehicles for proteasomal inhibitors were added) because the acrosomal shrouds detach from the spermatozoa and disintegrate. Most spermatozoa in this treatment show only the residual PNA binding to the newly exposed inner acrosomal membrane of the exocytosed spermatozoa (arrowheads); other spermatozoa are still in the process of exocytosis (arrow). (**d**) In the inhibitor group, fluorescence is even higher than in capacitated spermatozoa because proteasomal inhibition prevents the disintegration of acrosomal shrouds, whether still attached to sperm heads (arrow) or detached (arrowheads).

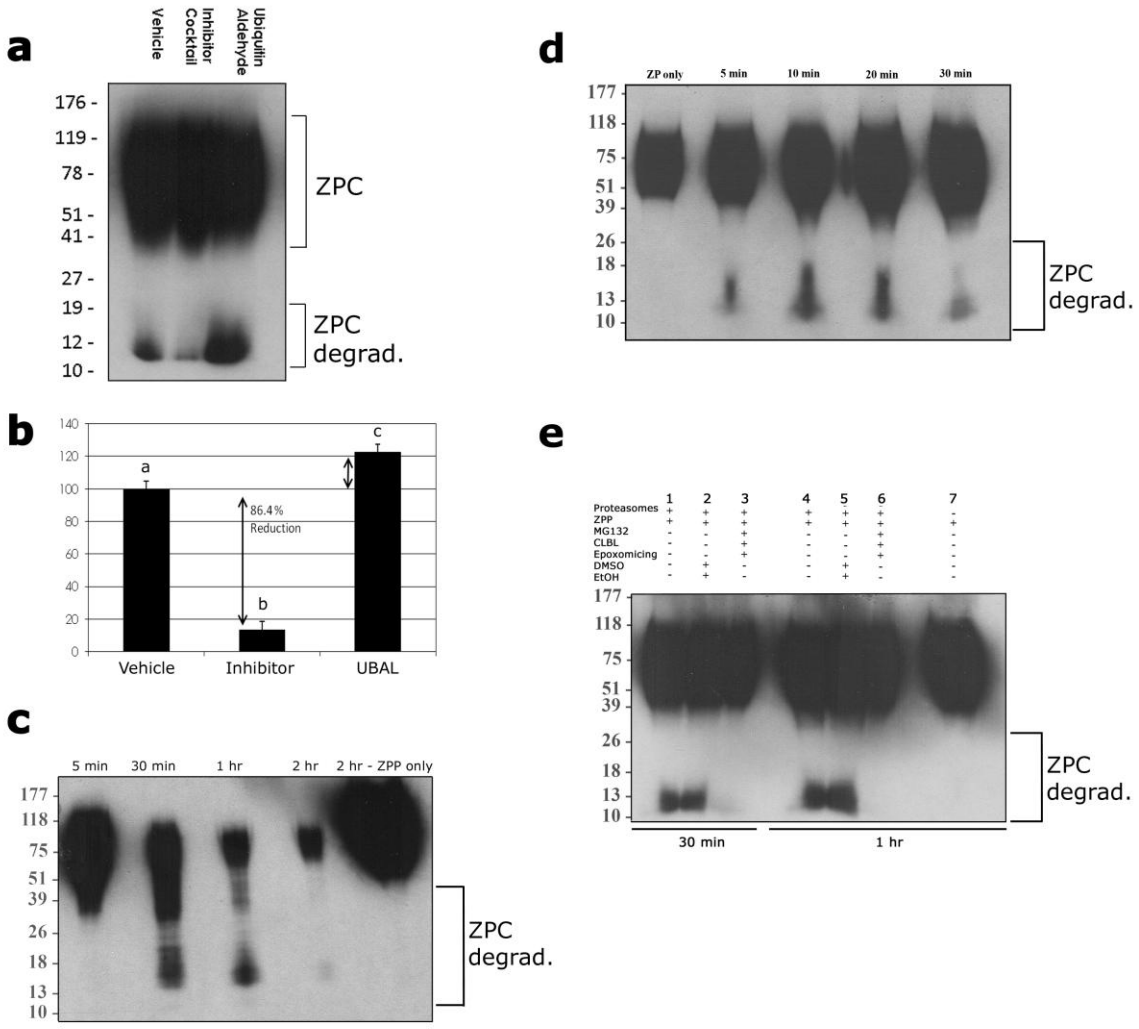

Fig. 2.4. *Proteolysis of ZPC in the presence of isolated sperm acrosomal proteasomes is similar to that in live sperm-ZPC coincubation-fractions.* (**a**) Western blot of coincubated fractions with anti-ZPC antibody. After two-hours of ZPP-sperm proteasome co-incubation, a familiar degradation product appears (vehicle lane), which is reduced by the addition of proteasomal inhibitors (Inhibitor Cocktail lane), and amplified by the stimulation of proteasomal activity with ubiquitin aldehyde (UBAL lane). (**b**) Densitometry data from three replicates (lower panel) averaged 86% reduction ($p<0.002$) in the presence of proteasomal inhibitors, and a 23% acceleration ($p<0.01$) of proteasomal proteolysis with UBAL. (**c**) Time-lapse Western blotting of ZPC, revealing the progress of ZPC degradation during zona-protein coincubation with sperm proteasomes. No degradation products were observed in ZPP preparation incubated for 2 h without addition of isolated proteasome (last lane). (**d**) Thirty-minute time lapse of sperm-ZPC coincubation, revealing the formation of degradation product as early as 5 min. after ZPC-proteasome mixing. (**e**) Replicate of the two-hour time lapse experiment with isolated sperm proteasomes and solubilized zona proteins (ZPP), with/without addition of proteasomal inhibitor cocktail (MG132, CLBL & epoxomicin), which eliminated the degradation of ZPC at 30 min (lanes 1-3) and 1 hr (lanes 4-7) after the onset of coincubation. Vehicles (DMSO, EtOH; lanes 2 &5) had no effect on degradation of ZPC; ZPP incubation for up to 1hr without addition of proteasomes (lane 7) did not produce a detectable degradation product.

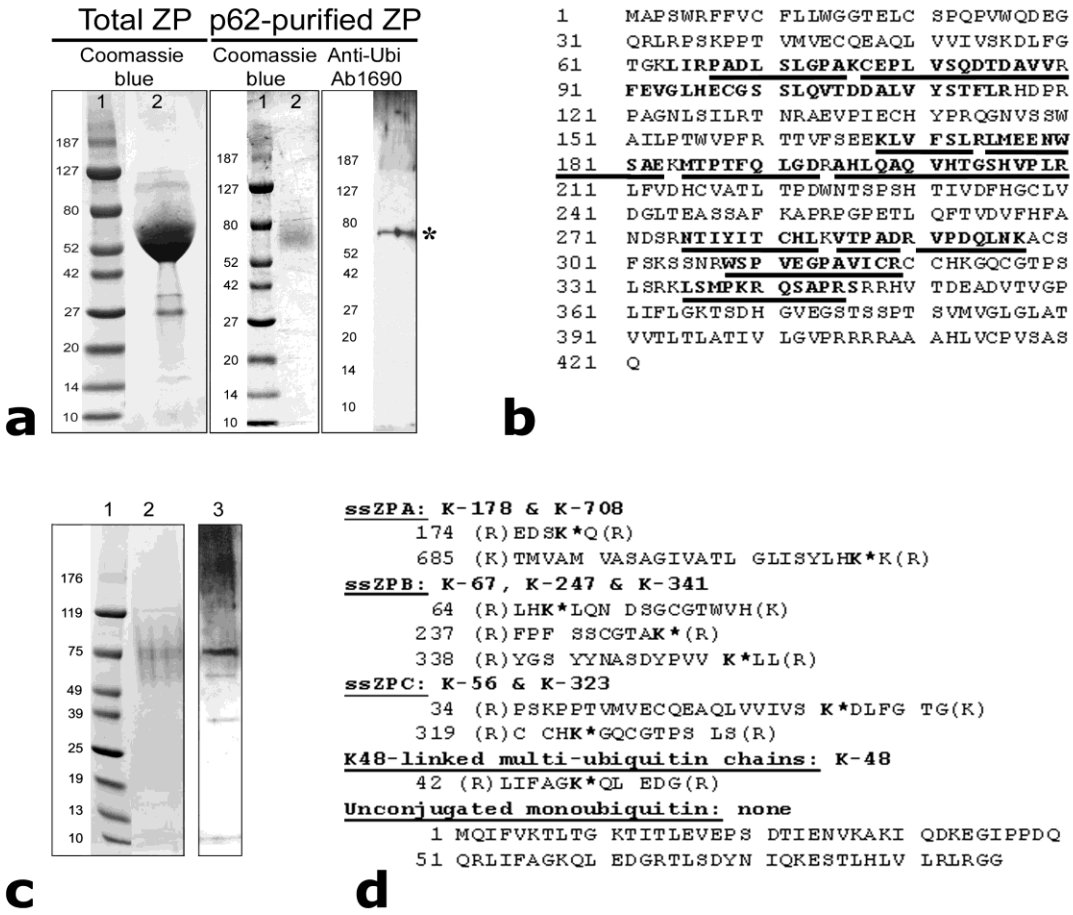

Fig.2.5. Porcine zona pellucida proteins are ubiquitinated prior to fertilization. (**a**) Zona pellucida fragments separated from minced porcine ovaries were solubilized (Left; Coomassie-stained PAGE gel-lane 2; lane 1=protein markers), and subjected to affinity purification of ubiquitinated proteins using the recombinant UBA domain of ubiquitin-binding protein p62 (center; PAGE gel, lane 2). The protein band between 70-80 kDa was reactive to anti-ubiquitin antibodies (Right; Western blot). (**b**) This band was excised and identified by MALDI-TOF MS as porcine sperm receptor component ZPC (identified fragments are underlined). (**c**). Ubiquitinated proteins from solubilized zonae from preselected, morphologically normal porcine metaphase-II oocytes were affinity purified on p62 matrix (lane 2; PAGE) and showed immunoreactivity to anti-ubiquitin antibodies (lane 3; Western). (**d**) Soluble proteins isolated by p62 affinity-purification were subjected to Nanospray LC-MS/MS spectroscopy adjusted for Gly-Gly modification, a fingerprint of ubiquitinated internal Lys-residues. Gly-Gly modifications were observed on all three components of porcine ZP, including ZPA, ZPB and ZPC, and in the positive control, the K-48 linked multi-ubiquitin chains, but not in the unconjugated monoubiquitin.

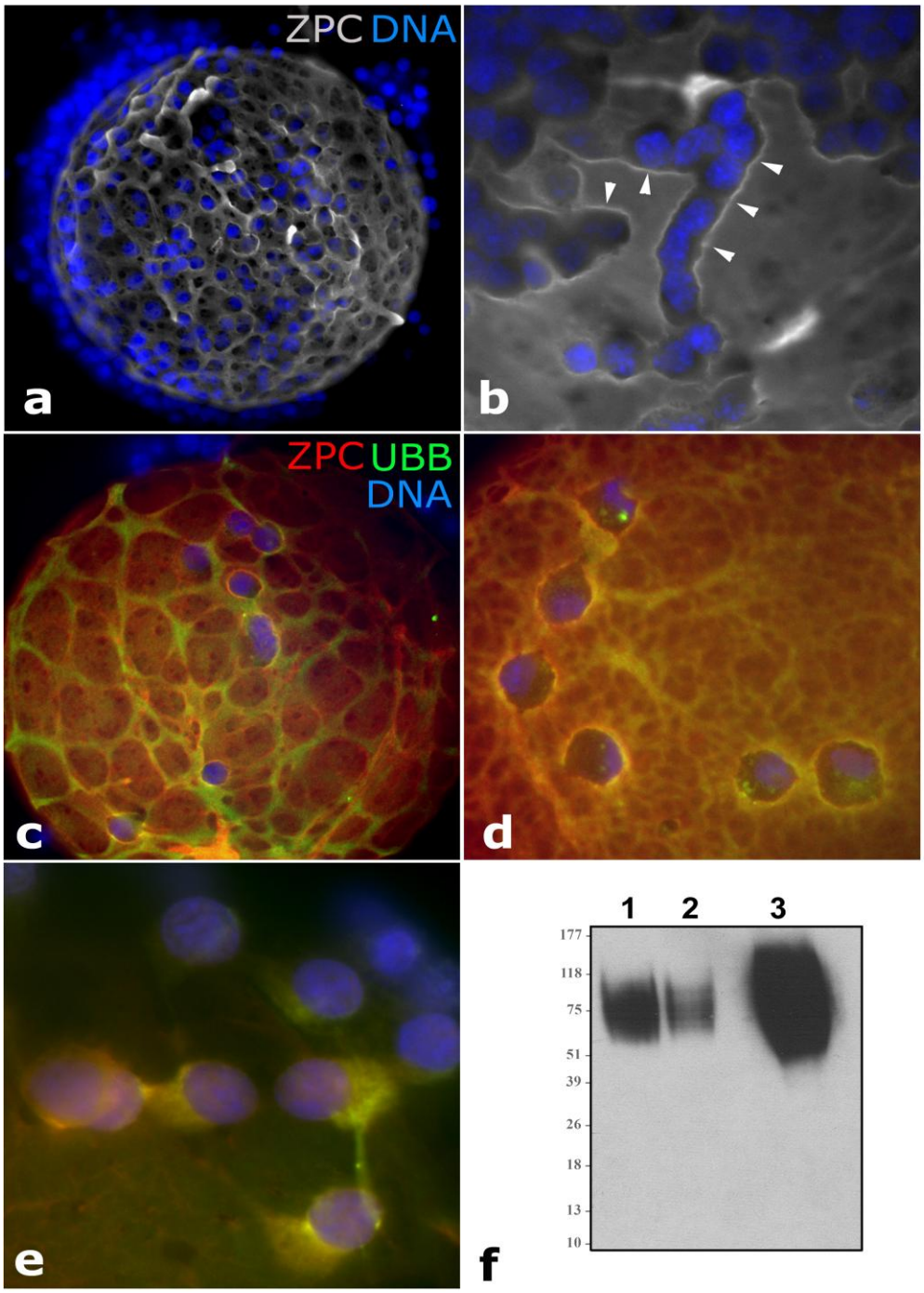

Fig. 2.6. Patterns of zona pellucida deposition and ZPC-ubiquitin colocalization in porcine oocyte-cumulus complexes isolated from small antral follicles. (**a, b**) Accumulation of ZPC (gray) in ridges (arrowheads) adjacent to zona-adhering corona radiata cells (blue = nuclei stained with DAPI). (**c-e**) Colocalization of ZPC (red) and ubiquitin (green) in the zona pellucida (c, d) and in the cytoplasm of corona radiata cells (e); DNA was counterstained with DAPI (blue). Western blotting of ZPC protein in the isolated cumulus/corona cells from 60 oocyte cumulus complexes (lane 1), in 60 zona-free oocytes (lane 2) and in soluble zona proteins isolated from 60 oocytes (lane 3).

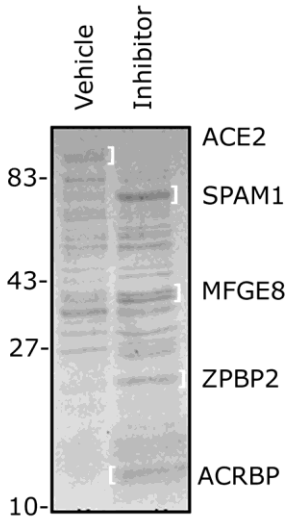

Fig. 2.7. Proteasomal inhibitors protect sperm acrosomal surface-associated proteins from degradation during ZPP-induced acrosomal exocytosis. Sperm-ZPP supernatants containing acrosomal shrouds and soluble/shroud bound zona proteins after 2 h of sperm-ZPP coincubation were separated on 1D PAGE gels. Bands that differed between vehicle control-fraction (left lane) and inhibitor fraction (right lane) were excised and subjected to LC-MS/MS identification. All of the identified proteins are known to be acrosomal components. ACE2 was the only protein diminished in the inhibitor-exposed fraction.

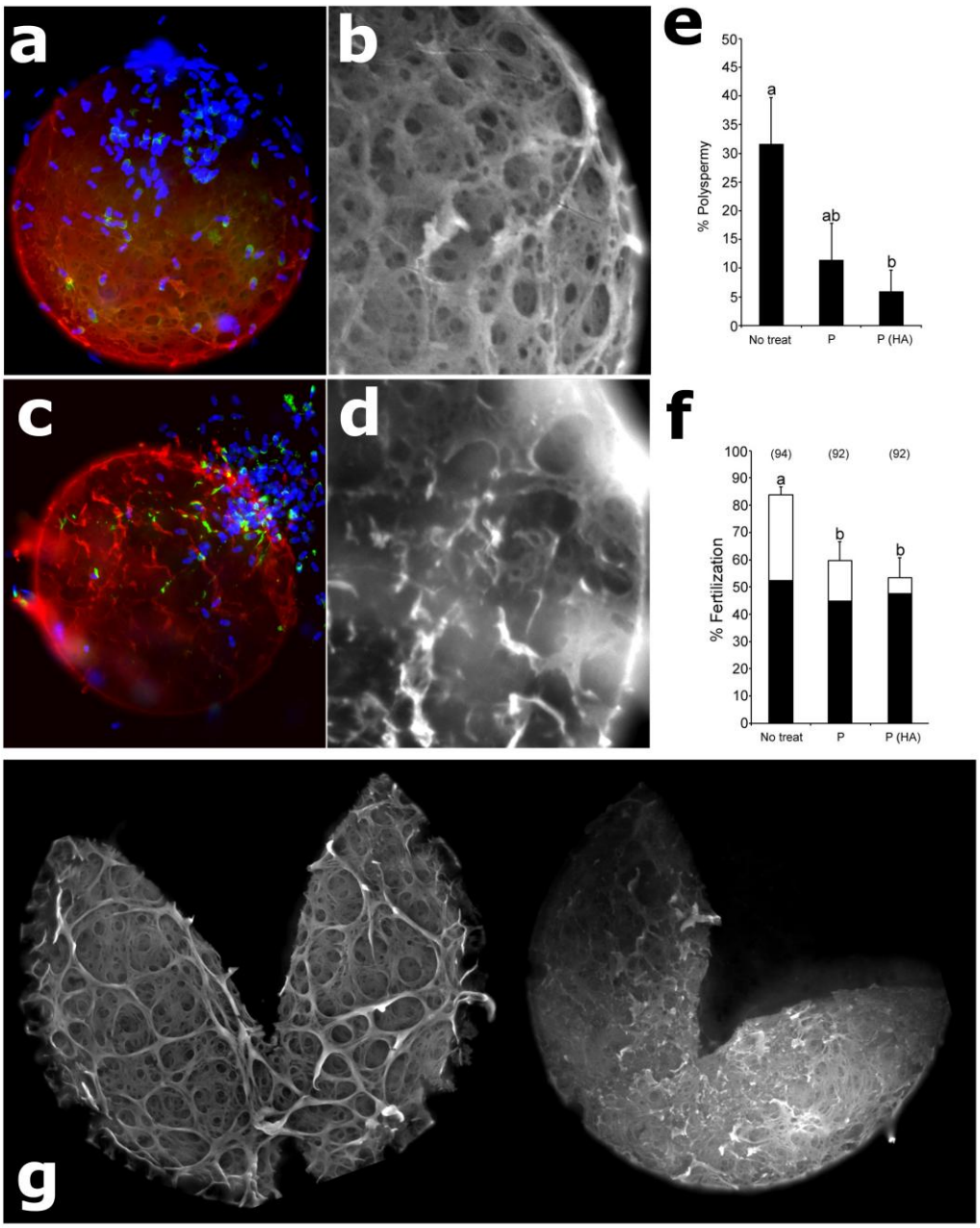

Fig. 2.8. Degradation of Intact Oocyte Zonae by Isolated Sperm Proteasomes. Maturing ova were incubated with purified, heat-activated sperm proteasomes for four hours with non-activated (**a, b**) or heat activated (**c, d**) sperm proteasomes, fertilized in vitro, and processed with anti-ZPC antibody (red), DNA stain DAPI (blue) and acrosomal shroud marker - lectin PNA-FITC (green). Note sperm detachment, and a striking abrasion and loosening of the zona in the active proteasome-treated ova (**c, d**). Preincubation with active proteasomes coincides with a reduced rate of polyspermic fertilization after IVF (**e, f**). IVF experiment was repeated three times, with total oocyte numbers shown above each column in panel **f**. Control (**g**; left) and proteasome treated (**g**; right) ova were also processed with anti-ZPC antibody immediately at the end of the 4 h coincubation, causing a pattern of zona digestion and abrasion (right zona) similar to that seen in IVF ova pre-treated with active proteasomes.

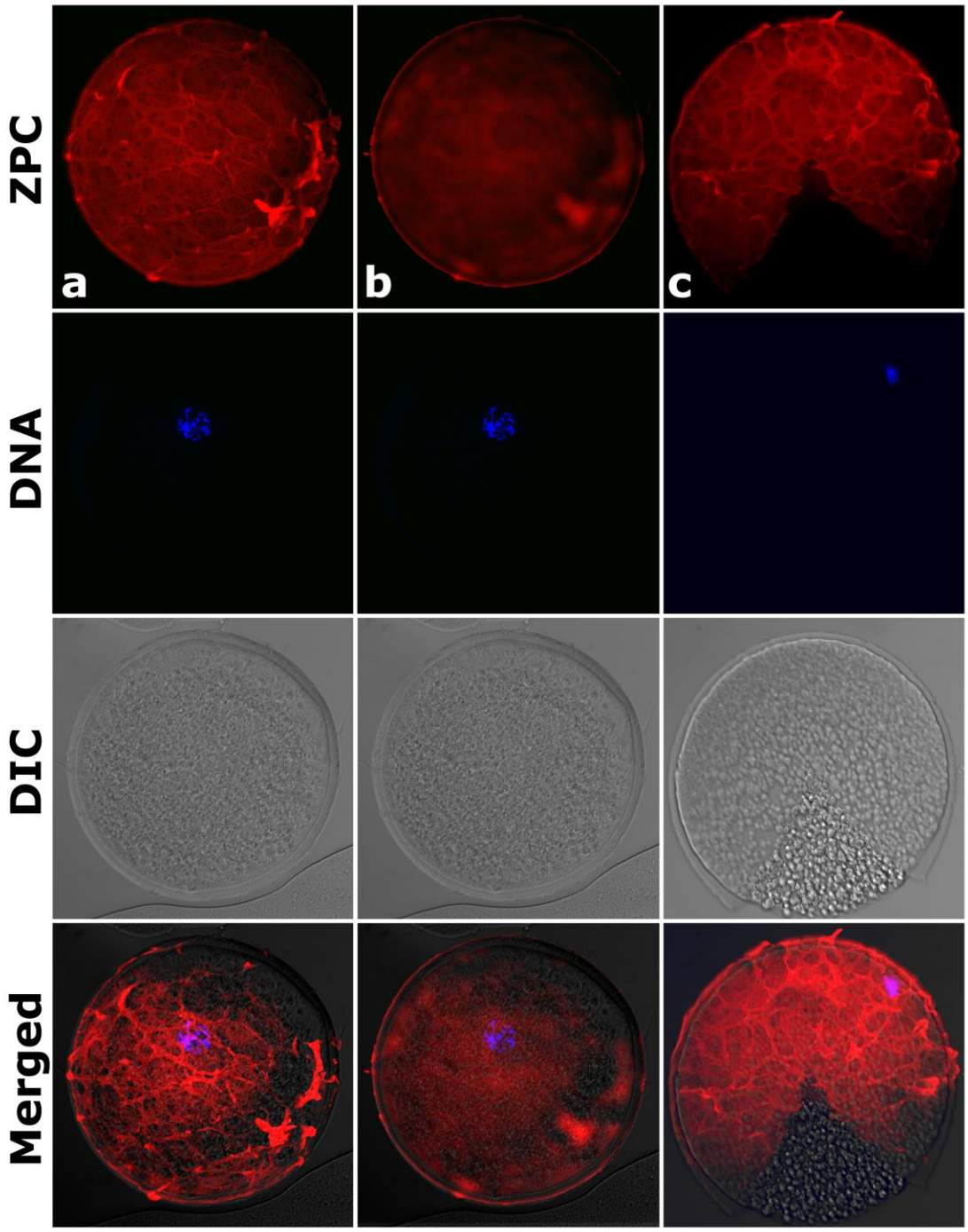

Supplemental Fig. 2.1. Immunolabeling of porcine ZP with anti-ZPC antibody MA-467, as also used for Western blotting. A representative, mature, metaphase II-stage oocyte is shown on an optical cross section across the equatorial plane (**a**) and surface plane (**b**). An oocyte with a cracked ZP is also shown (**c**) to demonstrate the difference between the fluorescence intensity of the ZP and the ooplasm, exposed by the crack.

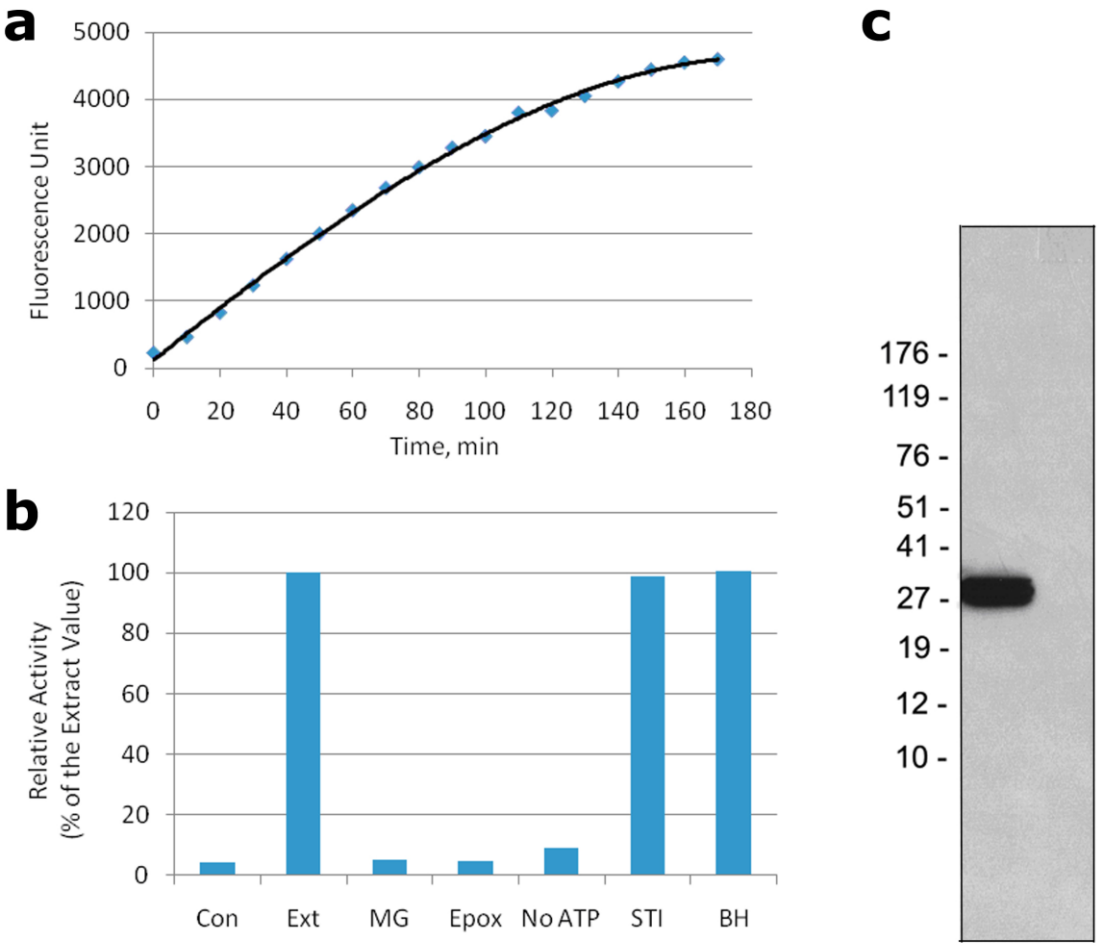

Supplemental Fig. 2.2. Isolation and characterization of the sperm acrosomal proteasomes. (**a**) Proteasomal activity of the purified sperm acrosomal proteasomes is demonstrated by time-dependent digestion of a specific fluorometric proteasomal substrate LLVY-AMC (chymotrypsin-like activity of the 20S proteasomal core) in a fluorometric 96-well plate assay. The reaction mixture containing 50 mM Tris, 5 mM $MgCl_2$, 1 mM EDTA, 1 mM DTT, 2 mM ATP and 100 µg of the sperm proteasome extract were prepared in Eppendorf tubes and then mixed with 100 µM LLVY-AMC (Biomol, www.enzolifescience.com). After vortexing, 200 µL of the mixture were quickly transferred to a 96-well plate and reaction product was measured in Fluoroskan Ascent late reader (Thermo Fisher Scientific Inc., www.thermo.com) at 380/460 nm wavelength, at 37^0C. The reaction progressed linearly for 2 hours, pattern typical of the said 20S core activity. (**b**) Effect of ATP, which is necessary for proteasome sustenance, and proteasomal and non-proteasomal protease-inhibitors on LLVY-AMC substrate digestion by the sperm proteasome. The reaction mixtures were prepared as described above. Inhibitors were added to the reaction mixtures before adding the substrate. Final concentrations of the inhibitors were 10 µM MG132 (MG; proteasomal inhibitor), 10 µM Epoxomicin (Epox; proteasomal inhibitor), 10 µg/ml Soybean trypsin inhibitor (STI), 1 mM benzamidine hydrochloride (Tantibhedhyangkul et al.). LLVY-AMC digestion was inhibited to the control level (Arcelay et al.) by MG132 and epoxomicin, or in the absence of ATP (No ATP), whereas non-proteasomal serine protease inhibitors, STI and BH did not show any effect (compared with the enzyme activity of the control, vehicle treated extract - Ext). (**c**) Western blotting of isolated sperm proteasomes. The extract was electrophoresed in 4-20% Tris-glycine gradient gels (PAGEr, www.lonza.com) , transferred and detected with an anti-proteasome antibody (Biomol, PW8195; www.biomol.com) recognizing a conserved motif of subunits α1-7 of the 20S core, by following the standard protocol. The extract showed the anticipated specific reaction at 27-29 kDa, verifying the presence of 20S α-subunits which migrate together on SDS-PAGE.

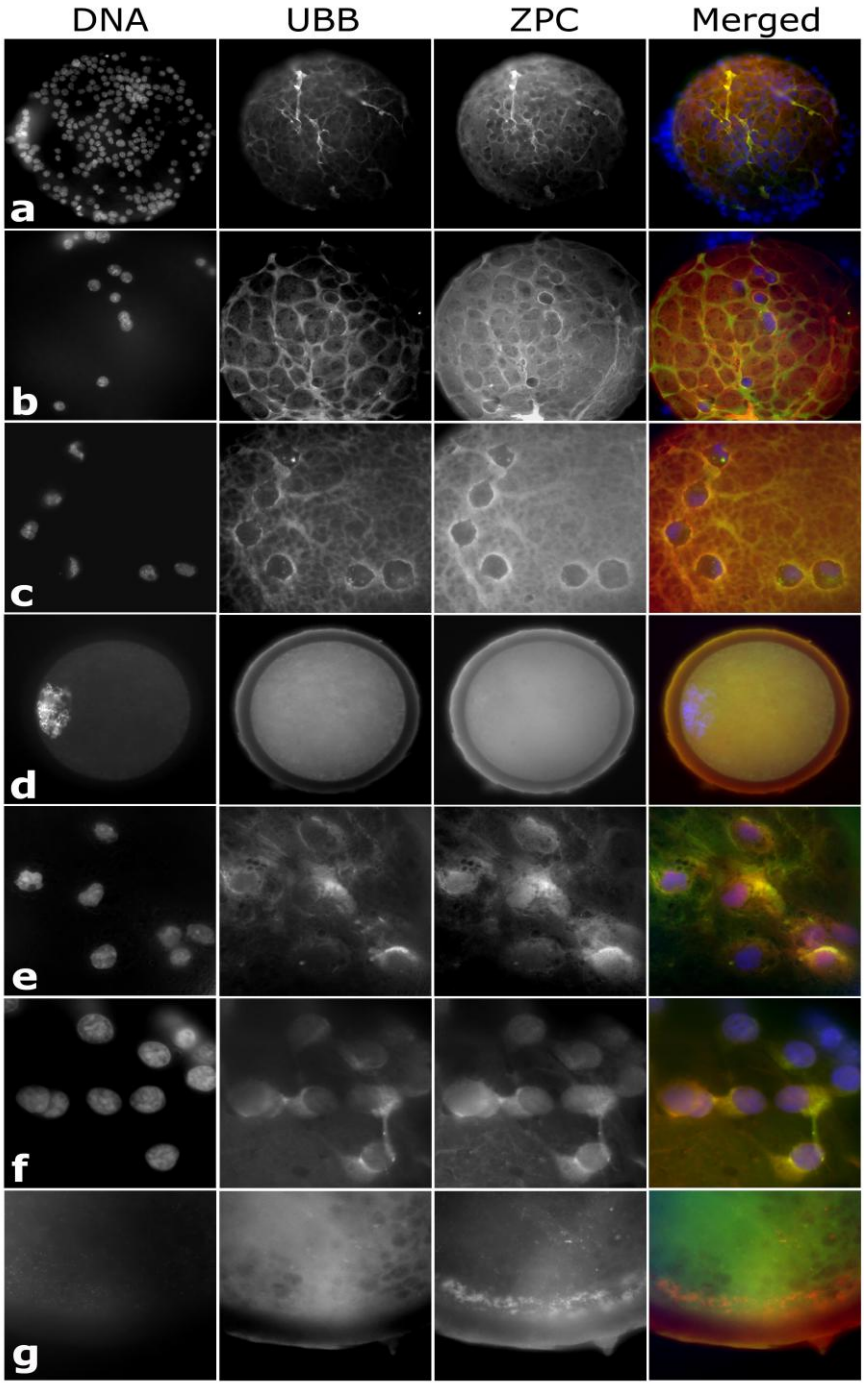

Supplemental Fig. 2.3: Duplicate colocalization of ubiquitin (UBB: green in merged images) with ZPC protein (ZPC; red in merged images) in growing porcine oocytes and cumulus cells. Oocytes were isolated from small/growing antral follicles (**a-c**), and from preantral follicles (**d**). Cumulus/corona radiata cells (**e, f**) are shown on the zona surface of oocytes isolated from small antral follicles. (**g**) Accumulation of ZPC in the cortex of an oocyte isolated from an atretic follicle. DNA was counterstained with DAPI (blue in merged images).

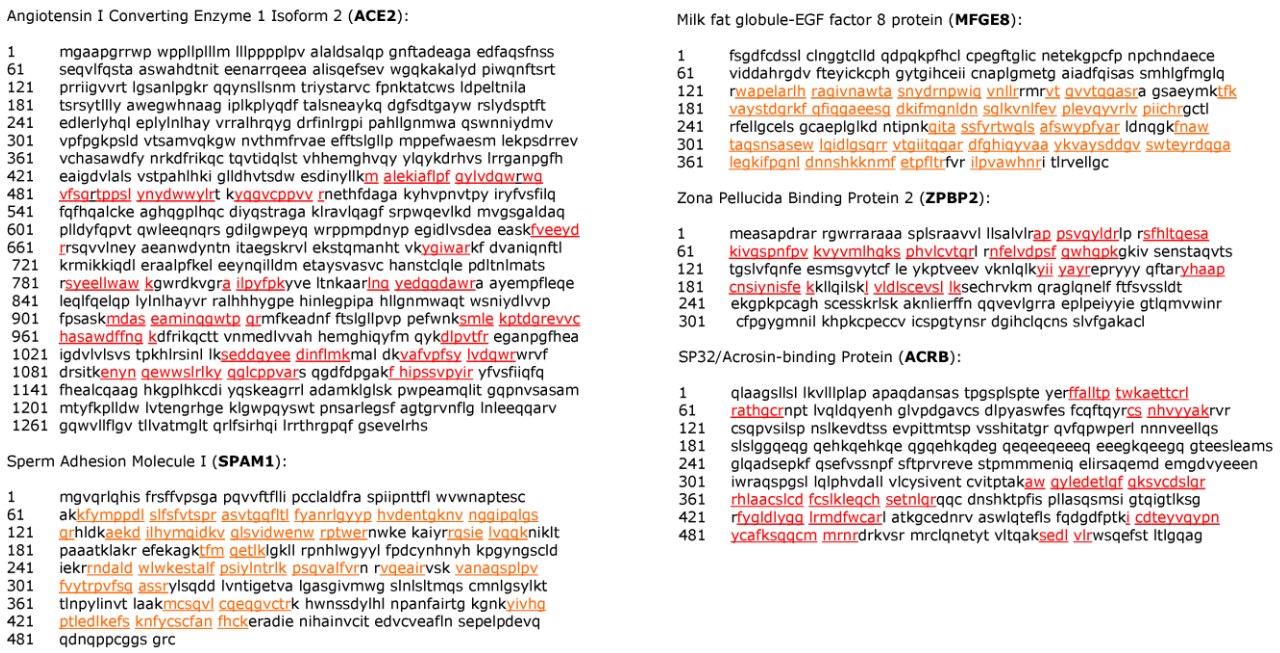

Supplemental Fig. 2.4. Proteomic identification of sperm acrosomal proteins that are protected from degradation by proteasomal inhibitors added to coincubated sperm-ZPP fractions. Sperm-ZPP mixtures were separated on SDS-PAGE and treatment-specific bands, as identified in Fig. 6, were excised, digested with trypsin and subjected to LC-MS/MS using an LTQ mass spectrometer (Thermo-Finnigan). Peptides were identified using the Sequest search algorithm. Peptides with probability scores ($p<0.05$) are shown in red. Note that a full length ACRBP-precursor protein sequence is shown for ACRBP. After translation/during capacitation, the 537 amino acid/~56 kDa precursor protein is processed proteolytically into 32 kDa functional protein and a small fragment (Baba et al. 1994b). The processed 32 kDa ACRBP has been shown to be further proteolyzed into two distinct fragments of 17 and 12.5 kDa (Baba et al. 1994b). N-terminal and C-terminal sequence coverage, shown here, suggests that the low mass doublet band of ACRBP seen in Fig. 6 is a mixture of at least two different fragments derived from the full length, 56 kDa ACRBP-precursor.

CHAPTER THREE

Identification and Characterization of RING-finger Ubiquitin Ligase UBR 7 in Mammalian Spermatozoa

Shawn W. Zimmerman[1], Young-Joo Yi[1], Miriam Sutovsky[1], Fred van Leeuwen[3], Peter Sutovsky[1,2]*

[1]Division of Animal Sciences and [2]Departments of Obstetrics, Gynecology & Women's Health, University of Missouri, Columbia, MO 65211-5300

[3]Maastricht University, School for Mental Health and Neuroscience, Department of Neuroscience, Universiteitssingel 50, 6229 ER Maastricht, THE NETHERLANDS

Key words: ubiquitin, proteasome, spermatozoa, fertilization, zona pellucida, pig

Short title: Identification of UBR7 in spermatozoa

Summary sentence: Ubiquitin ligase UBR7 is present in the acrosomal cap of round spermatids and within the acrosomal matrix of mature boar spermatozoa.

ABSTRACT

The ubiquitin-proteasome system (UPS) controls intracellular protein turnover in a substrate-specific manner. Through activation of three key enzymes, ubiquitin-activating enzyme E1, ubiquitin-conjugating enzyme E2, and ubiquitin-ligase E3, specific proteinaceous substrates are ubiquitinated and marked for degradation by the 26S proteasome. The E3 ubiquitin ligases mark specific substrates for recognition by an E2-carrier enzyme charged with activated ubiquitin. We used an E3-ligase substrate, mutant ubiquitin UBB^{+1} to identify E3 type ligases in a co-culture system composed of soluble porcine zona pellucida (ZP) proteins and boar sperm acrosomal fractions rich in UPS components. Electrophoresis of the reaction products yielded a unique protein band, identified by MS/MS as being similar to ubiquitin-ligase UBR7. Polymerase chain reaction (PCR) primers based on an expressed sequence tag (EST) of boar testis UBR7 amplified the expected product from boar testis and brain. Antibodies produced against a human UBR7 sequence detected UBR7 protein in boar, mouse and human sperm and boar testicular extracts by Western blotting. By immunofluorescence, UBR7 localized to the acrosomal cap of round and elongated, boar and mouse spermatids, and to the acrosome of testicular and ejaculated (boar) spermatozoa. During fertilization, UBR7 stayed with the zona pellucida-bound acrosomal shroud following acrosomal exocytosis, and disappeared as the shroud dispersed. However, inhibition of UBR7 activity did not alter the sperm's ability to fertilize mature oocytes; no change in fertilization rates was observed with anti-UBR7 antibodies present in the fertilization media. The presence of UBR7 in boar spermatozoa indicates that this ligase may be active during

spermiogenesis/acrosomal biogenesis and/or fertilization.

INTRODUCTION

Degradation of polyubiquitinated acrosomal and zona pellucida (ZP) proteins by the ubiquitin-proteasome system (UPS) is an essential process for invertebrate, ascidian and mammalian fertilization (Sanchez et al. 2011; Sawada et al. 2002; Sutovsky et al. 2004; Zimmerman et al. 2011). The UPS causes posttranslational modification of specific proteinaceous substrates by ubiquitination , followed by substrate degradation by a multi-subunit holoenzyme, the 26S proteasome (Hershko and Ciechanover 1998; Karabinova et al.) The UPS has been shown to participate in several steps of fertilization such as sperm capacitation, acrosomal exocytosis and sperm-vitelline coat/ZP penetration across multiple species and taxa (Huo et al. 2004; Morales et al. 2007; Morales et al. 1988; Sawada 2002; Sutovsky et al. 2004; Yokota and Sawada 2007; Zimmerman et al. 2011).

A specific sequence of enzymatic reactions leads to the formation of a multi-ubiquitin chain on an internal lysine (K) residue of the substrate protein that renders it recognizable to the 19S regulatory complex of the 26S proteasome (Glickman and Ciechanover 2002). Polyubiquitin isopeptide chains are typically formed by ubiquitin molecules attachment at either K48 or K63 residues of individual ubiquitin molecules within the multiubiquitin chain. Attachment at these residues then permits recognition by the 19S regulatory complex and initiation of the degradation process (Xu et al. 2009; Yi et al. 2010a).

This protein ubiquitination process is achieved by the sequential activation of three enzymes (Sutovsky 2003). The first enzyme in the ubiquitination cascade is the

ubiquitin-activating enzyme E1 (UBA1). It is tasked with forming a transient thiol-ester bond with a single ubiquitin molecule, a reaction referred to as ubiquitin activation. Active UBA1 is essential for the success of fertilization in the domestic pig; blocking by a specific UBA1 inhibitor results in the inability to properly fertilize porcine oocytes (Yi et al. 2011). Next, a ubiquitin-conjugating enzyme E2 (e.g. enzymes UBC4 & UBC5) establishes a transient thiol-ester bond with the activated ubiquitin molecule after the molecule's separation from the UBA1 enzyme. This complex is recognized by the third essential enzyme in the ubiquitination cascade, a E3-type ubiquitin ligase associated with the substrate protein. Once engaged, the E3 enzymes interact with the E2 enzymes in order for the E2-attached ubiquitin molecule to be transferred to the target protein. The ubiquitin molecule is attached to the substrate protein by catalyzing a covalent binding between ubiquitin's C-terminus and substrate's internal Lys-residue. Thus, the E3-type ligases are the substrate-specific elements of ubiquitination, responsible for determining which proteins are to be degraded.

Currently there have been about a dozen of the E2 enzymes identified in mammals. While most appear to be widely expressed, at least two have been identified as being testis and spermatozoa specific in rats and ascidians, respectively (Wing et al. 1996; Yokota et al.). Contrary to limited number of E2-type enzymes, there is a great variety of E3-type ligases. The E3-type ligases are categorized into two primary classes, HECT-domain and RING-finger ligases (Glickman and Ciechanover 2002). The hallmark of HECT ligases is a conserved cysteine residue positioned ~35 residues upstream of the

C terminus, while the RING-finger ligases contain zinc ions that allow for interaction with other proteins/enzymes (Pickart 2001). The RING-finger ligases are identified by the presence of cysteine and histidine residues that are distinctively spaced to allow for interaction of two zinc ions that results in a stabile E2-E3-substrate interaction (Pickart 2001). The zinc ion fingers are small protein motifs that can coordinate one or more zinc ions to help stabilize protein structure (Miller et al. 1985). A purified RING-domain alone is capable of acting as a ubiquitin ligase and activating the E2-type enzymes necessary for ubiquitin-conjugation (Furukawa et al. 2002).

The RING class of mammalian ubiquitin-ligases includes a unique family of ligases known as the UBR box-family. This family is characterized by the presence of a specific sequence known as the UBR box domain, which can be found throughout the various UBR-family members and their isoforms. The UBR-box domain is a heart-shaped Zn-finger domain with three zinc finger sites (Choi et al. 2010). These zinc fingers are capable of recognizing proteins that have outlived their utility based on the determinants of the N-end rule pathway of protein degradation (Kwon et al. 1998). The N-end rule pathway determines the half-life of proteins based on the N-terminal amino acid residue. The two primary destabilizing residues for mammals are Aspartic Acid and Glutamic Acid (Sriram et al. 2011). Once these proteins are identified based on their N-terminal residue, they are targeted for degradation through the UPS by the UBR box family of E3 ligases (Kwon et al. 1998). Most of the limited knowledge about the UBR family has come from work involving gene sequencing from mice and humans, as well

as protein expression in mammalian cells (Kwon et al. 1998; Tasaki et al. 2005; Tasaki et al. 2009). Herein, we sought to determine presence of the UBR- box family ligase in porcine gametes by using a *in vitro* assay involving solubilized zona pellucida and acrosome contents collected from boar spermatozoa. To capture the resident acrosomal ubiquitin ligases, a mutant form of ubiquitin UBB^{+1} was used as bait. The frame-shifted ubiquitin, UBB^{+1} integrates into elongating multi-ubiquitin chains with wild type ubiquitin (Shabek et al. 2009; Yi et al. 2010b). Based on this approach, we identified the UBR-family ligase UBR7 as a component of mammalian sperm acrosome and hypothesized that it may be involved in acrosomal biogenesis in testis and/or acrosomal function during fertilization.

MATERIALS AND METHODS

Boar semen collection and processing

All studies involving vertebrate animals were completed under the strict guidance of ACUC protocol number #A3394-01, approved by the Animal Care and Use Committee of the University of Missouri. Fresh boar spermatozoa were collected on a weekly basis and the sperm rich fraction was placed in a 50 ml tube and processed as described previously (Zimmerman et al. 2011). From the sperm rich fraction, 1 ml of collected spermatozoa was measured into a 15 ml Falcon tube and centrifuged at 350 x g in a Fisher Scientific Centrifuge for 5 min to remove the seminal plasma. The supernatant was removed and the pellet was resuspended in 1 ml HEPES-buffered

Tyrode lactate (TL-HEPES-PVA) medium containing 0.01% (w／v) polyvinyl alcohol (PVA) and centrifugedcentrifuged at 350 x g for 5 min. The sperm pellet was then resuspended in 1 ml of Beltsville thawing solution (BTS; 3.71 g glucose, 0.60 g trisodium citrate, 1.25 g ethylenediamine tetraacetic acid, 1.25 g sodium bicarbonate, 0.75 g potassium chloride, 0.06 g penicillin G and 0.10 g streptomycin in 100.0 ml distilled water) at a final concentration of 1 x 10^9 spermatozoa/ml. Sperm concentrations were estimated using a hemocytometer (Fisher Scientific, Houston, TX, USA). Semen was slowly cooled to room temperature (20–23 °C) by 2 h after collection. The semen was stored in styrofoam box at room temperature for 4 days unless otherwise specified.

Collection and in vitro maturation of porcine ova

Ovaries were collected at a local slaughterhouse and transported in a warm box (25–30˚C). Oocytes were aspirated using an 18 gauge needle and a 10 ml syringe. Cumulus oocyte complexes (COCs) from antral follicles, were washed three times in TL-HEPES-PVA medium containing 0.01% PVA and three times with the maturation medium (Abeydeera et al. 1998). A total of 50 COCs were transferred to 500 µL of the maturation medium that had been covered with mineral oil in a 4-well multi-dish (Nunc, Roskilde, Denmark) and equilibrated at 38.5˚C, 5% CO_2 in air. The medium used for oocyte maturation was tissue culture medium (TCM) 199 (Gibco, Grand Island, NY, USA) supplemented with 0.1% PVA, 3.05 mM d-glucose, 0.91 mM sodium pyruvate, 0.57 mM cysteine, 0.5 µg／ml LH (L5269; Sigma), 0.5 µg／ml FSH (F2293; Sigma), 10 ng／ml epidermal growth factor (E4127; Sigma), 10% porcine follicular fluid, 75 µg／ml penicillin

G and 50 μg/ml streptomycin. After 22 h of culture, the oocytes were washed twice and cultured in maturation media without hormones for 22 h at 38.5˚C, 5% CO_2 in air.

In vitro fertilization and culture of porcine ova

After oocytes were matured, cumulus cells were removed as previously stated, ova were washed three times with TL-HEPES-PVA medium and three times with Tris-buffered (mTBM) medium (Abeydeera et al. 1998) containing 0.2% BSA (A7888; Sigma). Thereafter, 20 MII stage oocytes were placed into each of four 50 μL drops of the mTBM medium, which had been covered with mineral oil in a 35-mm polystyrene culture dish. The embryos were allowed to equilibrate in the incubator for 30 min until spermatozoa were added for fertilization. One milliliter liquid semen preserved in BTS diluents was washed twice in PBS containing 0.1% PVA (PBS-PVA) at 350 x g for 5 min respectively. At the end of the washing procedure, the spermatozoa were resuspended in mTBM medium. After appropriate dilution, 50 μL of this sperm suspension were added to 50 μL of the medium that contained oocytes to give a final sperm concentration of $0.5x10^6$ spermatozoa/ml. Oocytes were co-incubated with spermatozoa for 6 h at 38.5 °C, 5% CO_2 in air. At 6 h after IVF, oocytes were transferred into 100 μL NCSU-23 medium (Yoshioka et al. 2002) containing 0.4% BSA (A6003; Sigma) for further culture. Different concentrations of UBR7 antibody (Abcam) were added to fertilization drops (final concentrations; 0–20 μg) at the time of sperm addition to observe the role of UBR7 during IVF. IVF studies were repeated three times for each treatment regimen.

Zona pellucida protein collection

After maturation, cumulus cells were removed by agitation in TL-Hepes containing 0.01% PVA and 0.5% hyaluronidase. Oocytes used for the coincubation experiments were exposed to 10 µL TBS (213 mM NaCl, 50 mM Tris) pH 2.0. This low pH solubilized the ZP and 10 µL of TBS pH 8.0 was then added to the oocytes to neutralize the solution. The solubilized zona pellucida proteins (sZP) were collected from the oocytes, placed in 500 µL tubes and stored in a -20°C freezer until required.

Crude acrosome collection

Freshly collected spermatozoa were measured into a 15 ml Falcon tube at a concentration of 1 x 10^9 spermatozoa/ml and centrifuged at 350 x g in a Fisher Scientific Centrifuge for 5 min to remove the seminal plasma. The supernatant was removed and the pellet was resuspended in 1 ml TL-Hepes containing 0.01% PVA and centrifugedcentrifuged at 350 x g for 5 min. The sperm pellet was then resuspended in 1 ml of a pre-chilled protease inhibitor cocktail (1 mM EDTA, 5 mM benzamidine hydrochloride, 5 µg/ml leupeptin, 1 µg/ml pepstatin A, and 1 mM PMSF). Suspended spermatozoa were sonicated at 30% amplitude for 30 sec and then placed in ice for 3 min. Spermatozoa were sonicated for an additional 30 sec at 30% amplitude followed by centrifugation at 12,000 rpm for 10 min at 4 ˚C. The supernatant was separated from the pellet and stored at -80 °C in 100 µL aliquots for further use.

Acrosome-ZPP coincubation experiments

Aliquots of acrosomal fraction were retrieved from a -80 °C freezer and allowed to defrost to room temperature prior to being used for coincubations; 5 µL of crude acrosomal content were used for each treatment group. Appropriate amounts of TL-Hepes-PVA were added to each group to bring the total reaction volume to 30 µL. Following the addition of TL-Hepes-PVA to the crude acrosomal contents, the groups received either a proteasomal inhibitor cocktail containing 100 µM MG 132 (cat # BML-PI102-0025), 100 µM CLβL (*clasto*-Lactacystin β-Lactone, cat # BML-PI108-0100) and 100 µM Epoxomicin (cat # BML-PI127-0100), a vehicle solution containing 100 µM EtOH and 100 µM DMSO or 5 µg/ml of a deubiquitinating inhibitor ubiquitin-aldehyde (all inhibitors were purchased from Enzo-Biomol; Plymouth Meeting, PA). All groups received 5 µg/ml of E3 ligase, mutant ubiquitin UBB^{+1} (cat # BML-UW8790-0100). The mutant ubiquitin UBB^{+1} protein used was a recombinant protein produced from *Escherichia coli* (*E. coli*). Once the treatments were added to the crude acrosomes, solubilized ZP protein purified from 100 oocytes was added followed by 1 µl of 200 µM ATP (Sigma, cat # A6559-25UMO). The incubations continued for 2 hrs at 38.5˚C and 5% CO_2 at which time the solutions were removed from the Falcon tubes, placed in 1.5 ml Eppendorf tubes and stored at -20˚C for analysis of proteins by Western blotting.

Polymerase chain reaction (PCR)

Total RNA was originally collected from boar testis tissue that had been snapped frozen in liquid nitrogen prior to RNA collection. Collected RNA was then converted to

cDNA using the High Capacity RNA-to-cDNA Kit from Invitrogen (Carlsbad, CA) and an Eppendorf Mastercycler (Eppendorf, Hauppauge, NY). A concentration of 200 ng of testis cDNA was amplified using primers for UBR7 (F:ACTCTGTGGAATGGGCTGCACTTA, R: CTGGCTGCAAACTTCAGGCGTTTA) designed by the IDT DNA primer design program (www.idtdna.com); primers were designed from a porcine clone EST sequence (GeneBank: DB817871.1). Sequences were amplified by using the GO-Taq-Green Master Mix (cat # PRM7122) from Promega (Madison, WI) according to manufacturer's protocol. Bands were separated on a 1.2% agarose gel that contained 1% ethidium bromide using a voltage of 100V and visualized under a UV light. Observed bands were excised from the gel using a sterile #10 scalpel blade, place in a sterile 1.5 ml Eppendorf tube and purified by following the protocol established for the Wizard SV Gel and PCR Clean-Up Kit from Promega (Madison, WI) prior to being confirmed by sequencing.

Antibodies

The band pattern of UBB^{+1} in the sperm acrosomal fractions coincubated with sZP was determined by using a custom-made antibody specific for the UBB^{+1} (antiserum UBI3-BL050897; (Fischer et al. 2003; van Leeuwen et al. 1998). Commercial antibodies for UBR7 were purchased from Abcam (Cambridge, MA, cat # ab59151) and Sigma-Aldrich (St. Louis, Mo, cat # SAB2103190). The rabbit anit-UBR7 antibody purchased from Abcam was developed against the human UBR7 internal sequence (MIQCVVCEDW FHGRHLGAIP PESGDFQEMV CQACMKRCSF LWAYAAQLAV ; aa 152-201) which showed a 98% homology to the predicted porcine UBR7 sequence. The Sigma rabbit anti-UBR7

was developed against the human UBR7 protein N-terminal sequence (MAGAEGAAGR QSELEPVVSL VDVLEEDEEL ENEACAVLGG SDSEKCSYSQ ; aa 1-50) and yielded a 98% homology when compared to the predicted porcine UBR7 sequence. For analysis using immune saturated antibodies, commercial antibodies were incubated with synthetic blocking peptides corresponding to the above amino acid sequences (Aviva Systems Biological, San Diego, CA), at a 1:20 dilution overnight at 4˚C prior to use.

Western blotting

Proteins from boar testis, boar spermatozoa, human and mouse spermatozoa, pig brain and sZP were extracted from respective tissues/samples by boiling samples at 95˚C for 5 min in 2X loading buffer containing 100 mM Tris, 300 mM NaCl, 4% SDS, 10% beta mercaptoethanol, 40% glycerol, and Bromphenol Blue. Total loading volumes for the gradient gel (4-20%, Lonza, Basel, Switzerland) did not exceed 30 µL per well. Separated proteins were transferred onto PVDF membrane purchased from Millipore (Billerica, MA) using the Owl wet transfer system (Fisher Scientific) at a constant 50 V for 4 h. Blocking of non-specific antibody binding was done by rocking membrane in a solution of 10% nonfat dry milk in TBS (104 mM NaCl, 96 mM Tris, pH 7.4) with 0.1% Tween for 1 h at room temperature. Rabbit anti-UBR7 antibodies and immune saturated antibodies were used as primary antibodies at a 1:2,000. Primary antibody incubation occurred overnight at 4˚C, washing between antibodies was done using 1% nonfat dry milk in TBS/Tween for 25 min. Secondary antibodies were anti-rabbit IgG HRP antibody (Zymed) and were used at a 1:10,000 dilution for 40 min at room temperature in 1%

nonfat dry milk in TBS-Tween. After secondary antibody-incubation, a final washing was done using TBS-Tween solution for 35 min. The membrane was incubated in a volume of 3 ml of chemiluminescent HRP substrate for 5 min prior to being exposed to Kodak film.

1D gel proteomics of sperm acrosomal fractions coincubated with sZP

Protein bands from coincubation experiments were excised using a sterile #10 scalpel blade from 1D SDS-PAGE gels stained with Coomassie Blue, followed by in-gel digestion with trypsin (Promega Gold MS grade). Peptides were partially purified by C-18 (ZIP tip) peptide clean-up prior to analysis by MALDI TOF-TOF MS & MS/MS. These results were then referenced for similarity of known porcine proteins by using the Applied Biosystems' GPS Explorer software version 3.6 prior to being submitted for cross reference with the NCBI mammalian protein database.

Immunofluorescence and evaluation of oocytes fertilized

Collection of testicular cells was accomplished by collecting fresh boar testis from the University of Missouri abattoir followed by immediate mincing to release all testicular cells. Crude cell suspension was centrifugedcentrifuged at 350 x g for 5 min, supernatant removed and pellet resuspended in TL-Hepes PVA at 37˚C. Cells were then centrifuged and resuspended in TL-Hepes PVA, then settled onto Poly-L-lysine coated cover slips in a suspension of KMT medium (100 mM KC1, 2 mM MgC12, 10 mM Tris-HC1; pH 7.0) for 3 min at room temperature. Following attachment, cells were fixed in 2% formaldehyde for 40 min at room temperature, washed with phosphate buffered

saline (PBS) three times and permeabilized with 0.1% Triton in PBS for 40 min at room temperature. Blocking of non-specific antibody binding was done using 5% normal goat serum (NGS) in PBS for 25 min at room temperature. Anti-UBR7 (Abcam/Sigma) was used as the primary antibody at a 1:100 dilution in 1% NGS/PBS overnight at 4˚C. Following primary antibody incubation, cover slips were washed in 1% NGS/PBS for 30 min at room temperature and exposed to a 1:200 dilution of goat anti-rabbit-TRITC and DAPI (DNA, Molecular Probes, Eugene, OR, USA) in 1% NGS/PBS for 40 min at room temperature. Cover slips were then mounted on slides using Vectashield (Vector Laboratories, Burlingame, CA) and sealed with nail polish.

For evaluation of fertilization, oocytes／zygotes were fixed with 2% formaldehyde for 40 min at room temperature, washed with PBS three times, permeabilized with PBS with 0.1% Triton-X-100 for 40 min at room temperature and stained using a 1:200 dilution of DAPI in 1% NGS/PBS for 40 min. Sperm penetration and the fertilization status of the zygotes (unfertilized, fertilized-monospermic or fertilized-polyspermic) were assessed under an epifluorescence microscope. Image acquisition for all immunofluorescence was performed with a Nikon Eclipse 800 microscope (Nikon Instruments Inc., Melville, NY, USA) with Cool Snap camera (Roper Scientific, Tucson, AZ, USA) and Meta-Morph software (Universal Imaging Corp., Downington, PA, USA).

Statistical analysis

Each result is presented as the mean ± SEM of three independent experiments. Data was processed using one-way analysis of variance (ANOVA) using the SAS package

9.2 (SAS Institute Inc., Cary, NC, USA) in a completely randomized design. Duncan's multiple range-test was used to compare values of individual treatment when the F-value was significant ($p < 0.05$).

RESULTS

Identification of UBR7 protein in porcine acrosomal fraction

We tested the hypothesis that an intrinsic ubiquitin ligase activity exists within sperm acrosome. Such an enzymatic activity was predicted to cause the integration of the externally added mutant, frame-shifted ubiquitin (UBB^{+1}) in the multi-ubiquitin chains formed *de novo* during coincubation of sperm acrosomal fraction and sZP(van Leeuwen et al. 1998; Yi et al. 2010b). The presence of the proteasomal inhibitor cocktail (protects the *de novo* formed ubiquitin-protein conjugates from degradation by acrosomal proteasomes) in the coincubation assay of acrosomal fraction, sZP and recombinant UBB^{+1} resulted in a ladder-like band pattern of UBB^{+1}, typical of polyubiquitination of mutant ubiquitin (Bardag-Gorce et al. 2003; Bardag-Gorce et al. 2002; Yi et al. 2010b) (**Fig. 3.1, lane 2**) when analyzed by Western blot using an anti-mutant ubiquitin antibody UBI3. No such mutant ubiquitin laddering effect was observed in the coincubation involving the vehicle solutions (**Fig. 3.1, lane 1**) or Ubiquitin Aldehyde (**Fig. 3.1, lane 3**), in which only one 10 kDa mass band doublet of non-ubiquitinated UBB^{+1} protein was seen. Based on this result it was determined that a ubiquitin-ligase activity is present in the boar sperm acrosome, this result set the stage

for isolation and identification of sperm ubiquitin-ligase(s). The mutant, frame-shifted UBB^{+1} was therefore used to bait E3-ligases that could be present and enzymatically active in the acrosomal content during the coincubation with sZP. We used 1D PAGE gels to separate proteins from the respective treatments groups of vehicle, inhibitor cocktail and UBB^{+1} only. Based on differences in band patterns of fractions incubated with proteasomal inhibitors (**Fig. 3.2A, lane 1**), control vehicle solutions (**lane 2**) or UBB^{+1} only (**lane 3**), several bands unique to the UBB^{+1} only treatments were excised and subjected to MALDI TOF-TOF MS MS/MS identification (**Fig. 3.2 red boxes**). Among the identified proteins that were unique compared to other treatment groups were the Zona Pellucida Sperm-Binding Protein 4 precursor (ZPBP4, ZP3-alpha or ZPB; aGI 47522906; NP_999210.1; predicted mass 49 kDa), contributed by sZP, and two fragments of an E3 ligase annotated as UBR7 specific for mouse (**Fig. 3.2B**). There was one protein band of ~25-26 kDa present in all treatments. No other protein bands unique to one treatment group were identified, most likely because the proteins of the acrosomal contents and solubilized ZP were degraded by acrosomal proteases during incubation.

UBR7 mRNA is present in boar testis

Amplification of testis mRNA that had been converted to cDNA using primers designed from a porcine clone EST sequence (GeneBank # DB817871.1) resulted in a

single amplicon of approximately 650 bps (**Fig. 3.3A**) in both the boar testis and pig brain (**Fig. 3.3A, lanes 1 & 3**). Control amplification of beta actin transcript (**Fig. 3.3A, lane 2**) was completed concurrently with the UBR7 samples to confirm amplification of proper sequences. The amplicon from the boar testis was purified from the ethidium bromide gel and sequenced for identification of the band. Sequencing resulted in a 100% identity to the predicted EST sequence present in Genebank # DB817871.1 for pig UBR7 (**Fig. 3.3B**). Based on these results, it was established that UBR7 mRNA was present in the boar testis as well as in the pig brain.

Presence of UBR7 protein in boar testis

Western blotting of porcine UBR7 ligase was conducted on proteins extracted from boar testis, boar spermatozoa, mouse testis, mouse spermatozoa, human spermatozoa and pig brain using two different peptide-specific human anti-UBR7 antibodies recognizing the N-terminal domain (Sigma;**Fig. 3.4A blue**) and an internal sequence of UBR7 protein (Abcam; **Fig. 3.4A green**). The N-terminal antibody (Sigma) detected a band of ~ 50 kDa in boar spermatozoa, testis (**Fig. 3.4B1, lane D, E**) and in the pig brain (**Fig. 3.4B1, lane F**). A similar band was observed prominently in the mouse testis and mouse spermatozoa (**Fig. 3.4B 1, lanes B, A**). No prominent band was seen in human spermatozoa (**Fig. 3.4B 1, lane C**). The immunosaturated Sigma antibody did not detect this band in boar testis, attesting to the specificity of Sigma antibody (**Suppl. Fig. 3.1 A, panel #2**). An unrelated antibody recognizing the internal sequence of UBR7 (Abcam), corresponding to the zinc finger region shared with several other proteins,

detected a doublet of protein bands in boar spermatozoa and in boar testis in the 60-65 kDa range (**Fig. 3.4B 2, lane D, E**). Additionally, a single band was observed in human spermatozoa at ~65 kDa (**Fig. 3.4B 2, lane C**) and multiple bands were seen in the pig brain extracts, ranging from ~40-90 kDa (**Fig. 3.4B 2, lane F**). A similar sized band was detected in mouse spermatozoa and mouse testis (**Fig 3.4B 2, lane A, B**). Immunosaturated Abcam antibody did not detect these presumed specific bands, while a minor non-specific band was observed after a prolonged exposure at ~29 kDa in boar testis (**Suppl. Fig. 3.1 A, panel #1**). These finding suggested that the Abcam antibody recognizes a protein other than UBR7, either a related UBR-family member, or an unrelated protein with a sequence similar to AA 152-201. Use of NCBI's blast protein search engine against the amino acid sequence used to produce the Abcam antibody identified several proteins that could potentially be recognized by Abcam anti-UBR7 antibody. The closest match, based on size, among those proteins was the metal-response element-binding transcription factor 2 (MTF2; access. # XP_ 003481559.1 or XP_001928492.4; alt. name NAM1); it shared a 31% AA identity with AA 152-201 of UBR7. The MTF2 protein's AA residue count of 593 predicts migration in the 60-65 kDa range on a PAGE gel (**Suppl. Fig. 3.2**). Furthermore, the Zn-finger domains of both UBR7 and MTF2 are of the RING-finger type, common for RING-finger E3 ubiquitin-ligases. In fact, MTF2 has two RING domains, although, to our knowledge, there is no data to demonstrate that MTF2 has a ubiquitin-ligase activity.

Localization of UBR7 in porcine and murine spermatids and spermatozoa

Immunofluorescence using both anti-UBR7 antibodies detected UBR7 in the acrosomal cap of boar round spermatids; acrosomal cap fluorescence using Abcam antibody is shown in **Fig. 3.5A** and immunofluorescence with Sigma antibody in **Fig. 3.6A**. During spermatid elongation UBR7 remained associated with the forming acrosomal cap and, upon reaching the final step of spermiogenesis, remained present only within the acrosome when using the Abcam antibody (**Fig. 3.5B**). Use of the Sigma antibody localized the UBR7 protein close to the equatorial segment in the matured boar sperm acrosome (**Fig. 3.6C**). In addition to acrosomal localization, the Sigma antibody also detected UBR7 association within the caudal manchete of elongating spermatids (**Fig. 3.6B**). In mouse germ cells the Sigma antibody showed localization in the acrosomal granule/cap of round spermatids (**Fig. 3.7A**) and in the fully formed acrosome of testicular and epididymal spermatozoa (**Fig. 3.7B**). The anti-UBR7 antibody produced by Abcam gave a similar localization in both acrosomal granule/cap of round spermatids (**Fig. 3.7 C**) and in the acrosome of the completely differentiated spermatozoa (**Fig. 3.7 D**). During porcine IVF, anti-UBR7 antibody from Abcam showed that following sperm-ZP binding and acrosomal exocytosis, UBR7 was retained within the acrosomal shroud (**Fig. 3.5C**) and became undetectable as the shroud dispersed at a later stage of fertilization, (**Fig. 3.5E**).

UBR7 immuno-block during porcine fertilization in vitro

Due to the presence of UBR7 in the intact acrosomes of fully differentiated testicular spermatozoa, and in the acrosomal shrouds of zona-bound fertilizing spermatozoa, we sought to determine if UBR7 was contributing to the fertilization

processes. Neither of the two anti-UBR7 antibodies in fertilization medium altered sperm zona binding or fertilization rates (**Fig. 3.8A**). Similarly, there was no effect on fertilization with the addition of blocking peptides corresponding to amino acid residues targeted by the respective antibodies (**Fig. 3.8B**), or the addition of the immunosaturated antibodies to the fertilization medium (**Suppl. Fig. 3.1, B)**.

DISCUSSION

Identification of the RING-finger ubiquitin ligase UBR7 in porcine testis and spermatozoa indicates that this UBR box family ligase may participate in spermatogenesis and/or sperm function during porcine fertilization. The UBR box-family ligases are thought to participate in cardiovascular development and during muscle protein recycling in mice (An et al. 2006; Krawiec et al. 2007). Furthermore, UBR box family members have been implicated in downstream synaptic synthesis for taste, smell and sight senses as well (Tasaki et al. 2007). To our knowledge, there is no data on UBR7 participation in spermatogenesis or fertilization.

The peptide sequences used to raise antibodies for the present study flank the UBR-box and zinc-finger/RING finger domain of UBR7 (AA residues 45-115). A polyclonal antibody against the N-terminal sequence (AA 1-50) of UBR7 recognized a protein band of appropriate size (~50 kDa) in sperm and testicular cell extracts and detected the UBR7 protein in spermatid acrosomal cap, caudal manchette and sperm acrosome. While the unrelated antibody targeting AA residues 152-201 labeled acrosomal cap/acrosome and reacted only with bands in 60-65 kDa range, i.e., above the predicted

mass of UBR7. The target peptide sequence overlaps in part with the PHD domain of UBR7 (aa 134-186), suggesting that this antibody could have recognized an unrelated protein with a PHD domain (Fong and Takeda 2008). However, this does not appear likely based on a NCBI Blast result, wherein the most identical domain (31% identity) overlapping with AA152-201 of UBR7 was that of RING-finger containing transcription factor MTF2. The PHD domain is found in UBR7 but not in other UBR-family members. The PHD domain is a zinc finger motif that has been shown to act as a transcription factor for gene transcription in *Drosophila* during normal development (Kessler et al. 2009). Furthermore, the PHD domain of the nuclear ring finger protein UHRF1 has been proposed to form a protein complex that may facilitate cellular proliferation and possibly prevent the onset of cancerous conditions in human adenocarcinomic epithelial cells (Jenkins et al. 2005). Consequently, the PHD domain of UBR7 is of interest with regard to a potential role of UBR7 in spermatogenesis or fertilization.

Based on its localization, the UBR7 may be participating in the acrosomal biogenesis during spermatid elongation, perhaps similar to the suggested activity of the Ring-finger E3 ligase Rnf19a (90 kDa) during acrosomal biogenesis in rat testis (Rivkin et al. 2009). The presence of Rnf19a in rat spermatocytes, round spermatids and epididymal spermatozoa, was determined using immunocytochemistry and western blotting. Localization of Rnf19a was in the acrosomal granule of developing spermatids, and co-immunoprecitpiated with the 19S proteasomal regulatory complex subunit PSMC3 (Rivkin et al. 2009). Similar to UBR7 in the present study, Rnf19a was also

present in the caudal manchette of the elongating spermatids (Rivkin et al. 2009). In addition to acrosomal biogenesis, UBR7 could participate in acrosomal function during fertilization. This idea was supported by the detection of UBR7 in the acrosomal shrouds of zona-bound acrosome -reacted fertilizing spermatozoa, but not by attempts to use the UBR7-specific antibodies and peptides to block fertilization. Addition of anti-UBR7 antibodies or blocking peptides during porcine IVF did not cause a significant change in the frequency of monospermic or polyspermic fertilization. However, the ability of any of these reagents to obliterate the enzymatic activity of UBR7 is not known, particularly because the target domains are outside of the UBR7's active site within the RING-finger domain/UBR box. If UBR7 is participating in sperm penetration through the ZP, this occurrence would fall in line with similar processes seen when the ascidian sperm receptor is ubiquitinated and degraded by the extracellular, sperm-borne ubiquitin-proteasome system (Sawada et al. 2002). While it has been shown that inhibition of the UBR box family is possible in cardiomyocytes with a heterovalent inhibitor RF-C11 (Lee et al. 2008), which we were unable to obtain from authors, lack of appropriate inhibitors for UBR family enzymes makes it difficult to test this hypothesis. Alternatively, considering the presence of UBR7 in mouse spermatozoa, a mutant animal lacking this enzyme in male germ line or specifically in spermatids could be developed. Deletion of the gene encoding for UBR family member UBR3, however, is embryonic lethal in mice, making the production of a UBR7 mutant mouse potentially difficult (Tasaki et al. 2007).

In conclusion, our results demonstrate the presence of UBR7 in mouse and boar testis and spermatozoa. Although the UBR7 protein is present in the sperm acrosome, it does not appear to be crucial for sperm function during fertilization. Further work is warranted to determine the precise roles of UBR7 in spermatogenesis and fertilization. Additional, studies should determine if UBR7 is participating in active ubiquitination of either acrosomal or ZP proteins during fertilization. If UBR7 is capable of identifying sperm or zona proteins for ubiquitination, then the inhibition of its ubiquitin-ligase activity should result in accumulation of protected acrosomal and/or ZP proteins. Collectively the research on gametic UBR7 provides a glimpse into the mechanism of spermatogenesis and may allow for manipulation of ubiquitin-dependent mechanisms during assisted fertilization.

ACKNOWLEDGMENTS

We would like to thank Dr. Kiho Lee for providing the mRNA samples for PCR analysis from boar testis. This work is supported by National Research Initiative Competitive Grant no. 2011-67015-20025 from the USDA National Institute of Food and Agriculture, and by the Food for the 21st Century Program of the University of Missouri-Columbia.

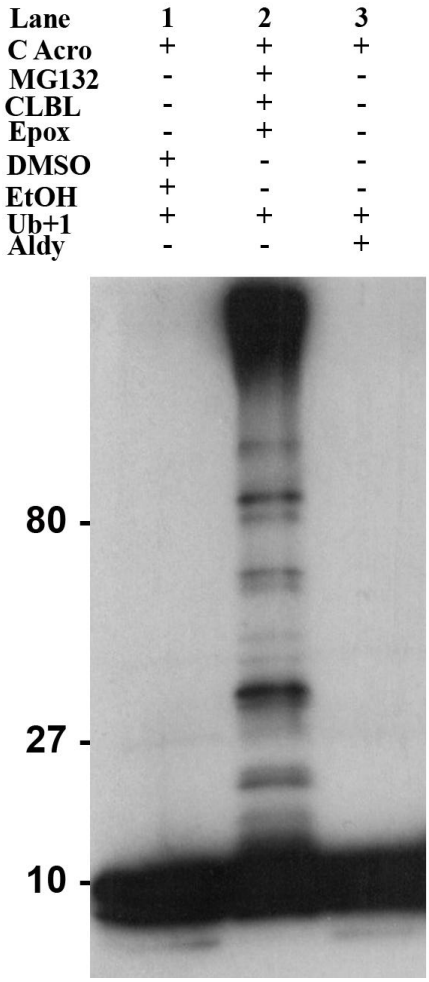

Fig. 3.1. Western blotting using an antibody against mutant ubiquitin UBB^{+1} (a ubiquitin-ligase substrate and a dose-dependent inhibitor of proteasomal proteolysis) shows the integration of UBB^{+1} into polyuibiquitin chains formed *de novo* during UBB^{+1} coincubation with sperm acrosomal fraction and solubilized porcine ZP proteins. Lane 1: Coincubation of the acrosomal fraction and sZP in the presence of vehicle solutions for proteasomal inhibitors (DMSO and EtOH). Lane 2: Presence of the proteasomal inhibitor cocktail in the coincubation mixture resulted in the retention of polyuibiquitinated UBB^{+1}proteins as seen by the presence of ladder of UBB^{+1} bands in this lane. Lane 3: Use of the proteasomal accelerator ubiquitin aldehyde showed no retention in ubiquitinated proteins. Equal UBB^{+1} and sZP protein load was used in all lanes.

A.

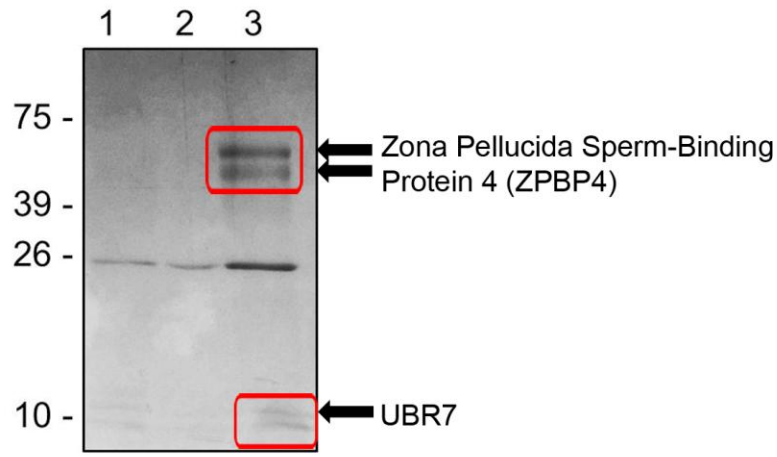

B. Ubr7 protein [Mus musculus]
GenBank: AAH51678.1

1 ypdpedevpd emiqcvvced wfhgrhlgai ppesgdfqem vcqacmrrcs flwayaaqla
61 vtrisaeddg llpnatgmgd edvskpenga pqdnglkeda pehgrdsvne vkaeqknepc
121 sssssesdlq tvf***kkenikt epqsscrlqe lqakqfvkkd aatywplnwr sklctcqdcm***
181 ***kmygel***dvlf ltdecdtvla yenkgkndqa tdrrdplmdt lssmnrvqqv eliceyndlk
241 telkdylkrf adegtvvkre diqqffeefq skkrrrvdgl qyycs

Fig. 3.2. Identification of the UBR7 protein in the sperm-acrosomal extracts. Presence of mutant ubiquitin (UBB^{+1}) protects acrosomal proteins from being degraded during sZP coincubation with sperm acrosome extracts. (A) Acrosome-sZP supernatants containing acrosomal shrouds and soluble zona proteins after 2 hr of coincubation were separated on 1D PAGE gels. Protein that differed between reaction mixtures containing proteasomal inhibitor MG132 (lane 1), vehicle (lane 2) and UBB^{+1} only (lane 3) were excised and subjected to MS/MS identification (red boxes). Tandem mass spectrometry confirmed the presence of Zona Pellucida Sperm-Binding Protein 4 (ZP3-alpha/ZPB) in the high molecular bands and a fragment of UBR7 was confirmed in the lowest band. (B) UBR7 amino acid sequence highlights the fragments identified using tandem mass spectrometry (red), a total of four sequences were identified for UBR7 in a redundant fashion**.** The sequence corresponding to the UBR box domain (aa 44-116) is underlined and the sequence for the PHD domain (aa 134-186) is in italic & bold.

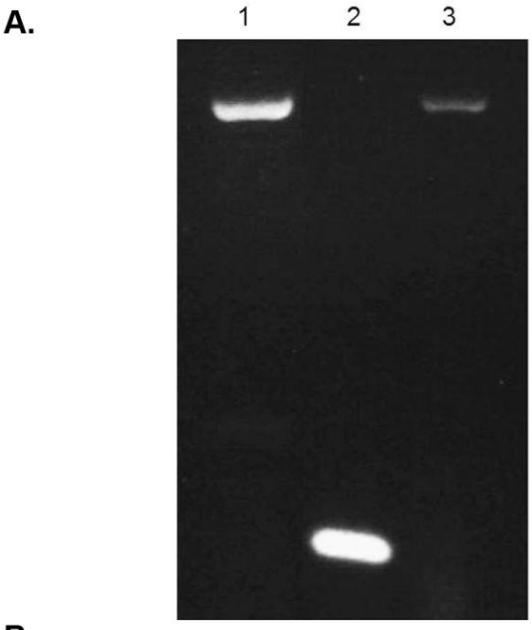

B.

GeneBank: DB817871

```
  1 tttttttttt ttttttcgg gaaaaaataa actggtttac tttctcaaaa ccaaatcaaa
 61 catcttaaag ttatgagcaa agaaccccgg ctagacgggg gtgggggctg gactctgtgg
121 aatgggctgc acttagctga gtcagaaaga agaatgctgg ttatgaaatc agcacaaaca
181 ctgtggctac tgttgttaag gagagtgaag gaagcccgag gctggaggag gaggcctctc
241 cagggagaga cggagagagg accaaaggtg aaatacgcct cttttattcc caggccagta
301 agtggcatct tcattggcct ggatgagaag gcgccttgct cccctctagc tgcaataata
361 ctgcatccca tccactcttc ttctcttttt ttgactgaaa ttcttcaaag aactgctgga
421 tgtcttctct cttaaccact gtgccttcat cagcaaatct cttgagatag tctttaagtt
481 cagtcttcaa gtcattgtat tcacaaataa gttccacttg ctggactctg ttcatgctgt
541 taagagtgtc cattaaaggg tccctcctgt cagctgcctg gtcaaccttg cctttgtttt
601 cataagccag aactgtgtca tattcatctg tcaggaacag gacatctagg tcgccataca
661 ttttcataca gtccttgcag gtacacaact tgctacgcca gttcacgggc caataggtgg
721 cagtgtcttt ctttataaac tgcttagctt taaacgcctg aagtttgcag ccagactgtg
781 attctgtgtt gagatgttgg ttcttaaatg ctgtctggag gtcagattca gaactagagc
841 tggtgcacgg ttcgttcgtc ggctctgctt tcactgccct cacagccgcc tgtccatgtt
901 ccgaaac
```

Fig. 3.3. Amplification of porcine UBR7 cDNA band originating from RNA collected from boar testis. (A) Boar testicular RNA was amplified, after conversion to cDNA, by primers designed against an EST sequence predicted to be porcine UBR7 (GeneBank: DB817871.1). Single bands of 650 bp appeared in boar testis (lane 1) and pig brain (lane 3) after amplification. β-actin (lane 2) was amplified from boar testis as an amplification control using primers specific for the β-actin sequence. (B) Sequencing of bands from lane 1 confirmed the identity of UBR7 cDNA.

A.) Putative E3 ubiquitin-protein ligase UBR7 [Sus scrofa]
NCBI Reference Sequence: XP_001926874.1

1 magaegtagr qselepvvsl vdvleedeel eneacavlgg sdsekcsysq gsvkrqalya
61 cstctpegee pagiclacsy echgshklfe lytkrnfrcd cgnskfknle cklfpdkaki
121 nssnkyndnf fglycickrp ypdpedeipd emiqcvvced wfhgrhlgaa ppesgdfqem
181 vcqacmkrcs flwayaaqla vtkgtaeedg lvlnvdgvgd qealqpenga hqdgapkedv
241 sehgqaavra vkaeptnepc tssssesdlq tafknqhlnt esqsgcklqa fkakqfikkd
301 tatywpvnwr sklctckdcm kmygdldvlf ltdeydtvla yenkgkvdqa adrrdplmdt
361 lnsmnrvqqv eliceyndlk telkdylkrf adegtvvkre diqqffeefq skkrrrvdgm
421 qyycs

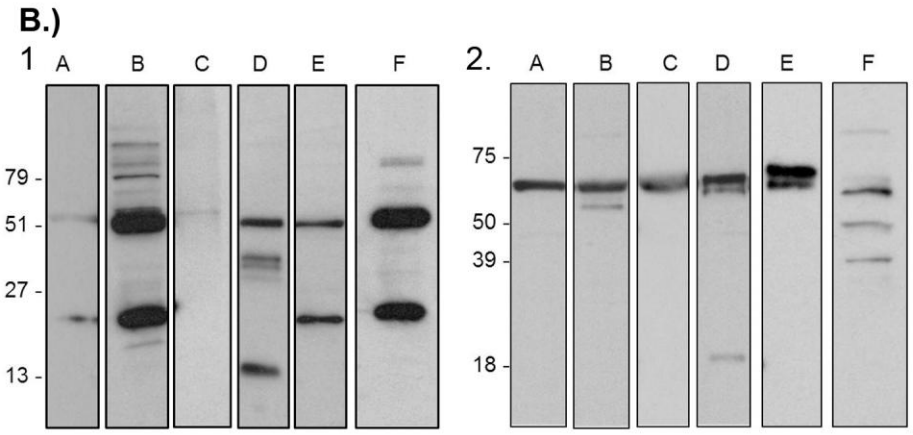

Fig. 3.4. Western blotting of UBR7 protein in the mammalian testis and spermatozoa. Proteins extracted from boar testis, ejaculated boar spermatozoa, mouse epididymal spermatozoa, mouse testis, human spermatozoa and pig brain were subjected to Western Blot analysis using two different anti-UBR7 antibodies. (A) Peptide sequences used to raise the anti-UBR7 antibody from Sigma (blue) and Abcam (green letters). (B) A band of ~ 50-55 kDa and a second, less prominent band at ~25 kDa was observed in boar testis (#1 lane E) (lane E)(lane E)(lane E)(lane E) and pig brain (lane F) using an antibody against the N-terminal amino acids (aa 1-50). A similar band pattern was seen in the mouse testis (lane B). A weak 50-55 kDa band was seen in the mouse (lane A) and human (lane C) sperm extracts. Western blotting with the Abcam anti-UBR7 antibody (aa, 152-201) produced a doublet of protein bands in boar testis and boar spermatozoa at 60-65 kDa (#2 lane E & D). Analysis of human sperm extracts resulted in a single protein band at ~60-65 kDa (lane C). This and other bands ranging from 39-90 kDa were seen in pig brain (lane F). Mouse spermatozoa (lane A) and mouse testis (lane B) produced a single band similar to human sperm at ~60-65 kDa.

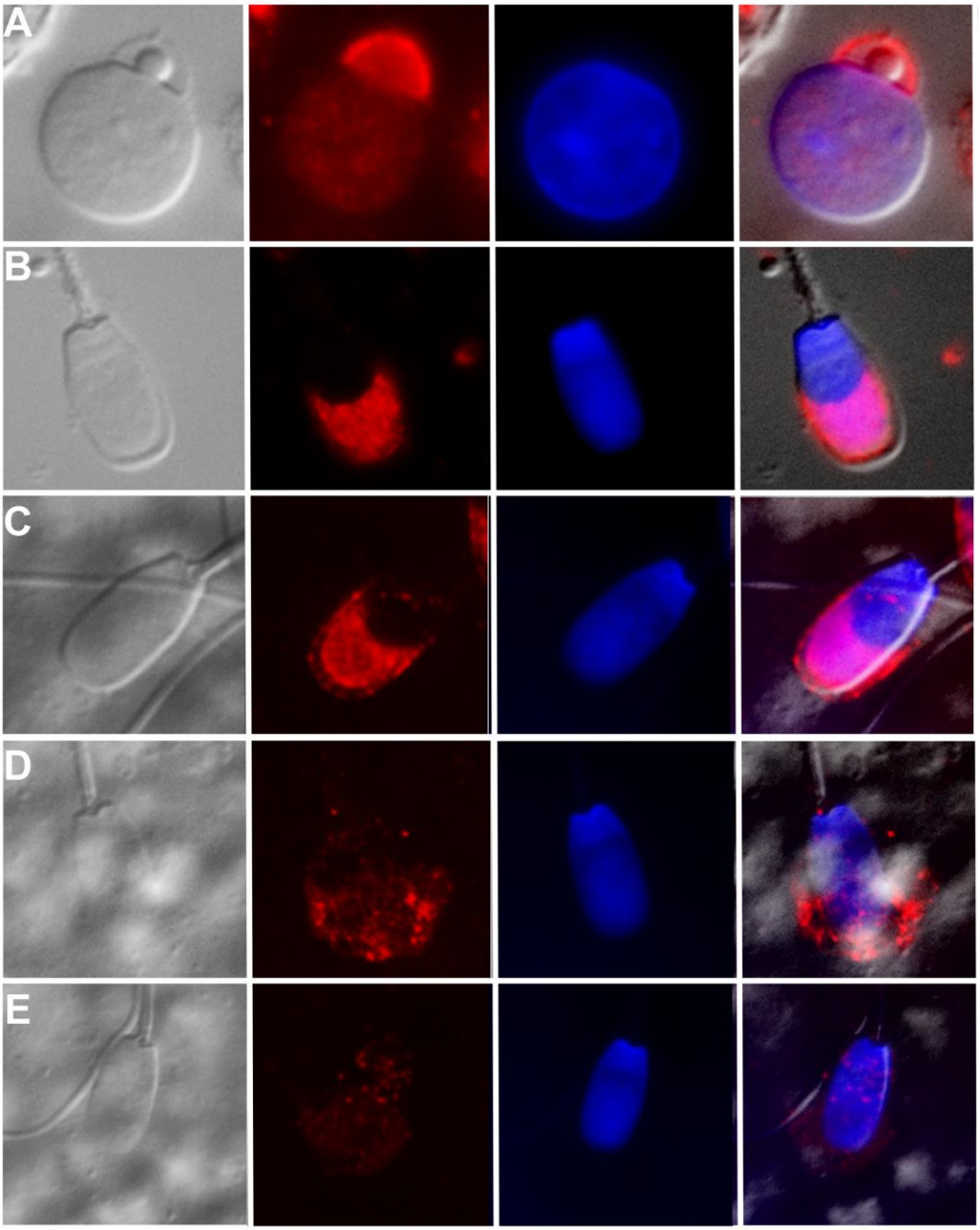

Fig. 3.5. Localization of the UBR7 protein in boar spermatids and spermatozoa using the Abcam antibody. DNA was counter-stained with DAPI (blue). (A) D detection of the UBR7 protein in the acrosomal cap of round and elongating spermatids. (B) UBR7 resided in the acrosome of fully differentiated testicular spermatozoa. (C) In the zona-bound spermatozoa after IVF, UBR7 remained localized in the acrosome. (D) Following the zona-induced acrosomal exocytosis, UBR7 remained with the acrosomal shroud/ghost. (E) As the acrosomal exocytosis/acrosomal shroud disintegration advanced, the UBR7 became almost undetectable.

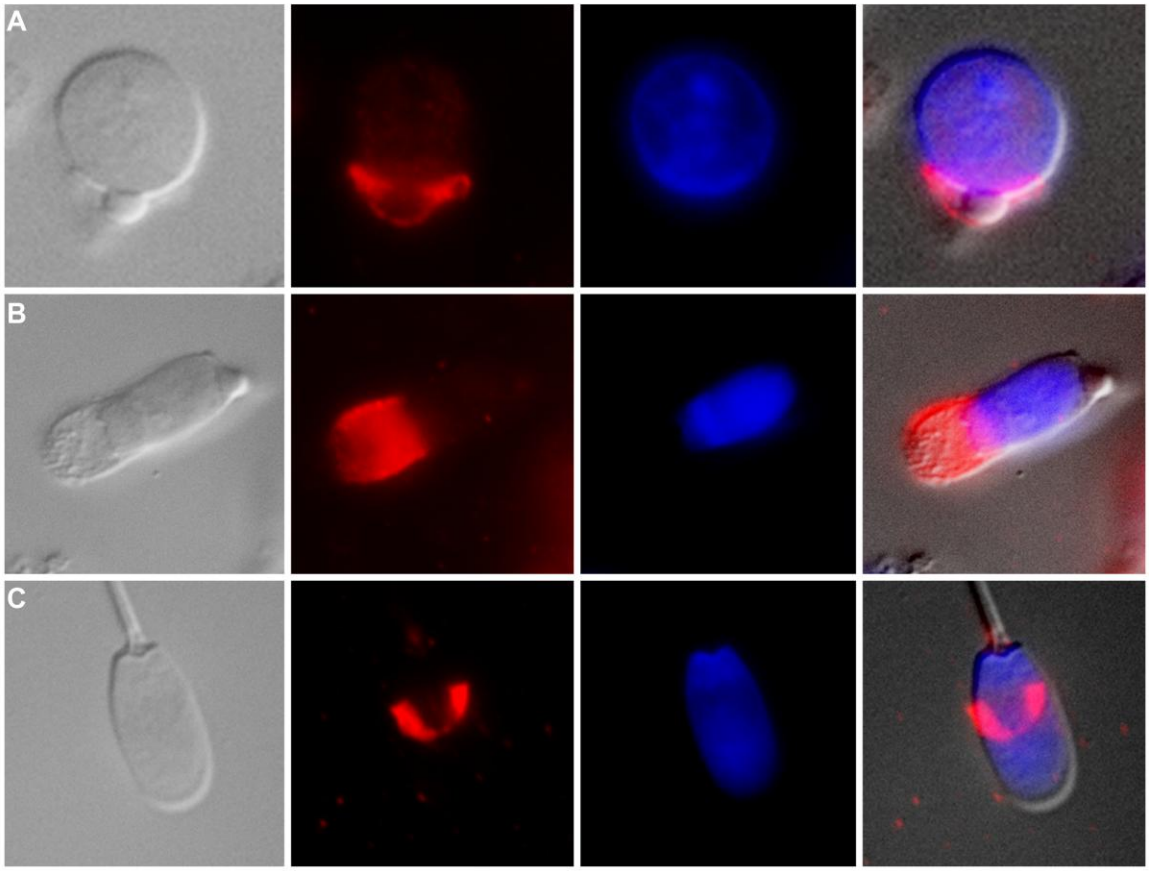

Fig. 3.6. Localization of the UBR7 protein in boar spermatids and spermatozoa using the Sigma antibody. DNA was counter-stained with DAPI (blue). (A) Anti-UBR7 purchased from Sigma detected UBR7 protein in the acrosomal cap of developing spermatids. (B) In the elongating spermatids, UBR7 protein also emerged in the in the caudal manchette. (C) UBR7 accumulated near the equatorial segment of the fully developed acrosome in the fully differentiated testicular spermatozoa.

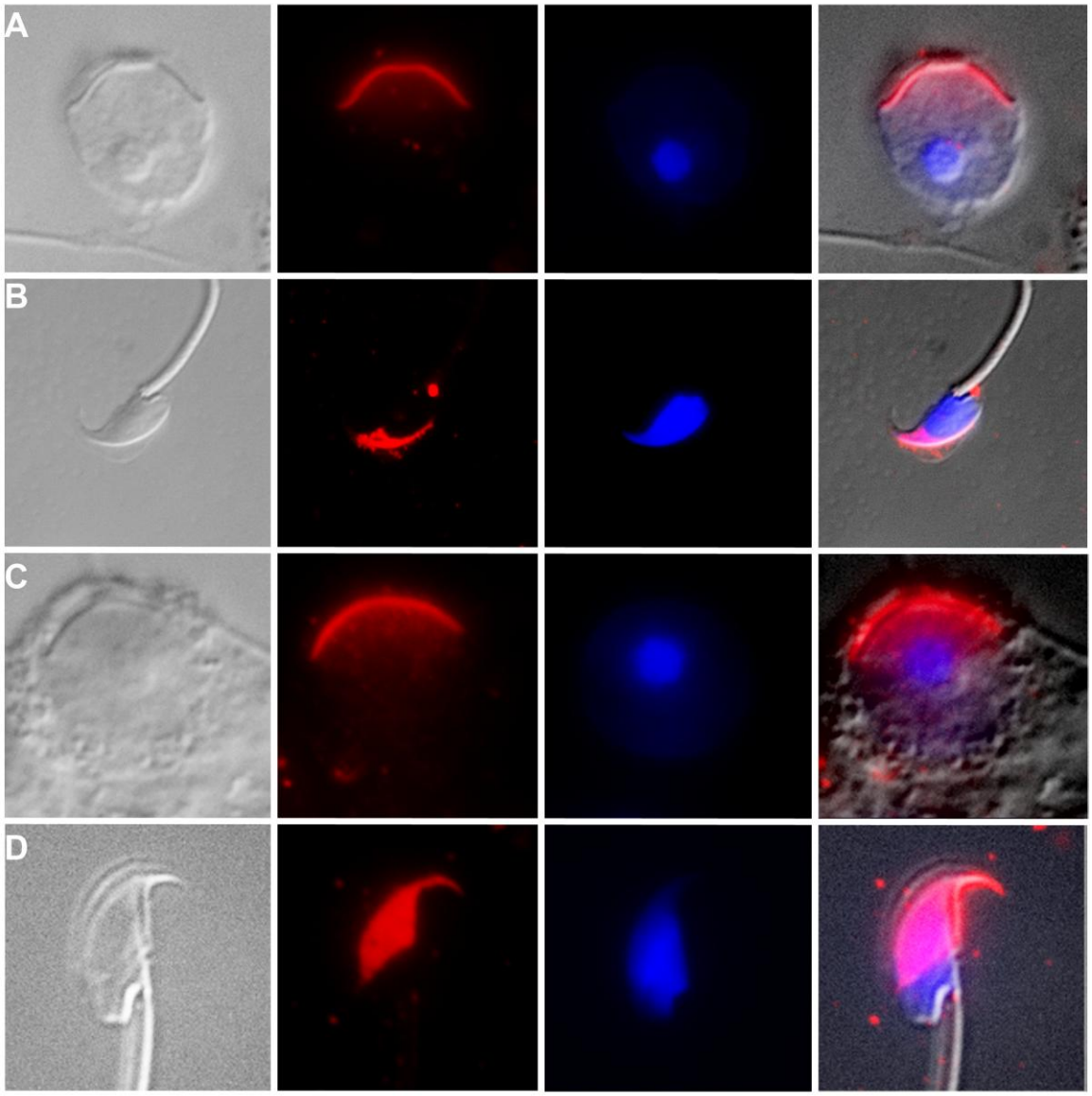

Fig. 3.7. Localization of UBR7 in mouse spermatids and spermatozoa using Abcam and Sigma antibodies. (A) UBR7 was visualized by the Sigma antibody in the acrosomal cap of round spermatids. (B) Sigma antibody detected UBR7 in the acrosome of epididymal spermatozoa. (C) Localization of UBR7 in the acrosomal cap of round spermatids, using Abcam antibody. (D) When the Abcam antibody was used on fully differentiated epididymal spermatozoa UBR7 remained localized in the acrosomal region.

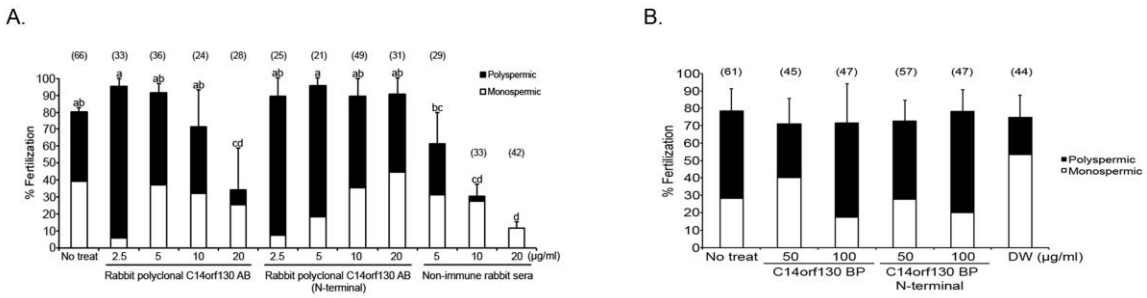

Fig. 3.8. Fertilization parameters of porcine oocytes fertilized in the presence of rabbit polyclonal antibody, raised against amino acids 152-201 (Abcam) or rabbit polyclonal anti-UBR7 N-terminal antibody (amino acids 1-50, Sigma). (A) Porcine oocytes were fertilized in the presence of different concentrations of antibodies or non-immune rabbit sera (control) for 6 hrs. (B) Effect of UBR7 blocking peptides on porcine IVF. Porcine oocytes were fertilized with UBR7 blocking peptide (AAPP11317, Aviva Systems Biology) that had been produced against the Abcam antibody sequence, or UBR7 blocking peptide, N-terminal (AAPS15306, Aviva) that was produced against the Sigma antibody sequence or a vehicle (distilled water, control) for 6 hrs. Each experiment was repeated three times. The numbers of inseminated ova are indicated in parentheses. All values are expressed as the mean percentages ± SEM. Superscripts (a-d) in each group of columns denote significant differences at $p<0.05$.

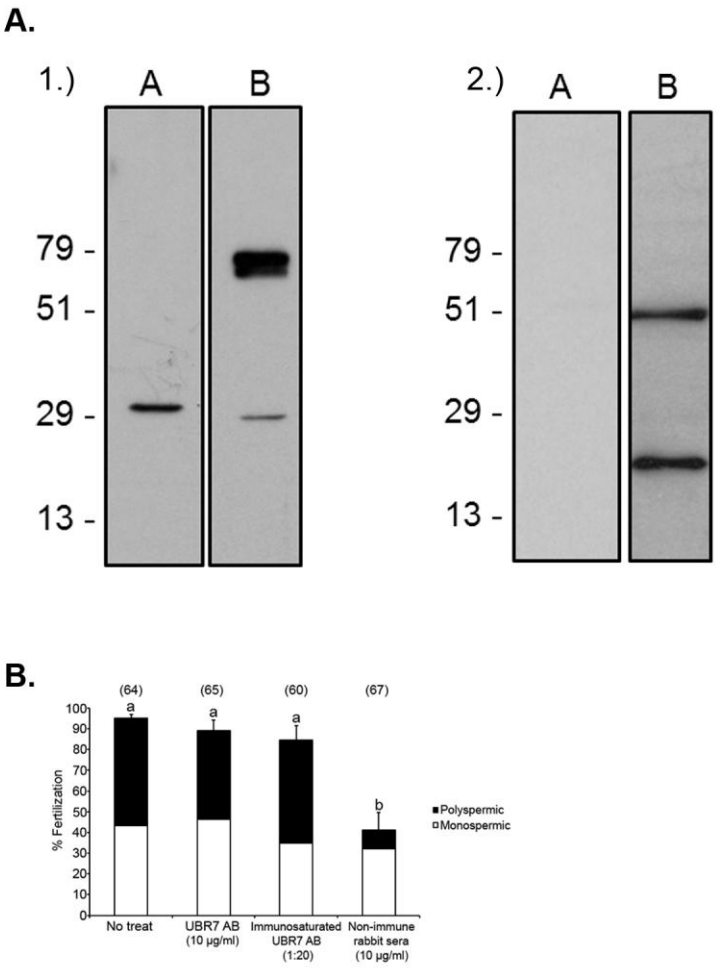

Supplemental Fig. 3.1. (A) (A)(A)Immuno-saturation of anti-UBR7 antibody eliminated the prominent band doublet in boar testis extracts. Proteins from boar testis were collected for Western Blot analysis using the anti-UBR7 antibody (Abcam/Sigma) that had been immuno-saturated (1:20) using peptide (AAPP11317/ AAPS15306) that was specific for the Abcam or Sigms sequence overnight at 4°C. (A) The immuno-saturated antibody did not recognize the double protein bands at the 70-75 kDa size (#1 A) when compared to the non-saturated active antibody (#1 B). A minor non-specific band was present at 29 kDa in both immune and non-immune saturated treatment groups. (B)(B)(B) Immuno-saturation of the second anti-UBR7 antibody (Sigma) eliminated the prominent bands in the boar testis extracts (#2 A/B). (B) Porcine IVF in the presence of immune-saturated UBR7 antibody. Rabbit polyclonal UBR7 (Abcam) antibody was incubated with UBR7 blocking peptide (AAPP11317) at 4˚C overnight (AB:BP ratio=1:20). Porcine oocytes were fertilized in the presence of antibody, immunosaturated antibody or non-immune rabbit sera for 6 hrs. Each experiment was repeated four times. The numbers of inseminated ova are indicated in parentheses. All values are expressed as the mean percentages ± SEM. Superscripts (a, b) in each group of columns denote significant differences at $p<0.05$.

Description	Max Score	Total Score	Predicted Size	% AA Identity
PREDICTED: putative E3 ubiquitin-protein ligase UBR7 [Sus scrofa]	111	111	50 kDa	98
PREDICTED: histone lysine demethylase PHF8 [Sus scrofa]	36.2	36.2	99 kDa	38
PREDICTED: lysine-specific demethylase 7 [Sus scrofa]	34.3	34.3	106 kDa	38
PREDICTED: metal-response element-binding transcription factor 2 [Sus scrofa]	29.6	29.6	60 kDa	31
PREDICTED: transcription initiation factor TFIID subunit 3-like, partial [Sus scrofa]	28.5	28.5	85 kDa	38
PREDICTED: zinc finger protein 280C [Sus scrofa]	27.7	27.7	83 kDa	31
PREDICTED: nuclear receptor subfamily 2 group C member 2 isoform 1 [Sus scrofa]	27.3	27.3	70 kDa	41
PREDICTED: protein fem-1 homolog C-like [Sus scrofa]	26.2	26.2	45 kDa	41
PREDICTED: zinc finger protein 280D [Sus scrofa]	26.2	26.2	107 kDa	25
PREDICTED: E3 ubiquitin-protein ligase UBR1 [Sus scrofa]	25	25	177 kDa	38
PREDICTED: tudor domain-containing protein 7 [Sus scrofa]	25	25	123 kDa	50
PREDICTED: leucine-rich repeat-containing protein 1 [Sus scrofa]	24.6	24.6	55 kDa	32
PREDICTED: PHD finger protein 20 [Sus scrofa]	24.6	24.6	46 kDa	35
PREDICTED: poly [ADP-ribose] polymerase 4-like, partial [Sus scrofa]	24.6	24.6	165 kDa	38
PREDICTED: cpG-binding protein [Sus scrofa]	24.3	24.3	76 kDa	62
PREDICTED: FERM, RhoGEF and pleckstrin domain-containing protein 1-like, partial [Sus scrofa]	23.9	23.9	104 kDa	59
PREDICTED: PHD finger protein 1 isoform 2 [Sus scrofa]	23.5	23.5	49 kDa	31
PREDICTED: histone-lysine N-methyltransferase MLL4-like [Sus scrofa]	23.5	23.5	295 kDa	43
PREDICTED: estrogen receptor-like [Sus scrofa]	22.7	22.7	28 kDa	35

Supplemental Fig. 3.2. Protein fragments of similar amino acid sequence to the peptide used to produce the Abcam UBR7 antibody, based on BLAST search of the NCBI's protein database. Further analysis revealed several zinc finger proteins that had a similar sequence alignment to the Abcam sequence. However, predicted size analysis determined that most of the found proteins did not have a mass of 60-65 kDa, as shown for the band recognized by the Abcam UBR7 antibody. One potential cross-reactive protein is the metal-response element-binding transcription factor 2 (MTF2, arrow). Sequence alignment revealed a 31% sequence identity between the target peptides of UBR7 and MTF2 (18 aa aligned total). Based on these results it was concluded that MTF2 was not likely to represent the bands present in the Abcam western blots.

CHAPTER FOUR

Acrosome remodeling during zona pellucida-induced acrosomal exocytosis in the domestic pig

Zimmerman S.[1],Yi Y-J [1], Sutovsky M.[1], Sutovsky P.[1,2]

[1]Division of Animal Science, University of Missouri, Columbia, MO 62511

[2]Departments of Obstetrics, Gynecology, and Women's Health, University of Missouri, Columbia, MO 62511;

Key words: ubiquitin, proteasome, sperm, fertilization, acrosome, pig

Short title: Acrosome remodeling by the 26S proteasome

Summary sentence: Visualization of acrosome remodeling during porcine *in vitro* capacitation and fertilization by environmental scanning electron microscopy.

Abstract

The Ubiquitin-Proteasome System (UPS) is considered vital to mammalian fertilization as it participates in sperm capacitation, acrosomal exocytosis (AE), and sperm-zona pellucida (ZP) penetration. Ubiquitin binds in redundant fashion to a variety of proteins and targets them for proteolysis by a multi-subunit protease, the 26S proteasome. Proteasomal inhibitors block sperm-zona pellucida penetration during porcine fertilization in vitro and prevent the degradation of solubilized zona pellucida proteins (sZP) by the capacitated boar spermatozoa or by the proteasomes isolated from boar sperm acrosomes. Based on these findings, we hypothesized that the sperm proteasomes participate in the remodeling of sperm acrosome during sperm capacitation and ZP-induced acrosomal exocytosis. Boar spermatozoa were capacitated and incubated with porcine sZP proteins with or without a proteasomal inhibitor cocktail composed of MG 132, CLβL and Epoxomicin. After the two hour coincubation, the entire reaction volume was fixed in primary fixative. Acrosomal membrane remodeling was examined by conventional and environmental scanning electron microscopy (SEM & ESEM), respectively. Upon co-incubation, the sZP binding to sperm acrosomes induces the process of acrosomal exocytosis that resulted in the formation of the membrane vesicle-composed acrosomal shrouds, which eventually detached from sperm heads and disintegrated. In the presence of the proteasomal inhibitor-cocktail, the acrosomal shrouds were retained, as compared to vehicle treatment groups. Rippling of the plasma/outer acrosomal membrane was observed during sperm

capacitation and visualized by ESEM. Vesiculation of the outer acrosomal membrane was observed in the presence of calcium ionophore, was visualized by SEM/ESEM, and inhibited by proteasomal inhibitors. Use of the ESEM procedure allowed for visualization of membranes located at the connecting piece while samples processed for SEM did not. These results indicate that proteasomal inhibitors prevent the ZP-induced acrosome remodeling. This suggests that in addition to being able to degrade ZP proteins, sperm proteasomes target substrates within the acrosome during capacitation and acrosomal exocytosis.

Introduction

The Ubiquitin Proteasome System (UPS) is a vital part of mammalian fertilization as it participates in sperm capacitation, acrosomal exocytosis (AE) and sperm penetration through the egg vitelline coat, and the zona pellucida (ZP) (Sutovsky et al. 2004; Yi et al. 2011; Zimmerman et al. 2011). Ubiquitin (UBB) is a small chaperone protein approximately ~8.5 kDa in size that binds covalently, in a redundant fashion to internal lysine residues of the specific substrates. This redundant ligation, termed ubiquitination, requires the activity of specific ubiquitinating enzymes including the ubiquitin activating enzyme E1 (UBA1), ubiquitin conjugating enzyme E2 (e.g. UBC4) and a ubiquitin ligase of E3 type (e.g. UBR7) (Glickman and Ciechanover 2002; Hershko and Ciechanover 1998). Upon formation of the redundant multi-ubiquitin chain with at least four UBB molecules linked through their internal Lys-residues, the substrate is recognized by a multi-catalytic protease known as the 26S proteasome. The 26S proteasome is a holoenzyme that consists of a 19S regulatory complex and the 20S core (Hershko and Ciechanover 1998). Initial recognition of the redundant multi-ubiquitin chain is accomplished through the 19S regulatory complex. The substrate is then unfolded and transferred to the 20S core where it is degraded into small peptides by the catalytic β-subunits PSMB 1, 2 & 5 (Hershko and Ciechanover 1998; Yi et al. 2010b).

The participation of the 26S proteasome in the fertilization process has been described in a number of mammalian and non-mammalian, including ascidans, *Drosophila,* porcine, mouse and human (Kawano et al. 2010; Lambert et al. 2002;

Morales et al. 2003; Sawada et al. 2002; Sutovsky et al. 2004; Zhong and Belote 2007; Zimmerman et al. 2011). In particular, proteasomal activity is required for sperm penetration of the vitelline coat in ascidians (Sawada et al. 2002) and the ZP in mammals (Sutovsky et al. 2004; Zimmerman et al. 2011). Some evidence suggests the 26S proteasome is also targeting acrosomal proteins during the destabilization of the acrosomal membranes by removal of cholesterol also known as sperm capacitation. Presence of proteasomal inhibitors may hinder some aspects of sperm capacitation by preventing acrosomal protein degradation (Chakravarty et al. 2008; Morales et al. 2007; Yi et al. 2011). Furthermore, the 26S proteasome appears to be active during the ZP-induced acrosomal exocytosis (AE) and this activity is prevented through the presence of proteasomal inhibitors (Zimmerman et al. 2011). The acrosome is a compartmentalized sperm accessory structure that, upon sperm-ZP binding, creates a microenvironment that allows spermatozoa to penetrate the ZP. The acrosome is derived from the Golgi and is divided into three distinct layers. First is the outer acrosomal membrane (OAM) which lies beneath the plasma membrane. Second, beneath the OAM lies the acrosomal matrix (AM) which, together with the vesiculated OAM, is responsible for creating a microenvironment conducive for fertilization. Finally, underneath the AM is the inner acrosomal membrane (IAM) which lies on top of the subacrosomal perinuclear theca and nuclear envelope. Within the acrosomal matrix reside proteins such as proacrosin binding protein, acrosin and zonadhesin that are thought to mediate sperm-zona interactions (Buffone et al. 2008). During the guinea pig AR, the fertilizing

spermatozoon releases the acrosomal matrix in stages or layers, until it has been completely expelled and creates a microenvironment (Kim et al. 2001). Conventional scanning electron microscopy allows for visualization of these stages of acrosomal exocytosis (Buffone et al. 2008), but is prone to sputter-coating or critical point drying artifacts (Dalo et al. 2008). Production of some of these artifacts can be prevented by use of an alternative EM method known as environment SEM (ESEM). The ESEM method allows for observation of samples in a wet state that allows for determination of external structures in a native configuration. Use of the environmental and low vacuum scanning electron microscopy has been shown to provide better cell membrane retention. For example, ESEM was used to determine the effect of aging on oocyte quality through comparison of aged oocyte microvillar domains to young oocytes (Dalo et al. 2008). However, while preserving cellular membranes ESEM still lacks some surface details that can be seen by conventional SEM, especially when visualizing the complex ZP matrix (Dalo et al. 2008; Familiari et al. 2006). Based on this evidence, we hypothesized that it may be possible to observe the fine-structural changes in the acrosomal integrity through the use of environmental scanning electron microscopy.

To study the participation of sperm-borne proteasomes in porcine fertilization, we have developed a coincubation system composed of capacitated boar spermatozoa and solubilized zona pellucida (sZP), in which the sZP induced AE and formation of the sperm acrosomal shroud in the absence of sperm attachment to a solid ZP-matrix (Zimmerman et al. 2011). The present study was designed to examine the effect of

proteasomal inhibitors on AE and acrosomal membrane/shroud remodeling visualized by conventional scanning electron microscopy (SEM) and environmental scanning electron microscopy (ESEM).

Materials and Methods

Zona pellucida collection

Oocytes were aspirated using an 18 gauge needle and a 10 ml syringe from ovaries collected from a slaughterhouse (Farmland Foods, Milon, MO). Cumulus oocyte complexes were placed in 500 µl of TCM-199 as previously described in (Zimmerman et al. 2011). After maturation the cumulus cells were removed by agitation in TL-Hepes containing 0.1% polyvinylacohol (PVA) and 0.5% hyaluronidase. Oocytes were exposed to 10 µl of non-reducing TBS (213 mM NaCl, 50 mM Tris) pH 2.0 to solubilized the ZP; 10 µl of TBS pH 8.0 was then added to the oocytes to neutralize the sZP-solution. The sZP were separated from the zona-free oocytes, placed in 500 µl tubes and stored in a -20°C freezer until further use.

Semen collection and sperm preparation

All studies involving vertebrate animals were completed under the strict guidance of ACUC protocol number #A3394-01, approved by the Animal Care and Use Committee of the University of Missouri. Fresh boar semen was collected on the day of co-incubations, transferred into 15 ml Falcon tubes and centrifuged at 350 x g in a hinged-rotor Fisher Scientific Centrifuge to remove the seminal plasma from the

supernatant. The pellet was resuspended in 14 ml of TL-Hepes-PVA and centrifuged at 350 x g for 5 min. Spermatozoa were slowly cooled to room temperature (20–23 °C), by remaining on the bench top, for 2 h after collection and diluted with Beltsville thawing solution/diluent (BTS; 3.71 g glucose, 0.60 g trisodium citrate, 1.25 g ethylenediamine tetraacetic acid, 1.25 g sodium bicarbonate, 0.75 g potassium chloride, 0.06 g penicillin G and 0.10 g streptomycin in 100.0 ml distilled water) to a final concentration of 10 x 10^6 spermatozoa/ml. The diluted semen was stored in styrofoam box at room temperature for up to 4 days unless stated otherwise. Unless otherwise noted, all chemicals used in this study were purchased from Sigma Chemical Co. (St Louis, MO, USA).

***Sperm capacitation and induction of acrosomal exocyto*sis**

A total of 30 million washed spermatozoa were added to 12 ml of capacitation medium containing TL-Hepes, 11 mM glucose, 5 mM pyruvic acid, and 20 mg/ml BSA and capacitated for 6 hrs at 38.5˚C (Wu et al. 2006). Following capacitation, spermatozoa were centrifuged at 350 x g in a Fisher Scientific Centrifuge for 5 min to remove the capacitation media. The supernatant was removed and the pellet was resuspended in 10 ml TL-Hepes-PVA and centrifuged again at 350 x g for 5 min. The sperm pellet was then resuspended in 6 ml TL-Hepes-PVA. A total of 10,000 spermatozoa were placed in a new Falcon tube and centrifuged at 350 x g in a Fisher Scientific Centrifuge for 5 min to remove the supernatant. In some experiments, spermatozoa were resuspended in 30 µl TL-Hepes PVA supplemented with 1 mM Ca^{2+}

Ionophore A23187 (Sigma-Aldrich; St. Louis, MO, Cat# C7522) to induce AE; sperm were incubated at 37 °C and 5% CO_2 for 1 hour.

Sperm-sZP coincubation experiments

Capacitated spermatozoa were centrifuged at 350 x g for 5 min, the supernatant was removed and the pellet resuspended in 10 ml TL-Hepes-PVA. The solution was centrifuged again at 350 x g for 5 min and the pellet was resuspended in 6 ml TL-Hepes-PVA. New 15 ml Falcon tubes were marked for the individual treatment groups; 10,000 spermatozoa were added per tube and then centrifuged at 350 x g for 5min. After removing the supernatant, appropriate amounts of TL-Hepes-PVA were added to the sperm pellets to bring the total reaction volume to 30 μl. Following the addition of TL-Hepes-PVA, the groups received either the proteasomal inhibitor cocktail containing 100 μM MG 132, 100 μM CLβL and 100 μM Epoxomicin, or vehicle solution containing 100 μM EtOH, and 100 μM DMSO (all inhibitors were purchased from Enzo-Biomol; Plymouth Meeting, PA). Once the respective treatment solutions were added to the sperm pellets, the sZP purified from 100 oocytes were added and mixed with the sperm pellets. The incubations continued for 2 hrs at 38.5˚C and 5% CO_2 at which time the entire solution was fixed for SEM/ESEM analysis.

In vitro fertilization

Cumulus cells were removed from mature metaphase-II oocytes with 0.1% hyaluronidase in TL-HEPES-PVA medium. Oocytes were washed once with TL-HEPES-PVA

medium and three times with Tris-buffered (mTBM) medium (Abeydeera et al. 1998) containing 0.2% (w/v) BSA (A 7888, Sigma). Thereafter, 25-30 oocytes were placed into each of four 50 µl drops of the mTBM medium, which had been covered with mineral oil, in a 35 mm polystyrene Petri dish. The dishes were allowed to equilibrate in the incubator for 30 min until spermatozoa were added for fertilization. The spermatozoa that were suspended in BTS were washed twice in PBS-PVA at 350 x *g* for 5 min. Next, the spermatozoa were resuspended in mTBM medium. After appropriate pre-dilution, 50 µl of this sperm suspension was added to 50 µl of the medium that contained oocytes to reach a final sperm concentration of 1 x 10^6 cells/ml. Oocytes were co-incubated with spermatozoa for 2 h at 38.5^{o}C, 5% CO_2. At 2 h after IVF, oocytes were transferred into a primary fixative for SEM/ESEM analysis.

SEM & ESEM

Following coincubation or IVF treatment, the entire coincubation mixtures or the individual oocytes, were fixed in a primary fixative composed of 5% paraformaldehyde, 50% glutaraldehyde, 0.1 M cacodylate buffer and 4 ml water. Samples were fixed for 40 min at room temperature at which time the fixative solution was removed. Samples were washed in PBS (137 mM NaCl, 3 mM KCl, 2 mM KH_2PO_4, and 8 mM Na_2HPO_4) and resuspended in ultrapure water and stored at 4 ˚C. Samples predetermined for SEM analysis were processed using a Pelco Biowave ProLaboratory microwave processing system with cold stage and vacuum chamber. All microwave steps were completed with samples under vacuum. Samples were rinsed for 5 min three times in 0.1M Cacodylate

Buffer, then placed in a 2% Osmium buffer and microwaved at 100W for 1min, following initial microwaving; samples were irradiation for 80 sec, microwaved for 3 min, irradiation for 40 sec, followed by 3 rinses in 2% Osmium buffer. After final buffer washes the samples were rinsed in ultra pure water and dehydrated through an Ethanol series of 40 sec each (20, 50, 70, 90, 100% x 3). After dehydration sample were critical point dried using the Tousimis Autosamdri-815 critical point drier. Following drying samples were mounted on a 13 mm carbon tab and sputter coated with 6 nM of Platinum and then viewed. Analyzing of ESEM samples were done by mounting samples on 13 mm carbon tab and then placing the samples in the FEI Quanta 600 FEG Extended Vacuum Scanning Electron Microscope with the following settings: 5.0 kV, 600 Pa, 2.0 °C, 14,000 x magnification and a 5.8 mm working distance. Conventional SEM samples were analyzed using the Hitachi S-4700 Scanning Electron Microscope with the following settings: 2.0 kV, 0.82 Torr, 26,000 x magnification and a working distance of 5.0 mm. Images were captured using the XTm software (FEI Company) at the specified magnifications.

Acrosome Analysis

Changes in acrosomal integrity were determined by visualizing differences acrosomal status within each treatment. Sperm were randomly counted within each treatment group and categorized based on the status of their acrosome. In both the non-capacitated and capacitated groups sperm were categorized into either non-capacitated by the appearance of a smooth plasma/outer acrosome membrane. Or

sperm were placed into capacitated status based on the appearance of ruffled plasma/outer acrosome membranes. For those sperm treated with Ca^{2+} ionophore sperm were placed in either the non-reacted group or reacted group. These determinations were based on the presence or absence of varying vesiculating membrane patterns on the sperm head. The sperm treatment groups involving exposure to sZP, these sperm where classified into either presence of acrosomal shroud or non-shroud. Determination of presence of acrosomal shroud was based on the results and images made in previous work using both TEM processing and flow cytometry analysis of fertilizing boar spermatozoa (Sutovsky et al. 2004; Yi et al. 2007a; Zimmerman et al. 2011).

Results

Remodeling of the outer acrosomal membrane during sperm capacitation and acrosomal exocytosis visualized by ESEM

Completion of the capacitation process resulted in a visible change in the structure of the plasma/outer acrosomal membrane as observed by ESEM (**Fig 4.1**). Changes in acrosome integrity could be determined in non-capacitated (**Fig. 4.1 A**) and capacitated (**B**) spermatozoa, and during the progress of AR (**Fig. 4.1 C-F**). Those spermatozoa that had completed the capacitation process (60% capacitated vs. 40% non-cap) displayed a plasma membrane/OAM that no longer had a smooth appearance as compared to the non-capacitated spermatozoa (**Fig. 4.2 A**). The plasma/OAM of capacitated spermatozoa had a rippled surface that was observed under high

magnification settings (**Fig. 4.2 B**). This rippled appearing surface was most likely due to the removal of cholesterol and the formation of lipid rafts that would have allowed the spermatozoa to undergo the AE process. Following the induction of AE in the presence of Ca^{2+} ionophore, vesiculation of the OAM and shedding of the acrosomal matrix from the sperm head were observed (**Fig. 4.3 A).** In some instances, the remnants of the acrosomal shroud were observed next to the spermatozoa that had undergone AE (**Fig. 4.3 B arrow**). Patterns varied from spermatozoon to spermatozoon within treatments, with some AE spermatozoa displaying membrane blebbing restricted to the equatorial segment (**Fig. 4.3 C**). While other spermatozoa were observed with what appeared to be random blebs of acrosomal membranes being shed from the individual spermatozoa (**Fig. 4.3 D**). Within a given Ca^{2+} ionophore treatment, varying stages of acrosomal exocytosis could be seen. Representative spermatozoa from varying stages of AE included those with extensive OAM vesiculation (**Fig. 4.4 A B**), those at an early stage prior to the formation of acrosomal shroud (**Fig 4.4 C**), and those that did not seem to respond to ionophore-treatment (**Fig. 4.4 D-F**). Determination of acrosome reacted spermatozoa showed that once exposed to Ca^{2+} ionophore 70% of sperm underwent AE (**Fig. 4.8**).

Similar to ionophore treatment, coincubation of the capacitated spermatozoa with sZP resulted in vesiculation of OAM and acrosomal matrix-release, as captured by ESEM. Spermatozoa treated with sZP in the presence of vehicle solutions (DMSO, EtOH) underwent AE as determined by the absence of OAM between equatorial segment and

proximal edge of the sperm head (**Fig. 4.5 A, C**). Spermatozoa incubated with sZP in the presence of the proteasomal inhibitor cocktail did undergo AE, as determined by the absence/ruffling of OAM. However, the detached acrosomal shrouds remained present within this environment upon the completion of acrosomal exocytosis, suggesting the resident proteasomes were unable to effectively degrade the acrosomal components in the presence of proteasomal inhibitors (**Fig. 4.5 B, D arrows**). This occurrence of acrosome retention was seen in 60% of spermatozoa exposed to sZP while those spermatozoa exposed to sZP in the presence of vehicle solution only showed 10% retention (**Fig. 4.8**).

SEM analysis of acrosomal remodeling

Conventional SEM was used to examine acrosomal remodeling of ZP bound spermatozoa following porcine IVF. Attempts to visualize acrosome remodeling using ESEM under IVF conditions produced collapsed oocytes and spermatozoa. This inability to retain shape was believed to be due to pressure inside the chamber and water within the samples, therefore differences in acrosomal integrity were not discernible (data not shown). The SEM fixation and preparation process resulted in a partial stripping of plasma membrane and OAM covering the acrosome, allowing for additional observations of changes in acrosomal integrity. As a result of fixation and preparation, the acrosomal cap of acrosome-intact spermatozoa was clearly distinguishable from the post-acrosomal sheath of the sperm head (**Fig. 4.6 A, D**). The posterior edge of the acrosomal cap, overlying the equatorial segment of the sperm head, became visible in

the zona-bound spermatozoa with exocytosed acrosomes, concurrent with the swelling of the acrosomal matrix (**Fig. 4.6 A, D arrows**). Those spermatozoa that had completed AE displayed appreciable shedding of the acrosomal matrix (**Fig. 4.6 B, C, arrows**). However, plasma membrane damage due to the harshness of the fixation and processing also damaged membranes covering the striated columns of the outer dense fibers located at the connecting piece of the sperm tail (**Fig. 4.7 A**). When compared to those spermatozoa prepared for and analyzed by ESEM (**Fig. 4.7 B**) the lack of striated columns of the outer dense fibers was very evident. While preparation for SEM did remove membranes located at the connecting piece consistently, ESEM was also prone to this membrane removal (**Fig. 4.1 C, D**). The high absences of these delicate membranes in the SEM trials lead to the conclusion that acrosomal analysis by traditional SEM was not representative of AE spermatozoa. Based on this conclusion, SEM samples were not used for determination of acrosomal integrity in isolated spermatozoa.

Discussion

The challenge with imaging of the acrosomal remodeling by scanning electron microscopy resides not with the size of the structures but with the processing. While conventional SEM is known for artifacts created by fixation, critical point drying and dehydration of samples (Dalo et al. 2008). It still produced very detailed results that allow for interpretations of surface structures. In an attempt to minimize processing artifacts samples were observed under wet conditions by use of an alternative SEM

method known as environmental SEM. While ESEM has been shown to lack high resolution imaging, in order to observe AE in its most native state we chose to analyze sperm samples using the ESEM technique (Dalo et al. 2008; Psenicka et al. 2010). Application of ESEM procedures allowed us to observe the fine-structural changes in the plasma/outer acrosomal membranes in spermatozoa at various stages of the fertilization process induced by in vitro capacitation, Ca^{2+} ionophore treatment and AE-induction by sZP. While use of a primary fixative containing cacodylate buffer has been questioned in regards to sample damage, it was chosen in order to ensure no contamination would occur from the fixative. Furthermore, use of this fixative has been shown to be adequate to determine interaction between cells, suggesting the potential for observation of sperm/sZP interaction (Maia-Brigagao and de Souza 2012). Additionally, use of this fixative has been shown to allow for visualization of acrosomal shrouds in boar spermatozoa (Sutovsky et al. 2004; Yi et al. 2007a). Although adequate, future work should be conducted to determined if use of the primary fixative containing PBS instead of cacodylate buffer may result in better preservation of sperm membranes.

While the conventional SEM analysis provided a greater detail/resolution than ESEM, it resulted in greater damage of sperm membranes, most conspicuous in the acrosomal region of the sperm head and the connecting piece of the sperm tail. Although some membranes did appear to be damaged at the connecting piece of the sperm tail on some observed spermatozoa exposed to Ca^{2+} ionophore in the ESEM images. The ESEM process allowed us to observe fine structural changes induced by

sperm capacitation (i.e. plasma membrane/OAM rippling) and exposure to sZP (i.e. OAM vesiculation). Despite the fact that ESEM provided analysis for structural changes other modes of SEM may have provided even greater detail. Use of low voltage SEM on rodent eggs has provided highly detailed images that resulted in determination of effect of age on unfertilized eggs (Dalo et al. 2008). Moreover, use of Cryo-SEM has been shown to capture images of boar sperm after being frozen and stored for AI (Hernandez et al. 2007). Although the acrosomal changes appeared to be difficult to determine as the individual spermatozoa where frozen together (Hernandez et al. 2007).

Using specific proteasomal inhibitors, we determined that the 26S proteasome is targeting substrates within the acrosome as spermatozoa undergo AE. Retention of acrosomal shrouds in the presence of a trio of proteasomal inhibitors is a direct result of inhibition of the proteasomal proteolysis activity in the sperm acrosome. These results agree with the proposal that the UPS is actively degrading acrosomal proteins during porcine fertilization (Chakravarty et al. 2008; Sanchez et al. 2009; Zimmerman et al. 2011). While the proteolytic activity resides within the 20S proteasomal core, inhibition of enzymatic activities associated with the 19S regulatory complex, and those that regulate substrate ubiquitination, can also alter the course of porcine fertilization. For example, inhibition of the ubiquitin activating enzyme (UBA1) during boar sperm capacitation altered the ubiquitination patterns of known acrosomal proteins such as spermadhesin AQN-1 (Yi et al. 2011). The presence of this E1 inhibitor also reduced the percentage of fertilized oocytes during porcine IVF (Yi et al. 2011). Furthermore,

proteasomal subunits may directly interact with acrosomal proteins as seen when antibodies produced against the 19S complex subunit PSMD4 were used for immunoprecipitation.

The acrosome-binding protein, acrosin inhibitor co-immunoprecipitated with PSMD4, a 19S subunit responsible for the recognition of multi-ubiquitin chains on the substrate proteins, suggests that proteasomes may be directly degrading acrosomal proteins from seminal plasma that maintain the uncapacitated state (Yi et al. 2010b). Inhibition of proteasomal activity both during capacitation and after capacitation made human spermatozoa unable to undergo AE (Chakravarty et al. 2008; Morales et al. 2007), even in the presence of progesterone (Morales et al. 2007). Chakravarty suggested that the proteasome-dependent step of AE occurs upstream of the Ca^{2+} influx in the acrosomal interior, mimicked by Ca^{2+} ionophore treatment. Proteomic analysis identified a number of proteins in the acrosomal shroud that are degraded by sperm proteasomes during the AE. These include known acrosomal proteins; SPAM1, lactadherin (MFGP8E), and the acrosomal membrane proteins ZPBP2/IAM38 and SP32 (Zimmerman et al. 2011). Protection of these known proteins from degradation by the proteasomal inhibitor cocktail is possibly resulting in the retention of acrosomal shrouds observed in the present study. Based on this evidence and our previous paper (Zimmerman et al. 2011) the action of sperm proteasomes during fertilization is likely two parts. First, proteasomes may be required for degradation of acrosomal proteins as the spermatozoa undergo the AE to allow for secondary sperm-ZP binding (Zimmerman

et al. 2011). According to some interpretation, the AE may even begin prior to initial sperm-ZP binding (Jin et al. 2011), which is consistent with acrosomal surface rippling observed in the present study following sperm capacitation. The acrosome is a Golgi derived organelle that covers the apical region of the fully developed sperm head. Within the acrosomal matrix and on the acrosomal membranes reside proteins such as proacrosin/acrosin and zonahesins (ZAN) that have been implicated in the fertilization process (Buffone et al. 2008). Release of the acrosomal matrix is believed to occur by layers, as opposed to all at once. Guinea pig spermatozoa have been shown to have three distinct acrosomal matrix layers which, upon release, allow for the creation of a microenvironment that allows for interaction between sperm head and zona surface (Foster et al. 1997). The resultant complex of vesiculated OAM and interdispersed AM components is commonly referred to as the acrosomal ghost or shroud. Besides containing essential proteins for fertilization, the acrosomal shroud may also contain concentrated amounts of ATP that is made available to resident proteasomes. Work done in pig showed that ATP is present on the acrosomal surface of both capacitated and non-capacitated boar spermatozoa (Yi et al. 2009c). The presence of ATP within the acrosomal shroud could, upon release, provide the energy needed for resident proteasomes to degrade both acrosomal and ZP proteins.

The present results support the hypothesis that the 26S proteasomes mediate the remodeling of the sperm acrosome during sperm capacitation and the AE. These findings fall in agreement with previous papers showing that UPS is active during

capacitation and the AE. While the use of the ESEM procedure may be a viable option for observing fine structural changes in acrosomal integrity, it may not be the best option for imaging changes in acrosomal composition. Compared to traditional SEM, the ESEM allows for observation of samples not burdened with some artifacts caused by sample processing but does not produce highly detailed images. Collectively, these results show that inhibition of the UPS by specific inhibitors alters the course of proteasomal remodeling induced by exposure to ZP-proteins.

Acknowledgements

The authors would like to thank Lou Ross and Cheryl Jensen for their help with SEM/ESEM sample processing and imaging. This work was in part supported by National Research Initiative Competitive Grants no. 2007-35203-18274 and no. 2011-67015-20025 from the USDA National Institute of Food and Agriculture, and by the Food for the 21st Century Program of the University of Missouri-Columbia.

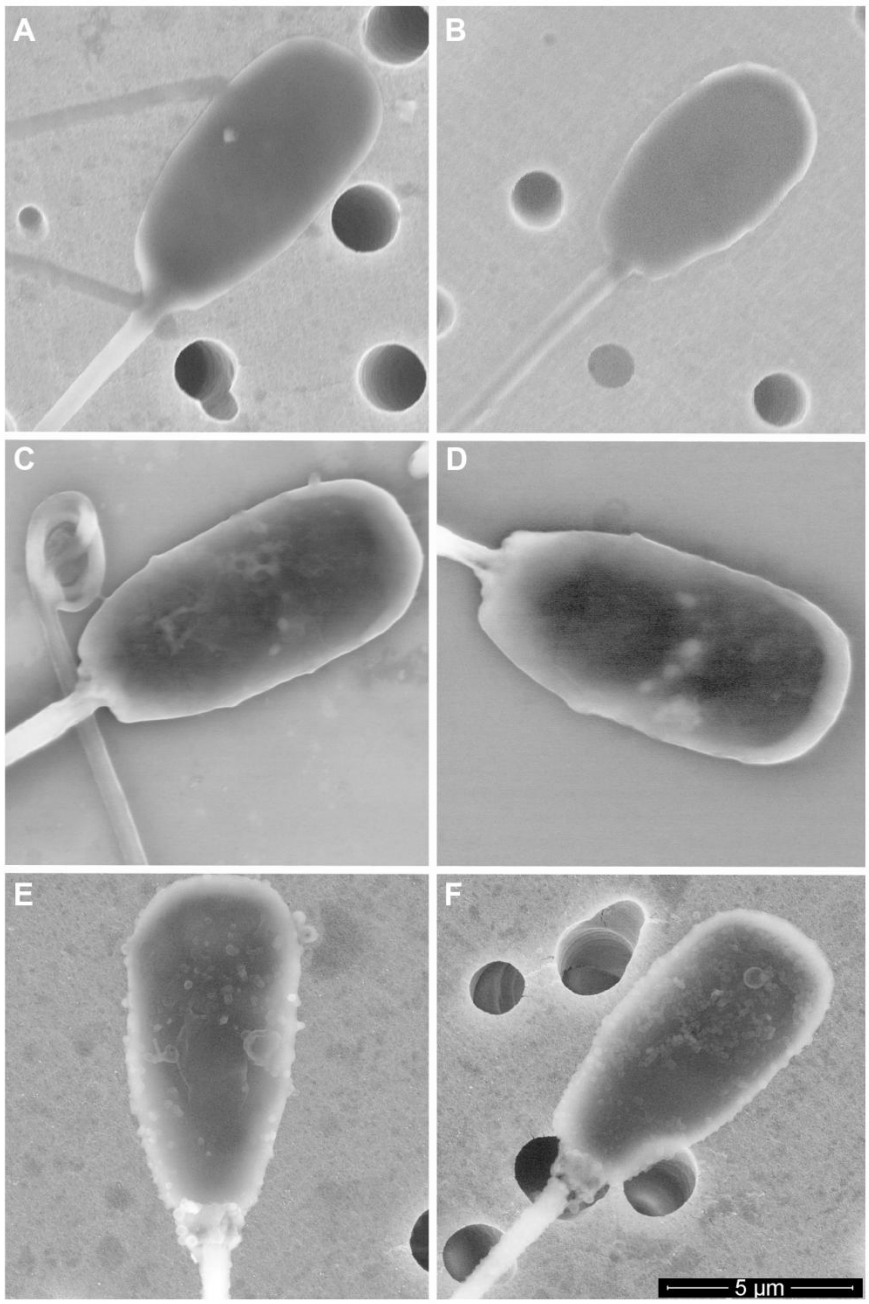

Fig. 4.1. Changes in the plasma/outer acrosomal membranes during capacitation and the AE of porcine spermatozoa, as visualized by ESEM. (A; B) Presence of a smooth plasma membrane/OAM of non-capacitated spermatozoa. (C; D) Upon completion of capacitation, most spermatozoa (6 out of 10) generally displayed ruffled plasma/outer acrosomal membrane. (E) Vesiculation of the acrosomal membranes was seen from spermatozoa that had initiated the AE upon stimulation with the of Ca^{2+} ionophore (7 out of 10). (F) Acrosomal shroud formation was observed to a varied degree in spermatozoa within the same sample stimulated by Ca^{2+} ionophore. Round holes originated from the carbon tabs which were used to mount the spermatozoa. Images were recorded using the FEI Quanta 600 FEG Extended Vacuum Scanning Electron Microscope set at 14,000 x magnification.

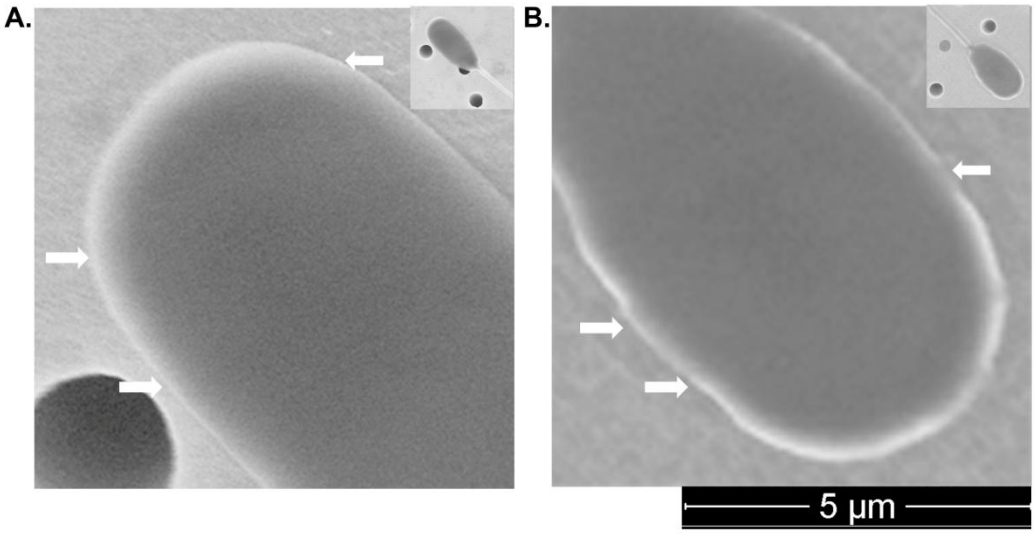

Fig. 4.2. Differences in the fine structure of acrosome-overlying membranes between non-capacitated and capacitated spermatozoa, visualized by ESEM. (A) Prior to capacitation, the plasma/outer acrosomal membrane (arrows) had a smooth appearance (7 out of 10). (B) Upon completion of the capacitation process, the plasma/outer acrosomal membrane became rippled (arrows), possibly in preparation for AE by the spermatozoa (6 out of 10). Note the difference in sperm head width and appearance between inserts of panels A& B. Round holes originated from the carbon tabs which were used to mount the spermatozoa. Images were recorded using the FEI Quanta 600 FEG Extended Vacuum Scanning Electron Microscope set at 14,000 x magnification.

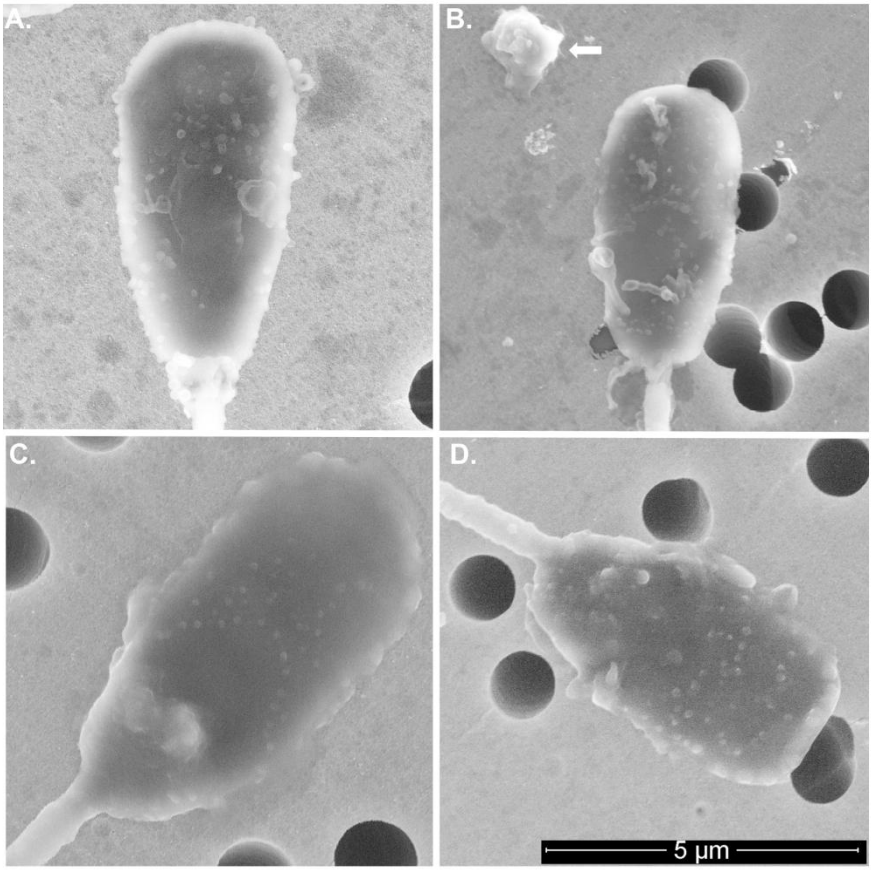

Fig. 4.3. Acrosomal exocytosis of capacitated boar spermatozoa exposed to of Ca^{2+} ionophore. (A) Blebbing and vesiculation of the plasma/outer acrosomal membranes of boar spermatozoon. Some of the vesicles separated from the acrosome and migrated distally towards the post acrosomal sheath and the sperm tail connecting piece. (B) Detached acrosomal shroud (arrow) next to a spermatozoon treated with Ca^{2+} ionophore. (C) Blebbing of acrosome along the equatorial segment of a spermatozoon exposed to Ca^{2+} ionophore for 1 hr. (D) Variation in patterns of acrosomal blebbing and vesicle size in Ca^{2+} ionophore treated spermatozoon. Round holes originated from the carbon tabs which were used to mount the spermatozoa. Images were recorded using the FEI Quanta 600 FEG Extended Vacuum Scanning Electron Microscope set at 14,000 x magnification.

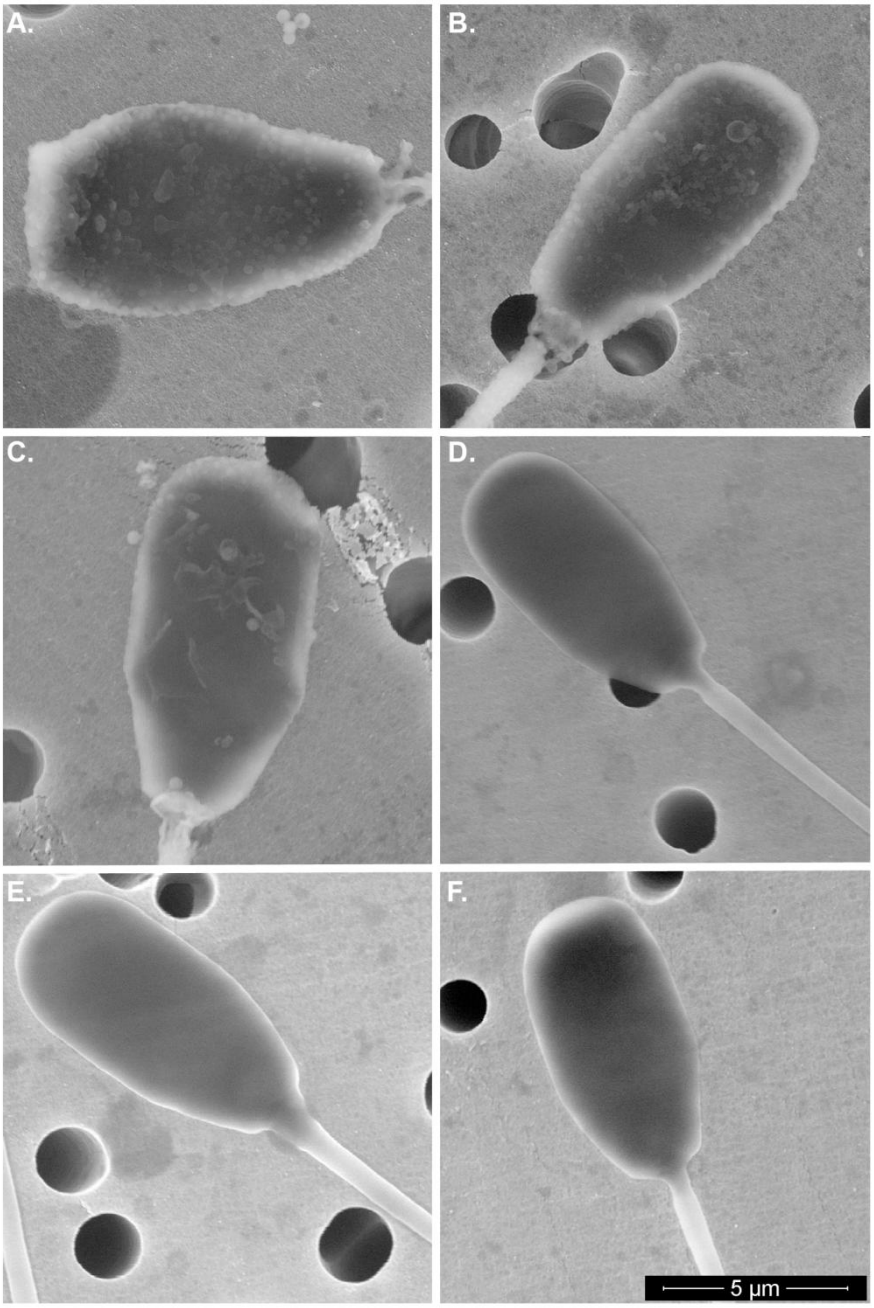

Fig. 4.4. Variation of acrosomal integrity in a population of spermatozoa treated with Ca^{2+} ionophore for 1 hr. (A) Extensive vesiculation of the sperm acrosome from one spermatozoon. (B-C) Patterns of acrosomal blebs varied within a given ionophore treatment from one boar spermatozoon to another. (D-F) Spermatozoa with smooth acrosomal membranes were also seen within the same treatment group, exposed to the Ca^{2+} ionophore (3 out of 10). Round holes originated from the carbon tabs which were used to mount the spermatozoa. Images were recorded using the FEI Quanta 600 FEG Extended Vacuum Scanning Electron Microscope set at 14,000 x magnification.

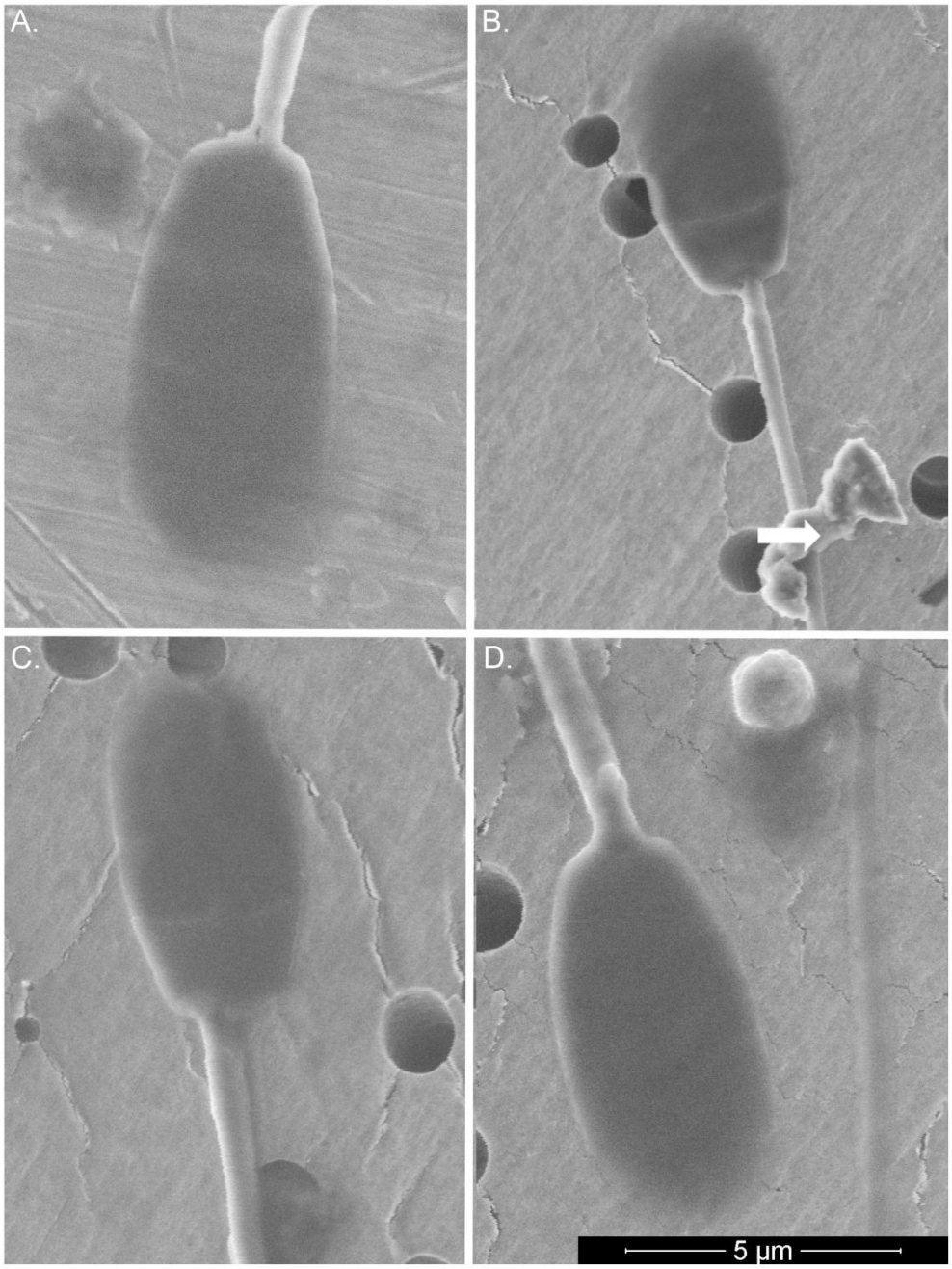

Fig. 4.5. Presence of proteasomal inhibitors prevents dispersion of acrosomal shrouds in spermatozoa co-incubated with sZP, as imaged by ESEM. (A, C) Capacitated spermatozoa co-incubated with sZP in the presence of vehicle solution of EtOH and DMSO resulted in expulsion of acrosomal contents as evident by the disappearance of the OAM. Dispersion of acrosomal contents resulted in the breakdown of the shroud. (B, D) Presence of the proteasomal inhibitor cocktail allowed the spermatozoa to undergo AE during coincubation with the sZP but prevented the dispersal of the acrosomal shrouds (6 out of 10, arrow in B), which in the absence of solid ZP-matrix detach from the exocytosed spermatozoa. Round holes originated from the carbon tabs which were used to mount the spermatozoa. Images were recorded using the FEI Quanta 600 FEG Extended Vacuum Scanning Electron Microscope set at 14,000 x magnification.

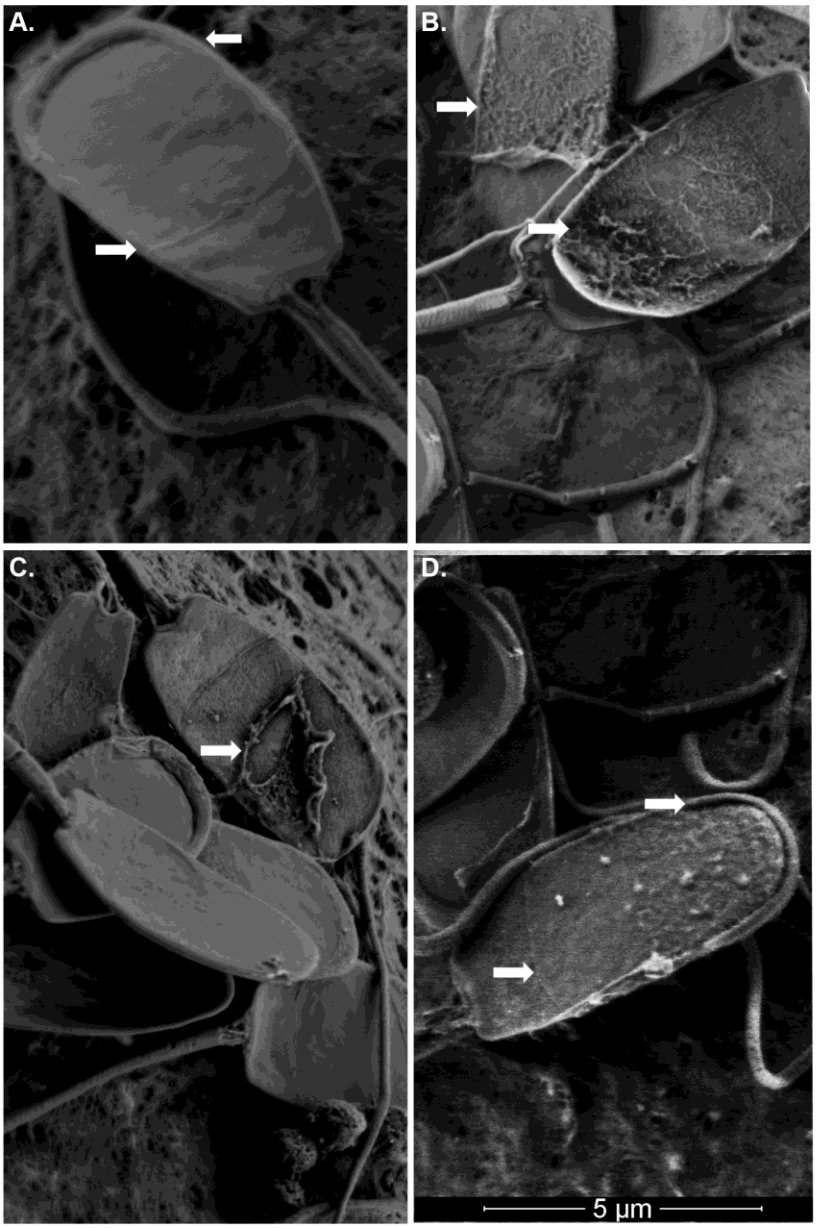

Fig. 4.6. Visualization of changes in acrosomal morphology and acrosomal exocytosis during porcine in vitro fertilization, using conventional SEM. (A, C) Due to plasma membrane damage by sample fixation and processing, the acrosomal matrix (upper arrow) was readily visible in the zona-bound spermatozoa prior to AE. The distal edge of the acosomal cap delineates the underlying equatorial segment (lower arrow). (B, C) Contary to ESEM, acrosomal shrouds (arrows) of the exocytosed, zona-bound spermatozoa were detectable but appeared to be poorly preserved. Images were recorded using the Hitachi S-4700 Scanning Electron Microscope set at 14,000 x magnification.

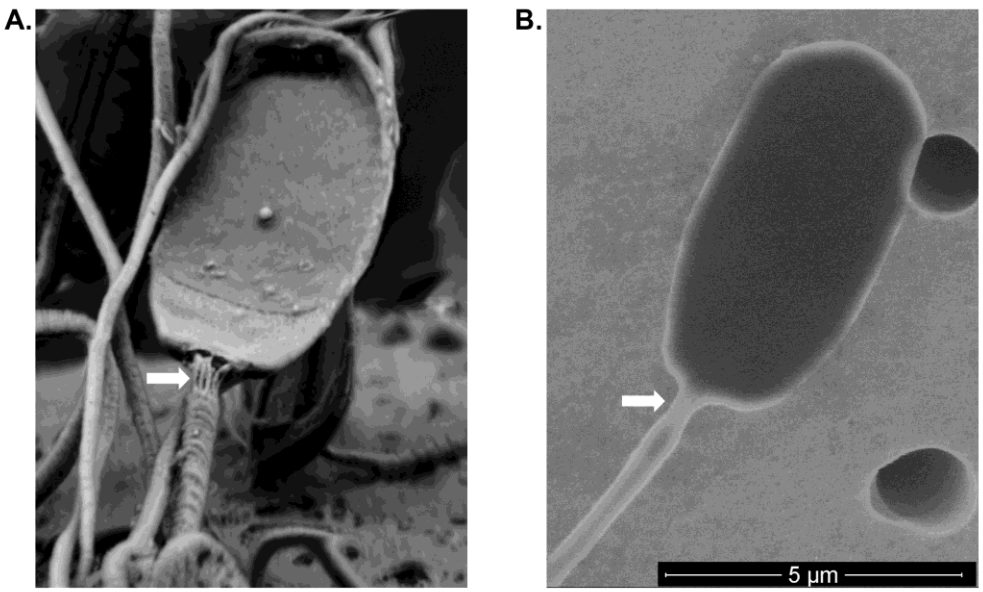

Fig. 4.7. Comparision of SEM and ESEM-captured surfaces of the membranes enveloping the connecting piece of boar spermatozoa. (A) Spermatozoon prepared for SEM analysis shows a lack of membranes at the connecting piece, revealing the striated columns of the outer dense fibers (arrow) located in this compartment. Lack of membranes at connecting piece lead to the determination that SEM samples were not representative of natural samples. (B) Spermatozoon prepared for ESEM retained the membrane covering the sperm tail connecting piece (arrow). Round holes (B) originated from the carbon tabs which were used to mount the spermatozoa. Images were recorded using the FEI Quanta 600 FEG Extended Vacuum Scanning Electron Microscope (ESEM) or Hitachi S-4700 Scanning Electron Microscope (SEM) set at 14,000 x magnification.

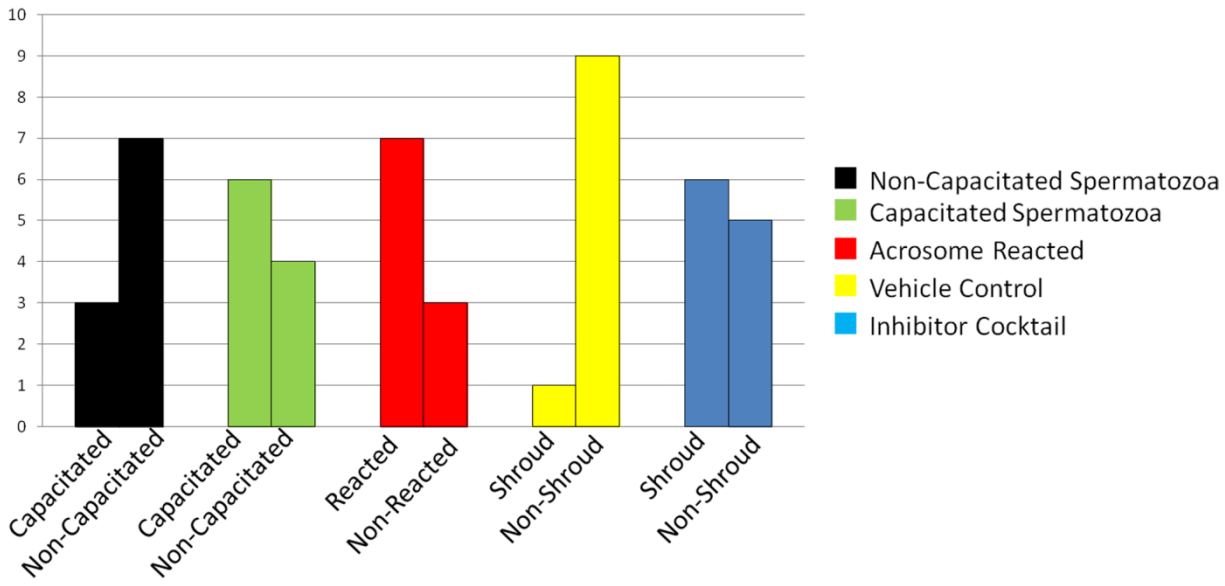

Fig. 4.8. Numerical values for acrosomal integrity during various stages of acrosomal exocytosis. Prior to capacitation the plasma/OAM was observed in a smooth appearance in 7 out of 10 spermatozoa (black bars). As the spermtozoa completed capacitation the plasma/OAM became ruffled, possible due to the removal of cholesterol and formation of lipid rafts, and could be visualized in 6 out of 10 spermatozoa (green). Once exposed to Ca^{2+} for 1 hr the sperm underwent AE and the presence of vesiculed arosomes could be seen in 7 out of 10 spermatozoa (red). In those treatments where spermatozoa were exposed to sZP the sperm completed the AE by dispersing the acrosomal shroud beyond identification (9 out of 10, yellow). However, use of the proteasomal inhibitor cocktail prevented this dispersion in every 6 out of 10 spermatozoa (blue).

CONCLUSIONS

The work conducted for this dissertation has provided substantial evidence that the Ubiquitin Proteasome System is active during porcine fertilization through both targeting and degradation of proteins. The presence of ubiquitinated lysines confirms the hypothesis that the porcine ZP glycoprotein ZPC is ubiquitinated prior to fertilization. Although the ZPC glycoprotein is ubiquitinated prior to fertilization there still remains active *de novo* ubiquitination during fertilization. Some of this active ubiquitination may be a result of a newly identified, in porcine, E3 ligase known as UBR7. The presence of these redundant ubiquitin chains results in the degradation of the ZPC glycoprotein as well as several acrosomal proteins by the 26S proteasome. Inhibition of the 26S proteasome, by proteasomal inhibitors, prevents the spermatozoa from successfully achieving fertilization. The use of proteasomal inhibitors prevents the ZP-induced acrosome remodeling by protecting several acrosomal proteins from degradation. Furthermore, the presence of proteasomal inhibitors also directly inhibits ZP protein degradation by resident sperm proteasomes during sperm-ZP penetration.

Collectively, this work provides the tools to modulate fertilization *in vitro* by altering the UPS. Whether it's by the use of active purified proteasomes to control polyspermy or proteasomal inhibitors to prevent overall fertilization, the UPS is the key. The results obtained within this dissertation greatly advance our understanding of the UPS during porcine fertilization and beyond. The remaining challenges will be to determine the requirement and activity of the UPS during other aspects of fertilization

i.e., spermiogenesis, capacitation and oocyte maturation, with the hope of producing better quality embryos through the deciphering and manipulation of sperm and oocyte derived ubiquitin proteasome systems.

VITA

Shawn Zimmerman was born and raised in the Chapman, Ks area. Shawn is the son and Susan and Ervin Zimmerman of Chapman and brother of Heather Mills of Wichita, Ks. Shawn graduated from Chapman High School in May 2000 and upon graduation Shawn attended Kansas State University in the Animal Science program. After completing his undergraduate degree in Animal Science in May 2005 he stayed at Kansas State University to attend graduate school. In August 2007 Shawn graduated with his Master's of Science degree in Reproductive Physiology under the mentoring of Dr. Tim Rozell.

In that same month Shawn began pursuing his PhD degree in Animal Science under the mentoring of Dr. Peter Sutovsky. Shawn continued his research under Dr. Sutovsky and will complete his PhD degree in Animal Science with an emphasis in Reproductive Physiology in May 2012.

Upon the completion of his degree, Shawn will become the Lead Embryologist for the Center for Reproductive Medicine and Robotic Surgery in St. Louis, Mo.

BIBLIOGRAPHY

Abeydeera LR, Wang WH, Prather RS, Day BN. 1998. Maturation in vitro of pig oocytes in protein-free culture media: fertilization and subsequent embryo development in vitro. Biol Reprod 58(5):1316-1320.

Akopian TN, Kisselev AF, Goldberg AL. 1997. Processive degradation of proteins and other catalytic properties of the proteasome from Thermoplasma acidophilum. J Biol Chem 272(3):1791-1798.

An JY, Seo JW, Tasaki T, Lee MJ, Varshavsky A, Kwon YT. 2006. Impaired neurogenesis and cardiovascular development in mice lacking the E3 ubiquitin ligases UBR1 and UBR2 of the N-end rule pathway. Proc Natl Acad Sci U S A 103(16):6212-6217.

Arcelay E, Salicioni AM, Wertheimer E, Visconti PE. 2008. Identification of proteins undergoing tyrosine phosphorylation during mouse sperm capacitation. Int J Dev Biol 52(5-6):463-472.

Austin CR. 1975. Membrane fusion events in fertilization. J Reprod Fertil 44(1):155-166.

Austin CR, Bishop MW. 1958. Role of the rodent acrosome and perforatorium in fertilization. Proc R Soc Lond B Biol Sci 149(935):241-248.

Baba T, Azuma S, Kashiwabara S, Toyoda Y. 1994a. Sperm from mice carrying a targeted mutation of the acrosin gene can penetrate the oocyte zona pellucida and effect fertilization. J Biol Chem 269(50):31845-31849.

Baba T, Kashiwabara S, Watanabe K, Itoh H, Michikawa Y, Kimura K, Takada M, Fukamizu A, Arai Y. 1989. Activation and maturation mechanisms of boar acrosin zymogen based on the deduced primary structure. J Biol Chem 264(20):11920-11927.

Baba T, Niida Y, Michikawa Y, Kashiwabara S, Kodaira K, Takenaka M, Kohno N, Gerton GL, Arai Y. 1994b. An acrosomal protein, sp32, in mammalian sperm is a binding

protein specific for two proacrosins and an acrosin intermediate. J Biol Chem 269(13):10133-10140.

Bagola K, Mehnert M, Jarosch E, Sommer T. Protein dislocation from the ER. Biochim Biophys Acta.

Bailey JL. 2010. Factors regulating sperm capacitation. Syst Biol Reprod Med 56(5):334-348.

Baker MA, Smith ND, Hetherington L, Taubman K, Graham ME, Robinson PJ, Aitken RJ. 2010. Label-free quantitation of phosphopeptide changes during rat sperm capacitation. J Proteome Res 9(2):718-729.

Bardag-Gorce F, Riley N, Nguyen V, Montgomery RO, French BA, Li J, van Leeuwen FW, Lungo W, McPhaul LW, French SW. 2003. The mechanism of cytokeratin aggresome formation: the role of mutant ubiquitin (UBB+1). Experimental and molecular pathology 74(2):160-167.

Bardag-Gorce F, van Leeuwen FW, Nguyen V, French BA, Li J, Riley N, McPhaul LW, Lue YH, French SW. 2002. The role of the ubiquitin-proteasome pathway in the formation of mallory bodies. Experimental and molecular pathology 73(2):75-83.

Bedford JM. 1998. Mammalian fertilization misread? Sperm penetration of the eutherian zona pellucida is unlikely to be a lytic event. Biol Reprod 59(6):1275-1287.

Bedford JM. 2008. Puzzles of mammalian fertilization--and beyond. Int J Dev Biol 52(5-6):415-426.

Belote JM, Miller M, Smyth KA. 1998. Evolutionary conservation of a testes-specific proteasome subunit gene in Drosophila. Gene 215(1):93-100.

Blackmore DG, Baillie LR, Holt JE, Dierkx L, Aitken RJ, McLaughlin EA. 2004. Biosynthesis of the canine zona pellucida requires the integrated participation of both oocytes and granulosa cells. Biol Reprod 71(2):661-668.

Bleil JD, Wassarman PM. 1980. Mammalian sperm-egg interaction: identification of a glycoprotein in mouse egg zonae pellucidae possessing receptor activity for sperm. Cell 20(3):873-882.

Bohring C, Krause E, Habermann B, Krause W. 2001. Isolation and identification of sperm membrane antigens recognized by antisperm antibodies, and their possible role in immunological infertility disease. Mol Hum Reprod 7(2):113-118.

Bohring C, Krause W. 2003. Characterization of spermatozoa surface antigens by antisperm antibodies and its influence on acrosomal exocytosis. Am J Reprod Immunol 50(5):411-419.

Brychcy M, Kuckelkorn U, Hausdorf G, Egerer K, Kloetzel PM, Burmester GR, Feist E. 2006. Anti-20S proteasome autoantibodies inhibit proteasome stimulation by proteasome activator PA28. Arthritis Rheum 54(7):2175-2183.

Buffone MG, Foster JA, Gerton GL. 2008. The role of the acrosomal matrix in fertilization. Int J Dev Biol 52(5-6):511-522.

Burkin HR, Paula Alves-Vieira A, Miller DJ. 2004. Localization of zona pellucida receptors on live sperm by fluorophore-conjugated solubilized zona pellucida proteins. Methods Mol Biol 253:79-93.

Chakravarty S, Bansal P, Sutovsky P, Gupta SK. 2008. Role of proteasomal activity in the induction of acrosomal exocytosis in human spermatozoa. Reprod Biomed Online 16(3):391-400.

Choi WS, Jeong BC, Joo YJ, Lee MR, Kim J, Eck MJ, Song HK. 2010. Structural basis for the recognition of N-end rule substrates by the UBR box of ubiquitin ligases. Nat Struct Mol Biol 17(10):1175-1181.

Choi YJ, Uhm SJ, Song SJ, Song H, Park JK, Kim T, Park C, Kim JH. 2008. Cytochrome c upregulation during capacitation and spontaneous acrosome reaction determines the fate of pig sperm cells: linking proteome analysis. J Reprod Dev 54(1):68-83.

Coux O, Tanaka K, Goldberg AL. 1996. Structure and functions of the 20S and 26S proteasomes. Annu Rev Biochem 65:801-847.

Dalo DT, McCaffery JM, Evans JP. 2008. Ultrastructural analysis of egg membrane abnormalities in post-ovulatory aged eggs. Int J Dev Biol 52(5-6):535-544.

Diaz ES, Kong M, Morales P. 2007. Effect of fibronectin on proteasome activity, acrosome reaction, tyrosine phosphorylation and intracellular calcium concentrations of human sperm. Hum Reprod 22(5):1420-1430.

Edwards SE, Buffone MG, Knee GR, Rossato M, Bonanni G, Masiero S, Ferasin S, Gerton GL, Moss SB, Williams CJ. 2007. Effects of extracellular adenosine 5'-triphosphate on human sperm motility. Reprod Sci 14(7):655-666.

Einspanier R, Schuster H, Schams D. 1993. A comparison of hormone levels in follicle-lutein-cysts and in normal bovine ovarian follicles. Theriogenology 40(1):181-188.

Ekhlasi-Hundrieser M, Gohr K, Wagner A, Tsolova M, Petrunkina A, Topfer-Petersen E. 2005. Spermadhesin AQN1 is a candidate receptor molecule involved in the formation of the oviductal sperm reservoir in the pig. Biol Reprod 73(3):536-545.

Familiari G, Relucenti M, Heyn R, Micara G, Correr S. 2006. Three-dimensional structure of the zona pellucida at ovulation. Microscopy research and technique 69(6):415-426.

Fischer DF, De Vos RA, Van Dijk R, De Vrij FM, Proper EA, Sonnemans MA, Verhage MC, Sluijs JA, Hobo B, Zouambia M, Steur EN, Kamphorst W, Hol EM, Van Leeuwen FW. 2003. Disease-specific accumulation of mutant ubiquitin as a marker for proteasomal dysfunction in the brain. Faseb J 17(14):2014-2024.

Fischer KA, Van Leyen K, Lovercamp KW, Manandhar G, Sutovsky M, Feng D, Safranski T, Sutovsky P. 2005. 15-Lipoxygenase is a component of the mammalian sperm cytoplasmic droplet. Reproduction 130(2):213-222.

Flechon JE, Degrouard J, Kopecny V, Pivko J, Pavlok A, Motlik J. 2003. The extracellular matrix of porcine mature oocytes: origin, composition and presumptive roles. Reprod Biol Endocrinol 1:124.

Fong GH, Takeda K. 2008. Role and regulation of prolyl hydroxylase domain proteins. Cell Death Differ 15(4):635-641.

Foster JA, Friday BB, Maulit MT, Blobel C, Winfrey VP, Olson GE, Kim KS, Gerton GL. 1997. AM67, a secretory component of the guinea pig sperm acrosomal matrix, is related to mouse sperm protein sp56 and the complement component 4-binding proteins. J Biol Chem 272(19):12714-12722.

Furukawa M, Ohta T, Xiong Y. 2002. Activation of UBC5 ubiquitin-conjugating enzyme by the RING finger of ROC1 and assembly of active ubiquitin ligases by all cullins. J Biol Chem 277(18):15758-15765.

Glickman MH, Ciechanover A. 2002. The ubiquitin-proteasome proteolytic pathway: destruction for the sake of construction. Physiol Rev 82(2):373-428.

Goeckeler JL, Brodsky JL. Molecular chaperones and substrate ubiquitination control the efficiency of endoplasmic reticulum-associated degradation. Diabetes Obes Metab 12 Suppl 2:32-38.

Green DP. 1987. Mammalian sperm cannot penetrate the zona pellucida solely by force. Exp Cell Res 169(1):31-38.

Green DP, Purves RD. 1984. Mechanical hypothesis of sperm penetration. Biophys J 45(4):659-662.

Gupta M, Gupta SK. 1994. Characterization of antigenic determinants on porcine zona pellucida-3 beta(ZP3 beta) glycoprotein by monoclonal antibodies. Indian J Exp Biol 32(6):376-381.

Gupta SK, Bagavant H, Chadha K, Gupta M, Yurewicz EC, Sacco AG. 1993. Mapping of immunogenic domains on porcine zona pellucida 3 alpha and beta glycoproteins by murine monoclonal antibodies. Am J Reprod Immunol 30(2-3):95-100.

Gupta SK, Yurewicz EC, Afzalpurkar A, Rao KV, Gage DA, Wu H, Sacco AG. 1995. Localization of epitopes for monoclonal antibodies at the N-terminus of the porcine zona pellucida glycoprotein pZPC. Mol Reprod Dev 42(2):220-225.

Guterman A, Glickman MH. 2004. Deubiquitinating enzymes are IN/(trinsic to proteasome function). Curr Protein Pept Sci 5(3):201-211.

Hagaman JR, Moyer JS, Bachman ES, Sibony M, Magyar PL, Welch JE, Smithies O, Krege JH, O'Brien DA. 1998. Angiotensin-converting enzyme and male fertility. Proc Natl Acad Sci U S A 95(5):2552-2557.

Hedrick JL. 2008. Anuran and pig egg zona pellucida glycoproteins in fertilization and early development. Int J Dev Biol 52(5-6):683-701.

Hendil KB. 1988. The 19 S multicatalytic "prosome" proteinase is a constitutive enzyme in HeLa cells. Biochem Int 17(3):471-477.

Hernandez M, Ekwall H, Roca J, Vazquez JM, Martinez E, Rodriguez-Martinez H. 2007. Cryo-scanning electron microscopy (Cryo-SEM) of semen frozen in medium-straws from good and sub-standard freezer AI-boars. Cryobiology 54(1):63-70.

Hershko A, Ciechanover A. 1998. The ubiquitin system. Annu Rev Biochem 67:425-479.

Honda A, Siruntawineti J, Baba T. 2002a. Role of acrosomal matrix proteases in sperm-zona pellucida interactions. Hum Reprod Update 8(5):405-412.

Honda A, Yamagata K, Sugiura S, Watanabe K, Baba T. 2002b. A mouse serine protease TESP5 is selectively included into lipid rafts of sperm membrane presumably as a glycosylphosphatidylinositol-anchored protein. J Biol Chem 277(19):16976-16984.

Hoshi M, Numakunai T, Sawada H. 1981. Evidence for participation of sperm proteinases in fertilization of the solitary ascidian, Halocynthia roretzi: effects of protease inhibitors. Dev Biol 86(1):117-121.

Huo LJ, Fan HY, Zhong ZS, Chen DY, Schatten H, Sun QY. 2004. Ubiquitin-proteasome pathway modulates mouse oocyte meiotic maturation and fertilization via regulation of MAPK cascade and cyclin B1 degradation. Mech Dev 121(10):1275-1287.

Husnjak K, Elsasser S, Zhang N, Chen X, Randles L, Shi Y, Hofmann K, Walters KJ, Finley D, Dikic I. 2008. Proteasome subunit Rpn13 is a novel ubiquitin receptor. Nature 453(7194):481-488.

Jenkins Y, Markovtsov V, Lang W, Sharma P, Pearsall D, Warner J, Franci C, Huang B, Huang J, Yam GC, Vistan JP, Pali E, Vialard J, Janicot M, Lorens JB, Payan DG, Hitoshi Y. 2005. Critical role of the ubiquitin ligase activity of UHRF1, a nuclear RING finger protein, in tumor cell growth. Mol Biol Cell 16(12):5621-5629.

Jin M, Fujiwara E, Kakiuchi Y, Okabe M, Satouh Y, Baba SA, Chiba K, Hirohashi N. 2011. Most fertilizing mouse spermatozoa begin their acrosome reaction before contact with the zona pellucida during in vitro fertilization. Proc Natl Acad Sci U S A 108(12):4892-4896.

Karabinova P, Kubelka M, Susor A. Proteasomal degradation of ubiquitinated proteins in oocyte meiosis and fertilization in mammals. Cell Tissue Res 346(1):1-9.

Kawano N, Kang W, Yamashita M, Koga Y, Yamazaki T, Hata T, Miyado K, Baba T. 2010. Mice Lacking Two Sperm Serine Proteases, ACR and PRSS21, Are Subfertile, but the Mutant Sperm Are Infertile In Vitro. Biol Reprod.

Kessler R, Hausmann G, Basler K. 2009. The PHD domain is required to link Drosophila Pygopus to Legless/beta-catenin and not to histone H3. Mech Dev 126(8-9):752-759.

Khor B, Bredemeyer AL, Huang CY, Turnbull IR, Evans R, Maggi LB, Jr., White JM, Walker LM, Carnes K, Hess RA, Sleckman BP. 2006. Proteasome activator PA200 is required for normal spermatogenesis. Mol Cell Biol 26(8):2999-3007.

Kim E, Yamashita M, Kimura M, Honda A, Kashiwabara S, Baba T. 2008. Sperm penetration through cumulus mass and zona pellucida. Int J Dev Biol 52(5-6):677-682.

Kim KS, Foster JA, Gerton GL. 2001. Differential release of guinea pig sperm acrosomal components during exocytosis. Biol Reprod 64(1):148-156.

Kim KS, Gerton GL. 2003. Differential release of soluble and matrix components: evidence for intermediate states of secretion during spontaneous acrosomal exocytosis in mouse sperm. Dev Biol 264(1):141-152.

Kloetzel PM. 2004. The proteasome and MHC class I antigen processing. Biochim Biophys Acta 1695(1-3):225-233.

Koegl M, Hoppe T, Schlenker S, Ulrich HD, Mayer TU, Jentsch S. 1999. A novel ubiquitination factor, E4, is involved in multiubiquitin chain assembly. Cell 96(5):635-644.

Kolle S, Sinowatz F, Boie G, Totzauer I, Amselgruber W, Plendl J. 1996. Localization of the mRNA encoding the zona protein ZP3 alpha in the porcine ovary, oocyte and embryo by non-radioactive in situ hybridization. Histochem J 28(6):441-447.

Kong M, Diaz ES, Morales P. 2009. Participation of the Human Sperm Proteasome in the Capacitation Process and Its Regulation by Protein Kinase A and Tyrosine Kinase. Biol Reprod.

Krawiec BJ, Nystrom GJ, Frost RA, Jefferson LS, Lang CH. 2007. AMP-activated protein kinase agonists increase mRNA content of the muscle-specific ubiquitin ligases MAFbx and MuRF1 in C2C12 cells. Am J Physiol Endocrinol Metab 292(6):E1555-1567.

Kwon YT, Reiss Y, Fried VA, Hershko A, Yoon JK, Gonda DK, Sangan P, Copeland NG, Jenkins NA, Varshavsky A. 1998. The mouse and human genes encoding the recognition component of the N-end rule pathway. Proc Natl Acad Sci U S A 95(14):7898-7903.

Lambert CC, Someno T, Sawada H. 2002. Sperm surface proteases in ascidian fertilization. J Exp Zool 292(1):88-95.

Lee MJ, Pal K, Tasaki T, Roy S, Jiang Y, An JY, Banerjee R, Kwon YT. 2008. Synthetic heterovalent inhibitors targeting recognition E3 components of the N-end rule pathway. Proc Natl Acad Sci U S A 105(1):100-105.

Lee VH. 2000. Expression of rabbit zona pellucida-1 messenger ribonucleic acid during early follicular development. Biol Reprod 63(2):401-408.

Lupas A, Koster AJ, Baumeister W. 1993. Structural features of 26S and 20S proteasomes. Enzyme Protein 47(4-6):252-273.

Luria A, Rubinstein S, Lax Y, Breitbart H. 2002. Extracellular adenosine triphosphate stimulates acrosomal exocytosis in bovine spermatozoa via P2 purinoceptor. Biol Reprod 66(2):429-437.

Maia-Brigagao C, de Souza W. 2012. Using environmental scanning electron microscopy (ESEM) as a quantitative method to analyse the attachment of Giardia duodenalis to epithelial cells. Micron 43(2-3):494-496.

Mao I, Liu J, Li X, Luo H. 2008. REGgamma, a proteasome activator and beyond? Cell Mol Life Sci 65(24):3971-3980.

Miller J, McLachlan AD, Klug A. 1985. Repetitive zinc-binding domains in the protein transcription factor IIIA from Xenopus oocytes. Embo J 4(6):1609-1614.

Mochida K, Tres LL, Kierszenbaum AL. 2000. Structural features of the 26S proteasome complex isolated from rat testis and sperm tail. Mol Reprod Dev 57(2):176-184.

Morales P, Diaz ES, Kong M. 2007. Proteasome activity and its relationship with protein phosphorylation during capacitation and acrosome reaction in human spermatozoa. Soc Reprod Fertil Suppl 65:269-273.

Morales P, Kong M, Pizarro E, Pasten C. 2003. Participation of the sperm proteasome in human fertilization. Hum Reprod 18(5):1010-1017.

Morales P, Overstreet JW, Katz DF. 1988. Changes in human sperm motion during capacitation in vitro. J Reprod Fertil 83(1):119-128.

Morales P, Pizarro E, Kong M, Jara M. 2004. Extracellular localization of proteasomes in human sperm. Mol Reprod Dev 68(1):115-124.

Moreno RD, Alvarado CP. 2006. The mammalian acrosome as a secretory lysosome: new and old evidence. Mol Reprod Dev 73(11):1430-1434.

Mtango NR, Latham KE. 2007. Ubiquitin proteasome pathway gene expression varies in rhesus monkey oocytes and embryos of different developmental potential. Physiol Genomics 31(1):1-14.

Mtango NR, Sutovsky M, Vandevoort CA, Latham KE, Sutovsky P. 2011. Essential role of ubiquitin C-terminal hydrolases UCHL1 and UCHL3 in mammalian oocyte maturation. J Cell Physiol.

Nakanishi T, Ikawa M, Yamada S, Toshimori K, Okabe M. 2001. Alkalinization of acrosome measured by GFP as a pH indicator and its relation to sperm capacitation. Dev Biol 237(1):222-231.

Naz RK, Dhandapani L. Identification of human sperm proteins that interact with human zona pellucida3 (ZP3) using yeast two-hybrid system. J Reprod Immunol 84(1):24-31.

Naz RK, Dhandapani L. 2010. Identification of human sperm proteins that interact with human zona pellucida3 (ZP3) using yeast two-hybrid system. J Reprod Immunol 84(1):24-31.

Oddo S. 2008. The ubiquitin-proteasome system in Alzheimer's disease. J Cell Mol Med 12(2):363-373.

Olds-Clarke P. 2003. Unresolved issues in mammalian fertilization. Int Rev Cytol 232:129-184.

Ortega J, Heymann JB, Kajava AV, Ustrell V, Rechsteiner M, Steven AC. 2005. The axial channel of the 20S proteasome opens upon binding of the PA200 activator. J Mol Biol 346(5):1221-1227.

Pasten C, Morales P, Kong M. 2005. Role of the sperm proteasome during fertilization and gamete interaction in the mouse. Mol Reprod Dev 71(2):209-219.

Peng J, Schwartz D, Elias JE, Thoreen CC, Cheng D, Marsischky G, Roelofs J, Finley D, Gygi SP. 2003. A proteomics approach to understanding protein ubiquitination. Nat Biotechnol 21(8):921-926.

Pickart CM. 2001. Mechanisms underlying ubiquitination. Annu Rev Biochem 70:503-533.

Psenicka M, Tesarova M, Tesitel J, Nebesarova J. 2010. Size determination of Acipenser ruthenus spermatozoa in different types of electron microscopy. Micron 41(5):455-460.

Qi H, Williams Z, Wassarman PM. 2002. Secretion and assembly of zona pellucida glycoproteins by growing mouse oocytes microinjected with epitope-tagged cDNAs for mZP2 and mZP3. Mol Biol Cell 13(2):530-541.

Rawe VY, Diaz ES, Abdelmassih R, Wojcik C, Morales P, Sutovsky P, Chemes HE. 2008. The role of sperm proteasomes during sperm aster formation and early zygote development: implications for fertilization failure in humans. Hum Reprod 23(3):573-580.

Rechsteiner M, Hill CP. 2005. Mobilizing the proteolytic machine: cell biological roles of proteasome activators and inhibitors. Trends Cell Biol 15(1):27-33.

Redgrove KA, Anderson AL, Dun MD, McLaughlin EA, O'Bryan MK, Aitken RJ, Nixon B. 2011. Involvement of multimeric protein complexes in mediating the capacitation-dependent binding of human spermatozoa to homologous zonae pellucidae. Dev Biol 356(2):460-474.

Reidlinger J, Pike AM, Savory PJ, Murray RZ, Rivett AJ. 1997. Catalytic properties of 26 S and 20 S proteasomes and radiolabeling of MB1, LMP7, and C7 subunits associated with trypsin-like and chymotrypsin-like activities. J Biol Chem 272(40):24899-24905.

Rivkin E, Cullinan EB, Tres LL, Kierszenbaum AL. 1997. A protein associated with the manchette during rat spermiogenesis is encoded by a gene of the TBP-1-like subfamily with highly conserved ATPase and protease domains. Mol Reprod Dev 48(1):77-89.

Rivkin E, Kierszenbaum AL, Gil M, Tres LL. 2009. Rnf19a, a ubiquitin protein ligase, and Psmc3, a component of the 26S proteasome, tether to the acrosome membranes and the head-tail coupling apparatus during rat spermatid development. Dev Dyn 238(7):1851-1861.

Rodriguez-Miranda E, Buffone MG, Edwards SE, Ord TS, Lin K, Sammel MD, Gerton GL, Moss SB, Williams CJ. 2008. Extracellular adenosine 5'-triphosphate alters motility and improves the fertilizing capability of mouse sperm. Biol Reprod 79(1):164-171.

Ross CA, Pickart CM. 2004. The ubiquitin-proteasome pathway in Parkinson's disease and other neurodegenerative diseases. Trends Cell Biol 14(12):703-711.

Rossato M, La Sala GB, Balasini M, Taricco F, Galeazzi C, Ferlin A, Foresta C. 1999. Sperm treatment with extracellular ATP increases fertilization rates in in-vitro fertilization for male factor infertility. Hum Reprod 14(3):694-697.

Sakai N, Sawada MT, Sawada H. 2004. Non-traditional roles of ubiquitin-proteasome system in fertilization and gametogenesis. Int J Biochem Cell Biol 36(5):776-784.

Sanchez R, Deppe M, Schulz M, Bravo P, Villegas J, Morales P, Risopatron J. 2009. Participation of the sperm proteasome during in vitro fertilisation and the acrosome reaction in cattle. Andrologia 43(2):114-120.

Sanchez R, Deppe M, Schulz M, Bravo P, Villegas J, Morales P, Risopatron J. 2011. Participation of the sperm proteasome during in vitro fertilisation and the acrosome reaction in cattle. Andrologia 43(2):114-120.

Sawada H. 2002. Ascidian sperm lysin system. Zoolog Sci 19(2):139-151.

Sawada H, Sakai N, Abe Y, Tanaka E, Takahashi Y, Fujino J, Kodama E, Takizawa S, Yokosawa H. 2002. Extracellular ubiquitination and proteasome-mediated degradation of the ascidian sperm receptor. Proc Natl Acad Sci U S A 99(3):1223-1228.

Sawada H, Yokosawa H, Someno T, Saino T, Ishii S. 1984. Evidence for the participation of two sperm proteases, spermosin and acrosin, in fertilization of the ascidian, Halocynthia roretzi: inhibitory effects of leupeptin analogs on enzyme activities and fertilization. Dev Biol 105(1):246-249.

Sekiguchi S, Kwon J, Yoshida E, Hamasaki H, Ichinose S, Hideshima M, Kuraoka M, Takahashi A, Ishii Y, Kyuwa S, Wada K, Yoshikawa Y. 2006. Localization of ubiquitin C-terminal hydrolase L1 in mouse ova and its function in the plasma membrane to block polyspermy. Am J Pathol 169(5):1722-1729.

Shabek N, Herman-Bachinsky Y, Ciechanover A. 2009. Ubiquitin degradation with its substrate, or as a monomer in a ubiquitination-independent mode, provides clues to proteasome regulation. Proc Natl Acad Sci U S A 106(29):11907-11912.

Sixt SU, Dahlmann B. 2008. Extracellular, circulating proteasomes and ubiquitin - incidence and relevance. Biochim Biophys Acta 1782(12):817-823.

Sriram SM, Kim BY, Kwon YT. 2011. The N-end rule pathway: emerging functions and molecular principles of substrate recognition. Nat Rev Mol Cell Biol 12(11):735-747.

Susor A, Liskova L, Toralova T, Pavlok A, Pivonkova K, Karabinova P, Lopatarova M, Sutovsky P, Kubelka M. 2010. Role of ubiquitin C-terminal hydrolase-L1 in antipolyspermy defense of mammalian oocytes. Biol Reprod 82(6):1151-1161.

Sutovsky P. 2003. Ubiquitin-dependent proteolysis in mammalian spermatogenesis, fertilization, and sperm quality control: killing three birds with one stone. Microsc Res Tech 61(1):88-102.

Sutovsky P. 2004. Visualization of sperm accessory structures in the mammalian spermatids, spermatozoa, and zygotes by immunofluorescence, confocal, and immunoelectron microscopy. Methods Mol Biol 253:59-77.

Sutovsky P, Manandhar G, McCauley TC, Caamano JN, Sutovsky M, Thompson WE, Day BN. 2004. Proteasomal interference prevents zona pellucida penetration and fertilization in mammals. Biol Reprod 71(5):1625-1637.

Sutovsky P, Prather RS. 2004. Nuclear remodeling after SCNT: a contractor's nightmare. Trends Biotechnol 22(5):205-208.

Tanaka K, Suzuki T, Hattori N, Mizuno Y. 2004. Ubiquitin, proteasome and parkin. Biochim Biophys Acta 1695(1-3):235-247.

Tantibhedhyangkul J, Weerachatyanukul W, Carmona E, Xu H, Anupriwan A, Michaud D, Tanphaichitr N. 2002. Role of sperm surface arylsulfatase A in mouse sperm-zona pellucida binding. Biol Reprod 67(1):212-219.

Tapia S, Rojas M, Morales P, Ramirez MA, Diaz ES. 2011. The laminin-induced acrosome reaction in human sperm is mediated by Src kinases and the proteasome. Biol Reprod 85(2):357-366.

Tasaki T, Mulder LC, Iwamatsu A, Lee MJ, Davydov IV, Varshavsky A, Muesing M, Kwon YT. 2005. A family of mammalian E3 ubiquitin ligases that contain the UBR box motif and recognize N-degrons. Mol Cell Biol 25(16):7120-7136.

Tasaki T, Sohr R, Xia Z, Hellweg R, Hortnagl H, Varshavsky A, Kwon YT. 2007. Biochemical and genetic studies of UBR3, a ubiquitin ligase with a function in olfactory and other sensory systems. J Biol Chem 282(25):18510-18520.

Tasaki T, Zakrzewska A, Dudgeon DD, Jiang Y, Lazo JS, Kwon YT. 2009. The substrate recognition domains of the N-end rule pathway. J Biol Chem 284(3):1884-1895.

Tengowski MW, Feng D, Sutovsky M, Sutovsky P. 2007. Differential expression of genes encoding constitutive and inducible 20S proteasomal core subunits in the testis and epididymis of theophylline- or 1,3-dinitrobenzene-exposed rats. Biol Reprod 76(1):149-163.

Tulsiani DR, Abou-Haila A. 2001. Mammalian sperm molecules that are potentially important in interaction with female genital tract and egg vestments. Zygote 9(1):51-69.

Urayama S, Harada Y, Nakagawa Y, Ban S, Akasaka M, Kawasaki N, Sawada H. 2008. Ascidian sperm glycosylphosphatidylinositol-anchored CRISP-like protein as a binding partner for an allorecognizable sperm receptor on the vitelline coat. J Biol Chem 283(31):21725-21733.

Ustrell V, Hoffman L, Pratt G, Rechsteiner M. 2002. PA200, a nuclear proteasome activator involved in DNA repair. Embo J 21(13):3516-3525.

van Leeuwen FW, de Kleijn DP, van den Hurk HH, Neubauer A, Sonnemans MA, Sluijs JA, Koycu S, Ramdjielal RD, Salehi A, Martens GJ, Grosveld FG, Peter J, Burbach H, Hol EM. 1998. Frameshift mutants of beta amyloid precursor protein and ubiquitin-B in Alzheimer's and Down patients. Science 279(5348):242-247.

van Tijn P, de Vrij FM, Schuurman KG, Dantuma NP, Fischer DF, van Leeuwen FW, Hol EM. 2007. Dose-dependent inhibition of proteasome activity by a mutant ubiquitin associated with neurodegenerative disease. J Cell Sci 120(Pt 9):1615-1623.

Vazquez JM, Martinez E, Pastor LM, Roca J, Matas C, Calvo A. 1996. Lectin histochemistry during in vitro capacitation and acrosome reaction in boar spermatozoa: new lectins for evaluating acrosomal status of boar spermatozoa. Acta Histochem 98(1):93-100.

Wing SS, Bedard N, Morales C, Hingamp P, Trasler J. 1996. A novel rat homolog of the Saccharomyces cerevisiae ubiquitin-conjugating enzymes UBC4 and UBC5 with distinct biochemical features is induced during spermatogenesis. Mol Cell Biol 16(8):4064-4072.

Wojcik C, Benchaib M, Lornage J, Czyba JC, Guerin JF. 2000. Proteasomes in human spermatozoa. Int J Androl 23(3):169-177.

Wojcik C, Di Napoli M. 2004. Ubiquitin-proteasome system and proteasome inhibition: new strategies in stroke therapy. Stroke 35(6):1506-1518.

Wu JT, Chiang KC, Cheng FP. 2006. Expression of progesterone receptor(s) during capacitation and incidence of acrosome reaction induced by progesterone and zona proteins in boar spermatozoa. Anim Reprod Sci 93(1-2):34-45.

Xu P, Duong DM, Seyfried NT, Cheng D, Xie Y, Robert J, Rush J, Hochstrasser M, Finley D, Peng J. 2009. Quantitative proteomics reveals the function of unconventional ubiquitin chains in proteasomal degradation. Cell 137(1):133-145.

Yanagimachi R. 1994. Mammalian fertilization. . Knobil E, Neill J, editors. New York: Raven Press.

Yanagimachi R. 2009. Germ cell research: a personal perspective. Biol Reprod 80(2):204-218.

Yao T, Cohen RE. 2002. A cryptic protease couples deubiquitination and degradation by the proteasome. Nature 419(6905):403-407.

Yi Y-J, Park C-S, Kim E-S, Song E-S, Jeong J-H, Sutovsky P. 2009a. Sperm-surface ATP in boar spermatozoa is required for fertilization: Relevance to sperm proteasomal function. Systems Biology in Reproductive Medicine 55(In press).

Yi YJ, Manandhar G, Oko RJ, Breed WG, Sutovsky P. 2007a. Mechanism of sperm-zona pellucida penetration during mammalian fertilization: 26S proteasome as a candidate egg coat lysin. Soc Reprod Fertil Suppl 63:385-408.

Yi YJ, Manandhar G, Sutovsky M, Jonakova V, Park CS, Sutovsky P. 2009b. Inhibition of 19S proteasomal regulatory complex subunit PSMD8 increases polyspermy during porcine fertilization in vitro. J Reprod Immunol 84(2):154-163.

Yi YJ, Manandhar G, Sutovsky M, Jonakova V, Park CS, Sutovsky P. 2010a. Inhibition of 19S proteasomal regulatory complex subunit PSMD8 increases polyspermy during porcine fertilization in vitro. J Reprod Immunol 84(2):154-163.

Yi YJ, Manandhar G, Sutovsky M, Li R, Jonakova V, Oko R, Park CS, Prather RS, Sutovsky P. 2007b. Ubiquitin C-terminal hydrolase-activity is involved in sperm acrosomal

function and anti-polyspermy defense during porcine fertilization. Biol Reprod 77(5):780-793.

Yi YJ, Manandhar G, Sutovsky M, Zimmerman SW, Jonakova V, van Leeuwen FW, Oko R, Park CS, Sutovsky P. 2010b. Interference with the 19S proteasomal regulatory complex subunit PSMD4 on the sperm surface inhibits sperm-zona pellucida penetration during porcine fertilization. Cell Tissue Res 341(2):325-340.

Yi YJ, Park CS, Kim ES, Song ES, Jeong JH, Sutovsky P. 2009c. Sperm-surface ATP in boar spermatozoa is required for fertilization: relevance to sperm proteasomal function. Syst Biol Reprod Med 55(2):85-96.

Yi YJ, Zimmerman SW, Manandhar G, Odhiambo JF, Kennedy C, Jonakova V, Manaskova-Postlerova P, Sutovsky M, Park CS, Sutovsky P. 2011. Ubiquitin-activating enzyme (UBA1) is required for sperm capacitation, acrosomal exocytosis and sperm-egg coat penetration during porcine fertilization. Int J Androl.

Yin Y, Lin C, Kim ST, Roig I, Chen H, Liu L, Veith GM, Jin RU, Keeney S, Jasin M, Moley K, Zhou P, Ma L. The E3 ubiquitin ligase Cullin 4A regulates meiotic progression in mouse spermatogenesis. Dev Biol 356(1):51-62.

Yin Y, Lin C, Kim ST, Roig I, Chen H, Liu L, Veith GM, Jin RU, Keeney S, Jasin M, Moley K, Zhou P, Ma L. 2011. The E3 ubiquitin ligase Cullin 4A regulates meiotic progression in mouse spermatogenesis. Dev Biol 356(1):51-62.

Yokota N, Harada Y, Sawada H. Identification of testis-specific ubiquitin-conjugating enzyme in the ascidian Ciona intestinalis. Mol Reprod Dev 77(7):640-647.

Yokota N, Harada Y, Sawada H. 2010a. Identification of testis-specific ubiquitin-conjugating enzyme in the ascidian Ciona intestinalis. Mol Reprod Dev 77(7):640-647.

Yokota N, Kataoka Y, Hashii N, Kawasaki N, Sawada H. 2010b. Sperm-specific C-terminal processing of the proteasome PSMA1/alpha6 subunit. Biochem Biophys Res Commun 410(4):809-815.

Yokota N, Sawada H. 2007. Sperm proteasomes are responsible for the acrosome reaction and sperm penetration of the vitelline envelope during fertilization of the sea urchin Pseudocentrotus depressus. Dev Biol 308(1):222-231.

Yoshioka K, Suzuki C, Tanaka A, Anas IM, Iwamura S. 2002. Birth of piglets derived from porcine zygotes cultured in a chemically defined medium. Biol Reprod 66(1):112-119.

Yu Y, Xu W, Yi YJ, Sutovsky P, Oko R. 2006. The extracellular protein coat of the inner acrosomal membrane is involved in zona pellucida binding and penetration during fertilization: characterization of its most prominent polypeptide (IAM38). Dev Biol 290(1):32-43.

Yurewicz EC, Sacco AG, Gupta SK, Xu N, Gage DA. 1998. Hetero-oligomerization-dependent binding of pig oocyte zona pellucida glycoproteins ZPB and ZPC to boar sperm membrane vesicles. J Biol Chem 273(13):7488-7494.

Zhong L, Belote JM. 2007. The testis-specific proteasome subunit Prosalpha6T of D. melanogaster is required for individualization and nuclear maturation during spermatogenesis. Development 134(19):3517-3525.

Zimmerman S, Sutovsky P. 2009. The sperm proteasome during sperm capacitation and fertilization. J Reprod Immunol 83(1-2):19-25.

Zimmerman SW, Manandhar G, Yi YJ, Gupta SK, Sutovsky M, Odhiambo JF, Powell MD, Miller DJ, Sutovsky P. 2011. Sperm proteasomes degrade sperm receptor on the egg zona pellucida during mammalian fertilization. PLoS One 6(2):e17256.

APPENDIX

Discovery of putative oocyte quality markers by comparative ExacTag proteomics

Michael D. Powell[1], Gaurishankar Manandhar[2], Lee Spate[2], Miriam Sutovsky[2], **Shawn Zimmerman[2]**, Shrikesh C. Sachdev[3], Mark Hannink[3], Randall S. Prather[2], and Peter Sutovsky[2,4]

1 Morehouse School of Medicine, Atlanta, GA, USA
2 Division of Animal Sciences, University of Missouri-Columbia, Columbia, MO, USA
3 Department of Biochemistry, University of Missouri-Columbia, Columbia, MO, USA
4 Department of Obstetrics, Gynecology and Women's health, University of Missouri-Columbia, Columbia, MO, USA

Published in: Proteomics Clin Appl. 2010 Mar;4(3):337-51.

Purpose—Identification of the biomarkers of oocyte quality, and developmental and reprogramming potential is of importance to assisted reproductive technology in humans and animals. Experimental design—PerkinElmer ExacTag™ Kit was used to label differentially proteins in pig oocyte extracts (oocyte proteome) and pig oocyte-conditioned in vitro maturation media (oocyte secretome) obtained with high- and low-quality oocytes. Results—We identified 16 major proteins in the oocyte proteome that were expressed differentially in high- versus low-quality oocytes. More abundant proteins in the high-quality oocyte proteome included kelch-like ECH-associated protein 1 (an adaptor for ubiquitin-ligase CUL3), nuclear export factor CRM1 and ataxia-telangiectasia mutated protein kinase. Dystrophin (DMD) was more abundant in low-quality oocytes. In the secretome, we identified 110 proteins, including DMD and cystic fibrosis transmembrane conductance regulator, two proteins implicated in muscular

dystrophy and cystic fibrosis, respectively. Monoubiquitin was identified in the low quality-oocyte secretome. Conclusions and clinical implications—A direct, quantitative proteomic analysis of small oocyte protein samples can identify potential markers of oocyte quality without the need for a large amount of total protein. This approach will be applied to discovery of non-invasive biomarkers of oocyte quality in assisted human reproduction and in large animal embryo transfer programs.

In an attempt to indentify oocyte quality markers oocytes were collected from ovaries obtained from a local slaughter house with the use of a 18 gauge needle attached to a 10 ml syringe. Oocytes were separated out into 100 oocytes groups and then matured in a serum free TCM-199 medium supplemented with FSH and LH (Gibco BRL; supplemented with 0.1% PVA w/v, 3.05 mM D-glucose, 0.91 mM sodium pyruvate and 10 μg/ml gentamicin) for 44hrs. Production of reduced developmental potential was done by using TCM-199 medium without the addition of FSH or LH. Upon completion of maturation media from both high and low quality-oocytes was collected and frozen at -80 ˚C until used for analysis. Medias from both classes of oocytes was analyzed by subjecting the solutions to Western blotting. Media was diluted in loading buffer containing 50mM Tris, 150 mM NaCl, 20% glycerol, 2% SDS, 5% β-mercaptoethanol, 1mM PMSF and 0.01% bromphenol blue and boiled for 5 min. Proteins were separated out on a 10% Tris-Glycine gel and then transferred to a PVDF membrane over a 4 hr period at 50V. Use of two anti-ubiquitin antibodies, mouse IgG MK-12-3 and mouse IgM FK-1 resulted in the presence of unconjugated ubiquitin bands

in low quality-oocytes and high mass bands of polyubiquitinated proteins were detected in the high quality-oocytes(Fig. 6). These results suggest that the ubiquitin proteasome pathway may be assisting in removal of maternal proteins during maturation and a possible oocyte quality marker.

Carbohydrate-Mediated Binding and Induction of Acrosomal Exocytosis in a Boar Sperm-Somatic Cell Adhesion Model[1]

Gary F. Clark,[3] **Shawn Zimmerman,[4]** David E. Lafrenz,[3] Young-Joo Yi,[4] and Peter Sutovsky[3,4]

Department of Obstetrics, Gynecology, and Women's Health,[3] Division of Reproductive and Perinatal Research, University of Missouri School of Medicine, Columbia, Missouri
Division of Animal Sciences,[4] University of Missouri, Columbia, Missouri

Published in: Biology of Reproduction **83**, 623–634.

The molecular basis underlying the binding of spermatozoa to their homologous eggs and the subsequent induction of acrosomal exocytosis remain a major unresolved issue in mammalian fertilization. Novel cell adhesion systems are now being explored to advance this research. Triantennary and tetraantennary N-glycans have previously been implicated as the major carbohydrate sequences that mediate the initial binding of spermatozoa to the specialized egg coat (zona pellucida) in the murine and porcine models. Mouse spermatozoa also undergo binding to rabbit erythrocytes (rRBCs), presumably via the interaction of their lectin-like egg-binding proteins with branched polylactosamine sequences present on these somatic cells. Experiments presented in this study confirm that boar spermatozoa also bind to rRBCs. However, unlike mouse

spermatozoa, boar spermatozoa also undergo acrosomal exocytosis within 30 min after binding to rRBCs. Both binding and induction of acrosomal exocytosis in this system did not require the participation of terminal Galalpha1-3Gal sequences that are found on rRBCs. Pronase glycopeptides derived from rRBCs inhibited the binding of boar sperm to porcine oocytes by 91% at a final concentration of 0.3 mg/ml under standard IVF conditions. Binding in this porcine cell adhesion model was also completely blocked at this concentration of glycopeptide. Thus, adhesion results from the interaction of the egg-binding protein expressed on the surface of boar spermatozoa with the glycans presented on rRBCs. This cell adhesion model will be useful for investigating the molecular basis of gamete binding and the induction of acrosomal exocytosis in the pig.

Initial experiments involving rabbit erythrocytes (rRBC) and boar spermatozoa were done by placing rRBCs in a Tris-buffered medium (mTBM) containing 0.2% BSA that was covered by mineral oil. Once in the medium the rRBCs were equilibrated for 30 min in the incubator prior to the addition of boar spermatozoa. Sperm that was to be used for coincubations was stored in Beltsville thawing solution (BTS) and was washed twice in PBS-PVA prior to being resuspended in mTBM medium. A final concentration of 1 $x10^6$ sperm/ml was added to the mTBM droplets containing the rRBCs. Spermatozoa and rRBCs were incubated for 30 min at 38.5 ˚C and then placed on SuperFrost microscope slides and sealed with clear nail polish (Fig 1, C).

Peroxiredoxin 2 and Peroxidase Enzymatic Activity of Mammalian Spermatozoa[1]

Gaurishankar Manandhar,[3] Antonio Miranda-Vizuete,[6] Jose R. Pedrajas,[7] William J. Krause,[4] **Shawn Zimmerman,**[3] Miriam Sutovsky,[3] and Peter Sutovsky[3,5]

Division of Animal Sciences,[3] Department of Pathology & Anatomical Sciences,[4] and Department of Obstetrics/ Gynecology and Woman's Health,[5] University of Missouri-Columbia, Columbia, Missouri Centro Andaluz de Biologı´a del Desarrollo (CABD-CSIC),[6] Departamento de Fisiologia, Anatomia y Biologia Celular, Universidad Pablo de Olavide, Sevilla, Spain Departamento de Biologı´a Experimental,[7] Facultad de Ciencias Experimentales, Universidad de Jae´n, Jae´n, Spain

Published in: Biology of Reproduction **80**, 1168–1177.

Peroxiredoxin 2 (PRDX2) is a highly efficient redox protein that neutralizes hydrogen peroxide, resulting in protection of cells from oxidative damage and in regulation of peroxidemediated signal transduction events. The oxidized form of PRDX2 is reverted back to the reduced form by the thioredoxin system. In the present study, we investigated the presence of PRDX2 in mouse and boar spermatozoa and in mouse spermatids using proteomic techniques and immunocytochemistry. Sperm and spermatid extracts displayed a 20-kDa PRDX2 band on Western blotting. PRDX2 occurred as a Triton-soluble form in spermatids and as a Triton-insoluble form in mature spermatozoa. Boar seminiferous tubule extracts were immunoprecipitated with PRDX2 antibody and separated by SDS-PAGE. Peptide mass fingerprinting by matrix-assisted laser desorption ionization-time of flight (TOF) and microsequencing by nanospray quadrupole-quadrupole TOF tandem mass spectrometry revealed the presence of PRDX2 ions in the immunoprecipitated band, along with sperm mitochondria-associated cysteinerich protein, cellular nucleic acid-binding protein, and glutathione peroxidase 4.

In mouse spermatocytes and spermatids, diffuse labeling of PRDX2 was observed in the cytoplasm and residual bodies. After spermiation, PRDX2 localization became confined to the mitochondrial sheath of the sperm tail midpiece. Boar spermatozoa displayed similar PRDX2 localization as in mouse spermatozoa. Boar spermatozoa with disrupted acrosomes expressed PRDX2 in the postacrosomal sheath region. Peroxidase enzyme activity of boar sperm extracts was evaluated by estimating the rate of NADPH oxidation in the presence or absence of a glutathione depletory (diethyl maleate) or a glutathione reductase inhibitor (carmustine). Diethyl maleate partially inhibited peroxidase activity, whereas carmustine showed an insignificant effect. These observations suggest that glutathione and glutathione reductase activity contribute only partially to the total peroxidase activity of the sperm extract. While the specific role of PRDX2 in the total peroxidase activity of sperm extract is still an open question, the present study for the first time (to our knowledge) shows the presence of PRDX2 in mammalian spermatozoa.

Collection of whole spermatozoa proteins was done by collecting the sperm rich fraction of a boar ejaculate from the University of Missouri Swine Complex. Once collected spermatozoa were centrifuged at 2,100 rpm for 5 min to remove seminal plasma, spermatozoa were then washed two more times in TL-Hepes-PVA prior to being resuspended in loading buffer (50 mM Tris [pH 6.8], 150 mM NaCl, 2% SDS, 20% glycerol, 5% b-mercaptoethanol, and 0.002% bromphenol blue). Samples were boiled for 5 min and then stored at -80 ˚C until needed for western blot analysis.

Ubiquitin-activating enzyme (UBA1) is required for sperm capacitation, acrosomal exocytosis and sperm–egg coat penetration during porcine fertilization

Y.-J. Yi,* **S. W. Zimmerman**,* G. Manandhar,* J. F. Odhiambo,* C. Kennedy,* V. Jona´ kova´ , P. Manˇ a´ skova´ -Postlerova´ ,_ M. Sutovsky,* C.-S. Park§ and P. Sutovsky*_

**Division of Animal Sciences and _Department of Obstetrics, Gynecology and Women's Health, University of Missouri-Columbia, Columbia, MO,USA, _Laboratory of Diagnostics for Reproductive Medicine, Institute of Biotechnology Academy of Sciences of the Czech Republic, Prague, Czech Republic, and §Research Center for Transgenic Cloned Pigs, Chungnam National University, Daejeon, South Korea*

Published in: Int J Androl. 2011 Sep 27

Protein ubiquitination is a stable, covalent post-translational modification that alters protein activity and ⁄ or targets proteins for proteolysis by the 26S proteasome. The E1-type ubiquitin-activating enzyme (UBA1) is responsible for ubiquitin activation, the initial step of ubiquitin–protein ligation. Proteasomal proteolysis of ubiquitinated spermatozoa and oocyte proteins occurs during mammalian fertilization, particularly at the site of sperm acrosome contact with oocyte zona pellucida. However, it is not clear whether the substrates are solely proteins ubiquitinated during gametogenesis or if de novo ubiquitination also occurs during fertilization supported by ubiquitin-activating and –conjugating enzymes present in the sperm acrosome. Along this line of inquiry, UBA1 was detected in boar sperm-acrosomal extracts by Western blotting (WB). Immunofluorescence revealed accumulation of UBA1 in the nuclei of spermatogonia, spermatocytes and spermatids, and in the acrosomal caps of round and elongating spermatids. Thiol ester assays utilizing biotinylated ubiquitin and isolated sperm

acrosomes confirmed the enzymatic activity of the resident UBA1. A specific UBA1 inhibitor, PYR-41, altered the remodeling of the outer acrosomal membrane (OAM) during sperm capacitation, monitored using flow cytometry of fluorescein isothiocyanate-conjugated peanut agglutinin (FITC-PNA). Although viable and motile, the spermatozoa capacitated in the presence of PYR-41, showed significantly reduced fertilization rates during in vitro fertilization (IVF; $p < 0.05$). Similarly, the fertilization rate was lowered by the addition of PYR-41 directly into fertilization medium during IVF. In WB, high Mr bands, suggestive of protein ubiquitination, were detected in non-capacitated spermatozoa by antibodies against ubiquitin; WB with antiphosphotyrosine antibodies and antibodies against acrosomal proteins SPINK2 (acrosin inhibitor) and AQN1 (spermadhesin) revealed that the capacitationinduced modification of those proteins was altered by PYR-41. In summary, it appears that de novo protein ubiquitination involving UBA1 contributes to sperm capacitation and acrosomal function during fertilization.

Initial experiments done using crude acrosome contents from boar spermatozoa were done by washing an aliquot of freshly collected boar spermatozoa three times in PBS and centrifuging each time at 2,100 rpm for 5 min. Once washed the sperm were suspended in cold Tris-buffered solution (TBS; 50 mM Tris, 150 mM NaCl, pH 7.4) supplemented with 1 mM dithiothreitol (DTT), 1 mM EDTA, 5 mM MgCl2 and 10% glycerol. Samples were sonicated for 1 min at 30% intensity, centrifuged at 2,100 rpm for 10 min and supernatants were collected. Supernatants were then re-centrifuged at

10,000 x g for 10 min and the final supernatant was collected and stored at -80 ˚C. Western blot of the crude acrosome contents showed the predicted UBA1 band at ~119 kDa when detected by a rabbit polyclonal anti-UBA1 antibody (Fig 1, A).

Interference with the 19S proteasomal regulatory complex subunit PSMD4 on the sperm surface inhibits sperm-zona pellucida penetration during porcine fertilization

Young-Joo Yi[1,2] Gaurishankar Manandhar[1] Miriam Sutovsky[1]
Shawn W. Zimmerman[1] Věra Jonáková[3] Fred W. van Leeuwen[4] Richard Oko[5]
Chang-Sik Park[2] Peter Sutovsky[1]

[1]Division of Animal Sciences, and Department of Obstetrics, Gynecology & Women's Health,University of Missouri-Columbia, Columbia, MO 65211, USA, [2]Research Center for Transgenic Cloned Pigs, Chungnam National University, Daejeon 305-764, South Korea, [3]Laboratory of Diagnostic for Reproductive Medicine, Institute of Biotechnology Academy of Sciences of the Czech Republic v.v.i., 142 20 Prague 4, Czech Republic, [4]School for Mental Health and Neuroscience, Department of Neuroscience, Maastricht University, Universiteitssingel 50, 6229 ER Maastricht, The Netherlands, [5]Department of Anatomy and Cell Biology, Queen's University, Kingston, Ontario, Canada

Published in: Cell Tissue Res. 2010 Aug;341(2):325-40.

Proteolysis of ubiquitinated sperm and oocyte proteins by the 26S proteasome is necessary for the success of mammalian fertilization, including but not limited to acrosomal exocytosis and sperm-zona pellucida (ZP) penetration. The present study examined the role of PSMD4, an essential non-ATPase subunit of the proteasomal 19S regulatory complex responsible for proteasome-substrate recognition, in sperm-ZP penetration during porcine fertilization in vitro (IVF). Porcine sperm-ZP penetration, but not sperm-ZP binding, was blocked in the presence of a monoclonal anti-PSMD4

antibody during IVF. Inclusion in the fertilization medium of mutant ubiquitin (UBB^{+1} and $UBB5^{+1}$), which are refractory to processing by the 19S regulatory complex and associated with Alzheimer's disease, also inhibited fertilization. This observation suggested that subunit PSMD4 is exposed on the sperm acrosomal surface, a notion that was further supported by the binding of non-cell permeant, biotinylated proteasomal inhibitor ZL3VS to the sperm acrosome. Immunofluorescence localized PSMD4 in the sperm acrosome. Immunoprecipitation and proteomic analysis revealed that PSMD4 co-precipitated with porcine sperm associated acrosin inhibitor (AI). Ubiquitinated species of AI were isolated from boar sperm extracts by affinity purification of ubiquitinated proteins using the recombinant UBA domain of p62 protein. Some proteasomes appeared to be anchored to the sperm head inner acrosomal membrane, as documented by co-fractionation studies. In conclusion, the 19S regulatory complex subunit PSMD4 is involved in the sperm-ZP penetration during fertilization. The recognition of substrates on the ZP by the 19S proteasomal regulatory complex is essential for the success of porcine/mammalian fertilization in vitro.

To determine the purity of both mutant forms of ubiquitin (UBB^{+1} and $UBB5^{+1}$) that were used in the IVF experiments 30 µg of each mutant form along with an equal amount of wild type ubiquitin was prepared for Western blot analysis by boiling each sample in loading buffer (50 mM Tris [pH 6.8], 150 mM NaCl, 2% SDS, 20% glycerol, 5% b-mercaptoethanol, and 0.002% bromphenol blue). Once transferred onto a PVDF membrane the proteins were probed using either an antibody specific for UBB^{+1} known

as UBI3 or a anti-ubiquitin antibody (MK 12-3) that would recognize a shared domain within both wild-type and mutant ubiquitin. Results confirmed high purity of both UBB^{+1} and $UBB5^{+1}$ through use of the anti-mutant ubiquitin antibody when two low bands were observed in the UBB^{+1} lane while larger massed bands were observed in the $UBB5^{+1}$ lane, additionally no bands were observed in the wild-type ubiquitin lane (Fig 6). A similar band pattern was seen when MK 12-3 was used to detect presence of ubiquitin in the UBB^{+1} and $UBB5^{+1}$ lanes with the addition of a single band in the wild-type lane also (Fig 6). Collectively these results confirmed the purity of the UBB^{+1} and $UBB5^{+1}$ mutant ubiquitin forms used in the IVF experiments and confirmed the specificity of the anti-mutant ubiquitin antibody UBI3.